Chapter 30

Perfluorinated membranes

M. Doyle[1] **and G. Rajendran**[2]

[1] *DuPont Microcircuit Materials, Research Triangle Park, NC, USA*
[2] *DuPont Central Research & Development, Wilmington, DE, USA*

1 INTRODUCTION AND OVERVIEW

The commercial development of single-ion conducting polymer electrolytes changed the field of electrochemical devices in a significant way. Electrochemists have spent many decades in a continuing search for newer, more highly conducting and more electrochemically stable electrolyte systems. With the development of single-ion conducting polymers, electrochemists have the ability to choose from a variety of polymers with both high conductivity for a given ion of interest as well as excellent stability and processability allowing the design of electrochemical devices in their most ideal formats. Traditional electrolyte systems such as sulfuric acid and potassium hydroxide, used for their low cost and high ionic conductivity but saddled with their extreme corrosivity and challenging confinement, are giving way to new polymeric electrolyte systems.

The broad class of polymer electrolytes to which perfluorinated ionomer membranes belong has application in a number of areas of commercial importance not limited to proton exchange membrane fuel cells (PEMFCs). Ionomers is a term that typically refers to single-ion conducting polymers with a fixed ion group covalently attached to a side chain of the polymer. A related term, ionenes, has been used for main-chain fixed ion group copolymers. All of these materials can be considered to be polyelectrolytes as well as ion-containing polymers, two commonly used terms outside of the fuel cell literature. The present review will focus on perfluorinated ionomer products, known by the trade names of Nafion® membranes and Nafion® solutions, that are commercially available from E.I. DuPont de Nemours and Company (DuPont).

A number of excellent review articles exist covering the subject of perfluorinated ionomer membranes with emphasis on transport processes,[1, 2] applications,[3] and structural studies and physical properties.[4, 5] Thus, the present review will only summarize briefly the important previous work while updating these reviews with recent experimental and theoretical studies shedding new light on the important factors in transport processes in these membrane systems. We make a special effort to gather physical (thermodynamic, thermal, mechanical, etc.) and transport property data together in this review so that current and future generations of engineers and scientists can utilize this section as a resource for experimental studies.

The most common commercial perfluorinated ionomer membranes used today in numerous industrial processes throughout the world are listed in Table 1. Physical structures of the Nafion®, Flemion®, and Aciplex® sulfonate (XR) and carboxylate (CR) form membranes have been shown in the literature.[6] The typical functional comonomer structures for each ionomer system are shown in Table 2.[5] We also list Dow's short side chain monomer structure here even though this ionomer is no longer offered commercially.

According to the literature, Aciplex® membranes from Asahi Chemical are available as AC-12 (1100 equivalent

---

Handbook of Fuel Cells – Fundamentals, Technology and Applications, Edited by Wolf Vielstich, Hubert A. Gasteiger, Arnold Lamm. Volume 3: *Fuel Cell Technology and Applications*. ISBN: 0-471-49926-9.

Table 1. Commercial perfluorinated ionomer membranes listed by trade name.

Trade name	Company	Membrane Type
Nafion® XR resin	DuPont	Perfluorosulfonic acid
Nafion® CR resin	DuPont	Perfluorocarboxylic acid
Flemion® XR resin	Asahi Glass	Perfluorosulfonic acid
Flemion® CR resin	Asahi Glass	Perfluorocarboxylic acid
Aciplex® XR resin	Asahi Chemical	Perfluorosulfonic acid
Aciplex® CR resin	Asahi Chemical	Perfluorocarboxylic acid

Table 2. Typical functional comonomer structures for each ionomer system.

XR (sulfonate) comonomer structures	
Nafion®, Flemion®	$CF_2{=}CFOCF_2CF(CF_3)OCF_2CF_2SO_2F$
Aciplex®	$CF_2{=}CFOCF_2CF(CF_3)OCF_2CF_2CF_2SO_2F$
Dow	$CF_2{=}CFOCF_2CF_2SO_2F$
CR (carboxylate) monomer structures	
Nafion®, Aciplex®	$CF_2{=}CFOCF_2CF(CF_3)OCF_2CF_2CO_2CH_3$
Flemion®	$CF_2{=}CFOCF_2CF_2CF_2CO_2CH_3$

weight (EW), 10 mil thick) and AC-4 (1000 EW, 4 mm thick), whereas Flemion® membranes from Asahi Glass are available as FL-12 (900 EW, 10 mil thick) and FL-4 (900 EW, 4 mil thick).[7] Asahi Glass have also developed reinforced ionomer membrane structures for fuel cell applications (see **Composite perfluorinate membranes**, Volume 3). Nafion® membranes, on the other hand, are available from DuPont as NE112 (2 mm thick), NE-1135 (3.5 mm thick), N115 (5 mm thick), and N117 (7 mm thick). Membranes such as N120 (1200 EW, 10 mm thick) and N105 (1000 EW, 5 mm thick) are also often cited in the literature.

Although ionomer membranes have been used for several decades in a number of commercial processes, their production volumes can only be deemed small in comparison to major commodity polymers. When the PEMFC reaches its eventual position as a power generation system in broad-based applications such as automotive propulsion, perfluorinated ionomers will reach a scale of production far exceeding the current levels. This change will bring about significant challenges for the polymer suppliers but also offers tremendous opportunities. It is likely that these future ubiquitous ionomer membranes will look different and cost less than the membranes that dominate the commercial landscape today.

2 DEVELOPMENT OF IONOMERIC MEMBRANES

2.1 Early work on ionomer-based chemical processes

Electrochemical separator membranes with fixed ion groups date back to before the 1950s with the use of polystyrene sulfonic acid and related acid-containing polymers as separators for electrochemical processes. The advantages of fixed ion group separators in the early days of usage were the same that exist today including the lack of corrosive mobile acids, high conductivity and selectivity, and thin film form leading to compact systems with low ohmic drop. The drawback of these systems was the chemical and electrochemical degradation that occurred with the instability of the C–H bonds in these early ionomers.

The concept of using an ion exchange membrane as the sole electrolyte in fuel cells is due to W. T. Grubb of General Electric (GE). US patent No. 2,913,511 to Grubb filed on June 29, 1955 describes a fuel cell with an ion-exchange membrane as the sole electrolyte and gaseous feed streams. These experiments were done using sulfonated poly(styrene-divinylbenzene) Amberplex C1 ion exchange membranes. A later patent (US patent No. 3,061,658), published in October 30, 1962 by R. H. Blackmer of GE, describes the use of humidified feed gases to improve the performance of these early membrane fuel cells. Early published literature on PEMFCs should be consulted for more information.[8, 9]

The first commercially available perfluorinated ionomer membranes were based on copolymers of tetrafluoroethylene (TFE) and perfluorovinyl ether monomers. The first use of a Nafion® membrane in a fuel cell was accomplished in 1966 by GE for National Aeronautics & Space Administration (NASA).[4, 10] A DuPont press release dated September 12, 1969 announced the availability of the new XR perfluorosulfonic acid copolymer composition suitable for use in PEMFCs. TFE can be homopolymerized and copolymerized without much difficulty given experience with handling fluorocarbon monomers and the necessary safety precautions associated with the hazards of these chemicals and their degradation products. The resulting random copolymers can have moderately high molecular weights and their behavior is dominated by the vast differences in the properties of the TFE segments and the polar and hydrophilic ion groups.

Although perfluorinated polymers were discovered over 60 years ago, with Roy Plunkett's discovery of polytetrafluoroethylene (PTFE) in an empty cylinder of TFE at DuPont's Jackson Laboratory in 1938, their nature is still an exciting research topic yielding new discoveries on an annual basis.[11] Their properties are dominated by the extreme behavior of the C–F bond, a topic that is the focus of a recent review article describing some of the many properties of fluoropolymers having diverse commercial application.[12] A recent surprising discovery of a means for melt processing PTFE demonstrates that this field is by no means stagnant and many exciting properties and applications remain to be exploited.[13]

While the use of perfluorinated ionomers has alleviated stability problems of other membranes systems to a large extent, there still exist real concerns around the long-term stability of polymers in electrochemical cells. Long-term performance of fuel cells will often require greater than 10 000 h of stable performance under operating conditions that are simultaneously oxidizing, reducing, and thermally demanding. A number of degradation mechanisms are known and well understood with perfluorinated ionomers including fouling and precipitation of multivalent salts within the membrane and conductivity loss due to ion exchange and immobilization, both of which occur with time in membrane chlor-alkali cells. Additionally, perfluorinated polymers can be reductively degraded in the presence of strong reducing agents such as lithium metal.

The primary concern related to polymer degradation in PEMFC environments is oxidation damage. Unfortunately this phenomenon, while often mentioned, is not well documented in the technical literature to the extent that the fundamental mechanisms can be articulated. The interested reader should refer to the article by LaConti (see **Mechanisms of membrane degradation**, Volume 3), for more information on these processes. Clearly perfluorinated ionomers are very stable to oxidation, as evidenced by their >10 years of continuous use in chlor-alkali cells and stability against even fluorine/nitrogen gas mixtures.

2.2 Chlor-alkali process — historical perspective

The use of perfluorinated ionomer membranes in the membrane chlor-alkali process has a long and rich history that continues to unfold as changes occur in the global chlorine and caustic industries. Chlorine and caustic soda are two of the largest industrial chemicals produced in the world and the largest by volume produced using an electrochemical process. The history of the chlor-alkali industry is punctuated by new technology, changing environmental regulations, and frequent fluctuations in the demand for these two products whose supply is linked due to their co-production.[14]

The membrane chlor-alkali process was developed in the 1960s and DuPont's membrane product Nafion® was invented in 1962 and first used in a chlor-alkali cell in 1964.[10] The perfluorosulfonate XR-type copolymer does not provide sufficient performance in chlor-alkali cells due to the problem of hydroxide crossover and dilution of the cathode product. This led to the development of multi-layer membranes with a thin layer of perfluorocarboxylate-type ionomer having significantly lower crossover of hydroxide under operating conditions. These membrane systems have been a tremendous success since their release with a steady increase in the use of membrane cells in new construction of chlor-alkali cell capacity and retrofit of older mercury cells as environmental regulations require their phase-out. Over 60 000 h of operation at 80 °C have been achieved with Nafion® membranes in chlor-alkali cells.[15]

A variety of membrane types and structures have been developed in the process of engineering the best performance in chlor-alkali cells over several decades of research and experimentation. These included laminating an open-weave Teflon® fabric into the polymer film with various characteristics such as degrees of open space, laminating different EW membranes together, surface treatments such as generating a thin layer of weakly acidic sulfonamide exchange sites on the surface, and composite membranes containing both carboxylate and sulfonate functional groups. All of these studies were targeted at reducing hydroxyl ion crossover, improving ionic conductivity and lowering power requirements of chlor-alkali cells.

Other early industrial applications of Nafion® membranes included solid polymer electrolyte (SPE) water electrolyzers, alkaline water electrolyzers, aqueous HCl electrolyzers, Na_2SO_4 electrolyzers, H_2/air fuel cells, H_2/halogen fuel cells, Zn/bromine cells, Zi/ferricyanide redox cells, Zn/ferric redox cells, Donnan dialyzers, electrochromic devices, ion-selective electrodes, and many other niche applications.[3]

2.3 Other industrial ionomer membrane processes

The excellent chemical and mechanical stability and facile cation transport valued in the PEMFC industry is useful for other electrochemical applications. In general, electrolytic processes are preferred economically for production of highly oxidized or reduced products that are difficult to manufacture by chemical routes. For example, a wide range of highly oxidized gases are synthesized industrially using electrolytic processes, including chlorine dioxide, ozone, hydrogen peroxide, fluorine, nitrogen trifluoride, and dinitrogen pentoxide. The advantages of using perfluorinated ionomer membrane-separated processes have been explored for all of these syntheses and commercial membrane-based processes exist in certain cases. These processes utilize cell designs and catalyst layer structures similar in concept to those used in the PEMFC.

An inorganic electrosynthesis of commercial importance in which perfluorinated ionomer membranes play a critical role is the HCl recycle process. Commercial processes for recycling HCl using electrochemical means generally utilize the Uhde process for which nine plants are in operation worldwide.[16] Challenges with Uhde-type HCl oxidation processes are the side reaction to form oxygen at the anode and the drying of the chlorine from the 1–2% water that typically is lost with the gaseous products. An improvement in the Uhde process can be achieved for the oxidation of anhydrous HCl to chlorine gas using a Nafion® membrane separated cell operating in a fuel cell-type mode with a gaseous anode feed stream.[17] Anhydrous HCl recycle is necessary in several large chemical industries such as the manufacture of isocyanates and production of fluorochemicals, which create anhydrous HCl as a co product and require dry chlorine gas as input.[16, 18] A 3-cell anhydrous HCl electrolyzer with $2\,\mathrm{m}^2$ of active area achieved stable operation at $1.2\,\mathrm{A\,cm}^{-2}$ at 1.7 V with current efficiencies of greater than 99%. High current densities afford essentially dry Cl_2 greatly reducing the downstream drying loads.

Nafion® membranes are also at the heart of a flow-through energy storage system referred to as Regenesys and commercialized recently by National Power.[19] The Regenesys system is based on electrochemical energy storage by the conversion of redox couples between two states of charge and storage of the chemicals until needed to return the power. The system offers power generation facilities the ability to meet peak demands with more flexibility and hence reduce capital expenditures on new facilities. The system was piloted in National Power's Aberthaw power station in South Wales, UK and will be commercialized at a plant in Didcot in Oxfordshire, UK. The commercial facility should have a storage capacity of 120 MW h and a nominal power output of 10 MW with a peak power output of 14.75 MW. The first utility-scale demonstration plant is reported to require $16\,000\,\mathrm{m}^2$ of Nafion® membranes.

3 MONOMER AND POLYMER SYNTHESIS

3.1 Side chain structure and synthesis

While numerous acid groups have been employed in ionomer systems over the years, the perfluorosulfonic acid group is still the dominant system in use for applications that demand the highest stability and ionic conductivity. This functional group presents a challenge to synthetic chemists as a limited number of routes to it exist. The most common approaches utilize sulfonyl fluoride or chloride precursors and create a non-ionic precursor polymer through polymerization followed by hydrolysis to the salt form.

Synthesis of the long-chain perfluorosulfonic acid monomer used in most commercial systems (Nafion®, Flemion®, Aciplex®) proceeds through reaction of SO_3 with TFE to create the cyclic sultone. Rearrangement of the cyclic sultone gives the rearranged sultone (RSU) which can be reacted with two equivalents of hexafluoropropylene oxide (HFPO) to produce sulfonyl fluoride adducts. Heating these compounds in the presence of sodium carbonate gives the vinyl ether.[2] These steps are illustrated in Figure 1.[20] The Nafion® membrane's comonomer is commonly referred to as perfluoro sulfonylfluoride ethyl propyl vinyl ether (PSEPVE). In an early patent on PSEPVE, the inventors describe co-polymers with vinylidene fluoride (VF2), TFE, and chloro-trifluoroethylene (CTFE) as well as with other perfluorinated vinyl ether monomers.[21]

The sulfonic acid form of the standard Nafion® membrane is specifically a copolymer of TFE and 2,2,3,3-tetrafluoro-3-[1′,2′,2′-trifluoro-1′-trifluoromethyl-2′-(1″,2″,2″-trifluoro-ethyloxy)ethoxy]sulfonic acid. The common name for this polymer is the Nafion® XR membrane and it can be identified as poly(TFE/4-methyl-3,6-dioxa-7-octene-1-sulfonic acid).

These chemical transformations involve dangerous reactants such as TFE under conditions of high pressure and temperature and as such present challenges for materials

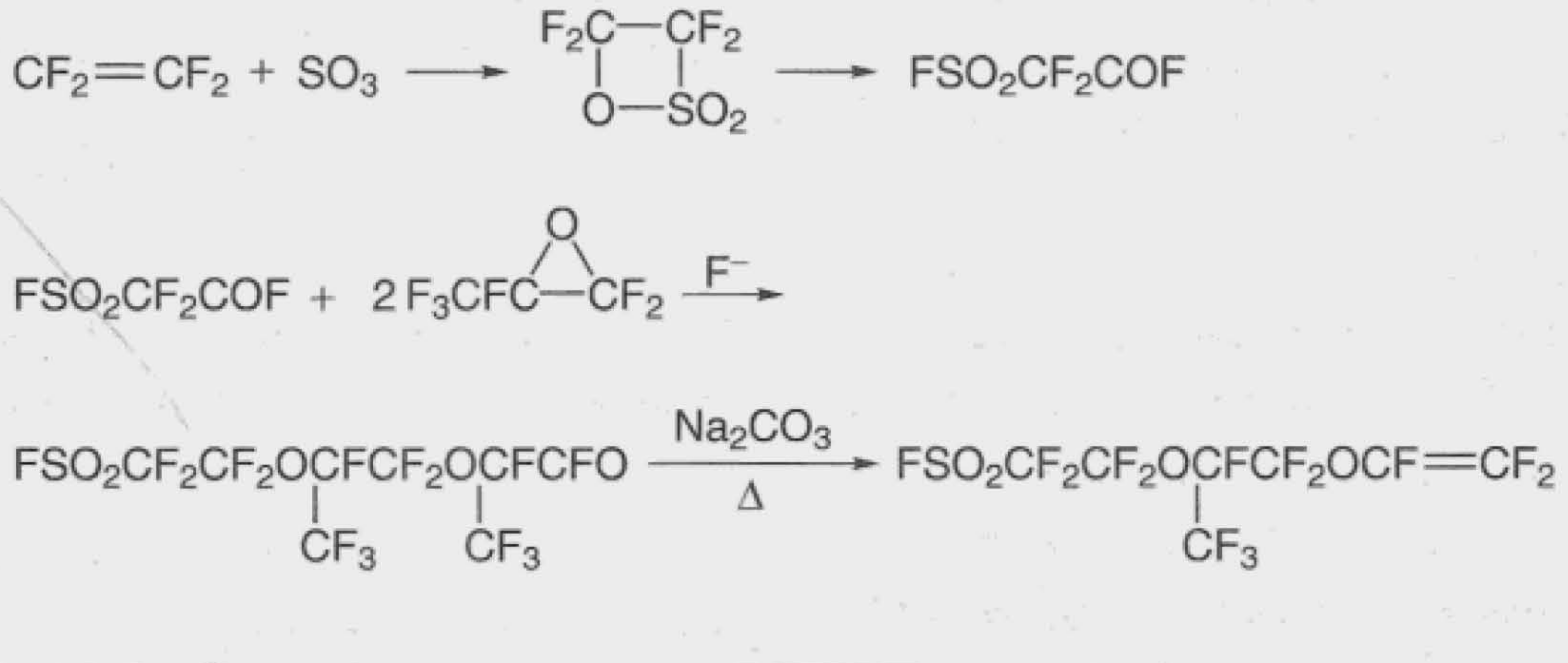

Figure 1. Synthesis process for Nafion® membrane comonomer PSEPVE.

of construction. Additionally, the synthesis of PSEPVE involves numerous steps and some of these steps present yields that could be improved. While the synthesis is carried out on a large scale today, substantial improvements in its quality and yield should be expected in the future when new capacity is justified for increased volume production. Polymerization is typically performed in perfluorocarbon solvents with a perfluorinated free radical initiator such as perfluoroperoxides.[22] Perfluorinated vinyl ether monomers are considered relatively unreactive during polymerization and can only be polymerized by a conventional free radical mechanism with a limited range of comonomers.[23] Modern controlled polymerization techniques, such as living radical, anionic, or cationic, cannot be used with fluorinated vinyl ethers so polymer architectures are limited.[24]

Copolymers of PSEPVE and TFE have many similarities to other perfluorinated systems in their stability and mechanical properties. These copolymers can be melt processed and fabricated into shapes prior to conversion to the salt form and depending on the comonomer content. The mechanical properties of the resin depend on the polymer's structure, including the comonomer content, distributions of the comonomers, and molecular weight and molecular weight distribution of the copolymer. The sulfonyl fluoride co-polymer is stable in water and acids. It is hydrolyzed completely in strong base to give a Na^+ salt form that can be converted to acid form using nitric acid. Nafion® membranes have been produced in a variety of forms including films, tubes, fibers, and laminates with other materials such as Teflon® fabrics.[20]

3.2 Short-chain perfluorosulfonyl fluoride vinyl ether monomer

The short-chain version of the perfluoro sulfonylfluoride vinyl ether monomer has been studied for as long as PSEPVE as a desirable comonomer for perfluorinated ionomers. Ionomers based on this monomer nearly reached commercial status in an experimental membrane produced by Dow Chemical in the early 1990s. Due to sampling to various research groups, numerous analyses were performed on these polymers in the study of their physical properties and fuel cell performance. The Dow membrane was based on a copolymer of TFE and $CF_2{=}CFOCF_2CF_2SO_2F$.

The short-chain perfluorosulfonyl fluoride vinyl ether is missing one hexafluoropropylene oxide (HFPO) unit from the synthesis procedure. The shorter side chain makes the ionic concentration higher for the Dow membrane with the same EW as a comparable Nafion® membrane. A consequence of this higher ion site density is higher ionic conductivities and water uptakes for these membranes under similar conditions. Testing of the Dow polymer in PEMFCs by Ballard in the 1987–1988 time frame showed significant improvements in performance compared to N117, with an approximately three times improvement in current density at 0.5 V under similar operating conditions.[15]

Unfortunately, the synthesis of the short-chain monomer is substantially more challenging than the PSEPVE monomer. One synthesis procedure for the short-chain monomer was illustrated in US Patent No. 4,358,412, based on $FSO_2CF_2C(O)$ and $CF_2(O)CF_2CF_2Cl$. At the present time, Dow is no longer producing this perfluorinated ionomer membrane.[15] Attempts to develop a simpler route to the monomer have apparently failed, at least for the present time.

3.3 Sulfonamide, methide, phosphate and other side chain structures

A good review of the novel ionomer structures examined for fuel cell applications was given by Savadogo.[15] Table 3 lists the more common acid groups utilized in perfluorinated ionomer membranes and some relevant properties of each. Although perfluorinated ionomers with perfluorocarboxylate ion groups ($-CO_2H$) are available, these are not suitable for use in PEMFCs due to their weak acid functional group which gives very poor ionic conductivity and water uptake in its proton form.[15] Other ion-containing moieties have been considered over the years in addition to the fluorosulfonate and fluorocarboxylate groups. A straightforward extension from the sulfonyl fluoride group affords the sulfonamide anion group. This anion has been studied over time for various applications in electroorganic synthesis but does not have either the stability or ionic conductivity required for fuel cell applications.

Table 3. Most common acidic functional groups used within perfluorinated ionomers.[77]

Monomer	Cost	Synthesis	Key Attributes
Fluorocarboxylate	Medium	Moderate	Poor conductivity
Fluorosulfonamide	High	Moderate	Poor conductivity and stability
Styrene sulfonate[a]	Low	Fewer steps	Moderate conductivity, poor stability
Fluorosulfonate	High	Moderate	High conductivity
Fluorosulfonimide	V. high	Challenging	High conductivity
Fluorosulfonyl methide	V. high	Moderate	High conductivity
Fluorophosphate	High	Challenging	Poor conductivity

[a] Monomer is not typically perfluorinated.

Trifluorostyrene type ionomers with perfluorinated backbones and anionic pendant groups having the structure $-P(O)(OMe)_2$ have been studied by Stone *et al.*[25] These phosphoric acid type ionomers exhibited poor conductivity compared to sulfonic acid type ionomers. Alternative acid groups based on the extremely weak Lewis basic fluorosulfonimide and fluorosulfonyl methide groups have seen study in recent years.[26] Other acid groups along these lines making use of strong highly delocalized acidic carbon or nitrogen groups are currently under examination and will be discussed in Section 8.

3.4 Polymerization and preparation of ionomer membranes

Traditional production of the TFE/vinyl ether class of copolymers consists of free radical polymerization in a fluorochemical solvent media.[23] Aqueous emulsion polymerization is also performed with water-soluble or emulsified comonomers. New polymerization methods for fluoropolymers such as supercritical CO_2 polymerization may find application for perfluorinated ionomers in the future. Typical molecular weight ranges for perfluorinated ionomers have been quoted in the $1-10 \times 10^5$ g mol^{-1} range.[5] The degree of branching is essentially zero for these copolymers which is typically measured based on the viscoelastic behavior of the ionomer in its sulfonyl fluoride precursor form. Other characteristics of the polymers, such as the head-to-head contents and polydispersity indices which are measures of the order of the monomers and their randomness, are not known.

Nafion® perfluorinated ionomer membranes are synthesized in their sulfonyl fluoride precursor form and converted to the sodium sulfonate form using a hydrolysis process. The hydrolysis reaction is traditionally carried out in a solution of 15 wt% KOH, 35 wt% dimethylsulfoxide (DMSO) and 50 wt% deionized water at 80 °C for a period of time between 30 min and several hours depending on the thickness of the resin pellet or film. DMSO is an excellent swelling agent for the hydrolyzed Nafion® membrane and allows hydrolysis to be carried out in short periods of time. Other solvent systems can also be employed, such as mixtures of water with long chain alcohols, but the rate of hydrolysis is generally slower and the risks of incomplete hydrolysis are greater.[27]

After the hydrolysis process, the material must be thoroughly washed with deionized water to remove the remaining hydrolysis solution and byproduct salt. This should be done several times with new rinsing solutions. Conversion of the K^+ form polymer thus obtained to the acid form is accomplished using a 10–15% solution of nitric acid (HNO_3). It is recommended to carry out this process twice with fresh nitric acid solution and fresh deionized water rinse steps after each acid treatment in order to ensure full attainment of equilibrium.

A concern with DMSO-based hydrolysis is the difficulty of removing trace DMSO from the hydrolyzed membrane. Fourier Transform infrared (FTIR) spectra continue to detect the presence of DMSO even after several successive washings of the hydrolyzed membrane. For applications that cannot tolerate the presence of trace DMSO, alternate hydrolysis procedures should be adopted. The degree of hydrolysis can be conveniently tested using ionic conductivity data and comparing to conductivity standards. For accurate measurements of the degree of hydrolysis, FTIR techniques are preferred.[28] Conversion from the SO_2F form to any ionic form can be verified by the disappearance of the 2704 cm^{-1} and 1469 cm^{-1} bands.

Ionomer membranes and resins are produced in their precursor form by melt processes as the SO_2F form of the polymer is thermoplastic. Extrusion of the membrane is commonly employed to make high-quality films in a variety of thicknesses in mass production. Films thus cast can be carried through hydrolysis baths to create the salt or acid form in post processing web-based operations. As hydrolysis and acid-exchange reactions require the use of hazardous and corrosive chemicals, proper safety precautions should be followed. Once the acid-form Nafion® membrane is completely rinsed, it should require no special precautions for handling.

3.5 Economics of industrial production of perfluorinated ionomers

The cost of perfluorinated sulfonic acid resin was quoted as $2000 per kilogram in 1999.[5] Fluoropolymers are expensive to manufacture for a variety of reasons. First, the monomers used are costly to manufacture often, requiring a large number of steps and dangerous to handle, making a number of additional precautions necessary for safe operation. The handling of TFE is a hazard that new producers should not consider without appropriate safety training. Second, the functional monomer used in the perfluorinated ionomer membrane (PSEPVE) is a chemical not used for other applications which limits its volume of production.

A significant driver of final polymer cost is the scale of production. An idea of the volume of production of the three major perfluorinated ionomer membranes can be estimated from the size of the membrane chlor-alkali market, the volume driver for these polymers for many years. The total global volume of perfluorinated ionomer membrane sales into the chlor-alkali market is estimated to be 150 000 m^2 year^{-1}. A similar volume of production for the fuel cell market is currently no greater than $50\,000\,m^2\,year^{-1}$. The average membrane thicknesses used in each application are 7 mm ($360\,g\,m^{-2}$ basis weight) and 3.5 mm ($190\,g\,m^{-2}$ basis weight), respectively, for chlor-alkali and fuel cell applications. This equates to a production capacity of approximately $65\,000\,kg\,year^{-1}$. This can be compared with the global production volume of Nylon at $1.2 \times 10^9\,kg\,year^{-1}$ or polystyrene at $2.4 \times 10^9\,kg\,year^{-1}$.[29] Clearly the perfluorinated ionomer membrane is still a specialty polymer made in small volumes when examined in this light.

DuPont made a press release to the Automotive industry on February 24, 1998 stating that future Nafion® membrane prices could be as low as $10 per kilowatt depending on production volumes and cell performance. Assuming that a typical fuel cell achieves about $0.6\,W\,cm^{-2}$ (0.6 V at $1\,A\,cm^{-2}$) at a membrane utilization of 80% (i.e., 80% in active area), this equates to $0.2\,m^2$ membrane per kilowatt. The important message was that the Nafion® membrane would not prevent the PEMFC from being cost competitive with internal combustion engines for automotive applications. The volume requirements quoted in the press release were 150 000 midsize vehicles annually which is a relatively small number compared to total annual vehicle sales.[30] This press release reinforces the strong volume dependence of the cost of manufacture of perfluorinated ionomers and should provide some reassurance that lower costs will be reached with economies of scale. More recently, the DuPont Nafion® business has been using a concept of 10 : 5 : 1 to provide a roadmap for future price reductions for perfluorinated ionomers for fuel cell applications. The numbers represent the projected relative prices for Nafion® membranes in the years 1998, 2001, and 2010. The current price of Nafion® membranes for fuel cell applications is estimated at $100 per kilowatt.

Another practical industrial barrier to new ionomers is the need to create sources and manufacturing facilities for new monomers, new polymer, and post-processing operations such as hydrolysis and film casting or extrusion. Capital investments for these operations on a large scale can be significant and the skills required to operate these facilities are not easy to accumulate. These facts argue for making use of existing facilities and skill sets in the search for new and better-performing perfluorinated ionomers. As perfluorinated ionomers can otherwise achieve most if not all of the attributes needed for high performance PEMFCs, it is necessary to focus efforts on achieving lower cost through economies of scale and other cost reduction measures. A number of means exist for potentially reducing cost of ionomers in fuel cells, including larger scale production, improvements in monomer synthesis and yields, improvements in polymer membrane production, reductions in the quantity of polymer used through composites, thin layers, etc., and changes in structure to simplify the polymer.

How low does the ionomer cost have to reach for widespread usage of PEMFCs? A number of papers in the literature quote fuel cell stack cost goals in the range of $30 per kilowatt or lower for the demanding automotive application.[31, 32] This is translated into precious metal costs of <$5 per kilowatt in one study, representing a Pt loading goal of $0.25\,mg\,cm^{-2}$.[32] This study states that reductions in precious metal usage and cost are the main driver for stack cost reduction. Another study quotes a membrane cost goal of $<\$20\,m^{-2}$.[31] Assuming a fuel cell power density in the range of $0.3\,W\,cm^{-2}$, the membrane cost goal would equate to <$6 per kilowatt.

4 STRUCTURE AND CHARACTERIZATION

4.1 Structural studies and techniques

The relationship between ionomer structure and performance characteristics such as ionic conductivity continues to be a critical driving force for much of the structural research on ionomer membranes and provides the foundation for fundamental modeling work on these materials.[33–40] See **First principles modeling of sulfonic acid based ionomer membranes**, Volume 3, for a description of fundamental studies of this nature. Structural studies of ionomers remain the most common fundamental research topic even after over 30 years of intensive research which indicates the richness of the behavior exhibited by these systems and the capability of new experimental techniques to continue to provide deeper understanding.

The presence of ionic clustering in many ionomer materials including ethylene-methacrylate ionomers and perfluorinated sulfonic acid and carboxylic acid ionomers is well established.[41, 42] Detailed theoretical models for ionic clustering have been proposed to describe small angle X-ray and neutron scattering data, dynamic mechanical properties, and certain characteristics of ionic conductivity and electrochemical performance such as the hydroxyl ion exclusion properties of perfluorinated ionomer membranes used in the membrane chlor-alkali process.

Gierke *et al.*[1, 33] first proposed the cluster-network model for perfluorinated ionomers, which is still used to describe the fundamental relationship between ionomer cluster structure and electrochemical properties.[43] This model emphasizes the fact that the solvent swelling and ionic conductivity of these ionomers are dominated by the cluster network, while certain other characteristics such as anion exclusion and hydrodynamic permeability are dominated by intra-cluster transport processes.[34] These latter processes are presumed to involve transport inside of channels, possibly cylindrical in nature, that connect adjacent clusters. This model continues to be the basis for fundamental modeling efforts ranging from macroscopic pore models to molecular dynamics studies.[36, 37]

More recent microstructural models of perfluorinated ionomer membranes have been based on a three-phase model.[41, 44, 45] In this model, the ionomer consists of three regions, one being the hydrophobic fluorocarbon backbone region, the second being the hydrophilic ionic cluster region, and the third being an interfacial region with intermediate behavior. The hydrophobic fluorocarbon region is the location of any crystallinity in the polymer, while the hydrophilic region accommodates the majority of the absorbed solvent and is therefore critical to ionic and solvent transport characteristics.

It is not possible to review all previous structural studies on perfluorinated ionomers and several review articles are available to bring the reader up to date on previous work. The sections to follow will highlight selected topics of a more recent nature in the field and provide references for deeper study.

4.2 Scattering studies — SAXS and SANS

Small-angle X-ray scattering (SAXS) studies were one of the first means to conclusively identify ion clustering in ionomer systems and remains an important experimental technique for probing ion cluster structure. Often these studies are complemented with other techniques including small-angle neutron scattering (SANS) and mechanical or thermal analyses. Early SAXS studies of perfluorinated ionomer membranes demonstrated the presence of two scattering maxima at low angles, one related to crystallites in the polymer and the other to the presence of ion clusters.[46] These and later studies have led to a conclusion among researchers on the existence of ion clusters in perfluorinated ionomers and general agreement on their size and behavior under various conditions. More recent SAXS studies of the Nafion® membrane focused on the changes in morphology brought about by swelling with water/methanol mixtures.[47]

A recent structural model is the multiplet cluster model for random ionomers proposed based on dynamic mechanical and X-ray scattering studies by Eisenberg and co-workers.[45] This model postulates the existence of multiplets of associated fixed ion sites that are accompanied by regions of reduced mobility. If these multiplets grow larger by addition of more ion sites, they can become what are traditionally referred to as ion clusters. These multiplets are postulated to raise the T_g of the polymer but are not large enough to exhibit their own T_g as is the case for ion clusters. While this model can be considered a three-phase model, its importance is its ability to rectify data from diverse techniques including structural, thermal, and mechanical properties of ionomers.

A number of recent structural studies using SANS and SAXS address new questions around the structure of ionomer solutions, suspensions, and gels. An efficient method for dissolving high EW perfluorinated ionomer membranes was first developed in the early 1980s.[48, 49] A standard method involves dissolution at 250 °C under pressure in a 50/50 mixture of water and an aliphatic alcohol such as ethanol which affords a clear, homogeneous appearing solution. The commercial availability of these solutions led to their usage in a variety of applications, the most important being recast films for coatings on electrode surfaces and production of ultra-thin ionomer membranes and catalyst-loaded ionomer layers that have good adherence to the membrane surface. The structure of these ionomers in solution and their properties have tremendous practical importance on the performance and morphology of the films and composite structures. While we refer to these as solutions, they are in fact colloidal dispersions of partially associated ionomer particles and ionomer chains in a pseudo-equilibrium that depends on the solvents present and the thermal history of the solution. These colloidal particles can be cast into films referred to as recast films due to the fact that they are often produced via dissolution of extruded membranes.

Early studies of Nafion® solutions using scattering techniques concluded that the ionomer chains form rod like colloidal particles.[50, 51] A more recent study by Loppinet and co-workers used both SANS and SAXS techniques to study the structure of ionomer solutions in various solvents. These authors used several techniques to determine the radius of the rod like particles and obtained values in the 2.0–2.5 nm range. This radius was found to be independent of the solvent for low interfacial energy solvents.[52]

Moore *et al.* examined the structure of Dow's short-side chain perfluorosulfonate ionomers having various EWs including 635, 803, 909, 1076, and 1269 g eq^{-1}. Wide angle X-ray diffraction (XRD), SAXS, and differential scanning calorimetry (DSC) data as well as water uptake were examined as a function of the EW. The 635 EW ionomer had the highest water uptake and no sign of crystallinity. Dissolution of the Dow ionomers was studied in DMSO and 1-propanol/water mixtures. Melting temperatures varied only slightly with EW leading to the conclusion that these are block-type copolymers rather than random copolymers.[53]

A further study by Gebel and Moore gathered SANS and SAXS data on the Dow short-side chain perfluorosulfonate ionomer over the same wide EW range. Scattering data taken from the very low EW membrane were fit using a model of a connected rod like network with a 1.5 nm rod radius. Higher EW membrane structures were dominated by interfacial phenomena using a local order model with radii from 1.5 to 2.5 nm and interdomain distances roughly constant at 4.0 nm.[54]

The nature of the recast films formed from Nafion® solutions has been studied by several authors including Gebel *et al.*[54] Recast films are weaker than extruded membranes and more readily dissolved into organic solvents unless heat-treated under specific conditions. Li^+ and Na^+ form solutions were shown to give the best quality films while K^+, tetrabutylammonium (TBA^+), or divalent cations lead to films that crack more easily upon drying. SAXS data show that heating at elevated temperature causes an increase in the crystallinity of the recast film, explaining its changes in mechanical and solvent properties. These authors attributed the temperature effect to an annealing process leading to an increase in size of initially small lamellar crystals and formation of long-range order, with the added high-boiling solvents such as DMSO acting as plasticizers to facilitate these processes.[55]

To alleviate some of the challenges of the recast films, Moore *et al.* studied the conversion of these films into a new film that they referred to as solution-processed Nafion® films.[56] A study of the morphology of the solution-processed Nafion® films found that they are very similar to as-received (extruded) membranes. In contrast, recast Nafion® films have poor mechanical properties and high solubility in organic solvents. Higher disorder and lack of crystallinity and higher water content and ionic conductivity are due to the morphological differences. Critical issues include obtaining strong mechanically-pliant films in both wet and dry form with low dissolution in water/alcohol solutions. A patent to Grot describes the use of DMSO, Tetraethyl pyrophosphate (TEP), or 2-ethoxyethanol as an additive while evaporating to dryness at 125 °C to improve the mechanical properties of the solution-cast film.[57] A variety of solvents can be used to create solvent-cast films including alcohols, amides, dimethyl sulfoxide, and glycols.

No evidence for crystallinity is seen in recast films, which explains some of their properties. Casting the films at higher temperature from solvents such as DMSO can give crystalline films; heat treatments to recast films can also give crystalline films. Heat treatment to 200 °C is optimal for making films that are mechanically robust and solvent resistant, although some difference is seen between different solvents and cationic forms of the ionomer solution.[55] Recast films do show the same SAXS peak as the as-received ionomer membranes which is indicative of ionic clustering, suggesting that ionic domains are present in the recast films. The presence of ionic clustering in the absence of crystallite formation has been explained on the basis of the increased mobility of side chains relative to the backbone. However, the T_g for the ionic clusters is 30 °C lower than that in the as-received membrane indicating that the clusters have a different morphology, possibly accommodating a smaller fraction of the ion groups in the polymer.[56]

The superacidic nature of Nafion® membranes makes the use of some organic solvents with the H^+-form ionomer difficult at elevated temperatures creating a challenge for researchers seeking to create solutions and cast films from organic solvents. For example, it has been reported that the presence of triethyl phosphate or propylene carbonate in the film if heated to over 80 °C causes a blackening of the film due to the decomposition of the organic solvent. These discolorations can generally be removed by vigorous treatment with nitric acid.[55]

A recent study of note by Ludvigsson and co-workers employed Nafion® solution cast films 1 micrometer thick cast onto single crystal silicon wafers.[58] Irradiation of the films with xenon ions in vacuum caused growth of large, pronounced crystallites 0.5–10 mm in size. FTIR spectra showed that the proton is localized on the fluorosulfonate group in the crystalline regions of these films. XRD spectra showed that the crystalline regions have spherulitic morphology consisting of lamellar crystalline plates of folded polymer chains. Full crystallization did not occur in dried films stored for extended periods of time without the xenon ion irradiation. Exposure to water caused the crystallites to disappear immediately.

4.3 High resolution microscopy — TEM and AFM

Studies of ionic cluster formation and its dependence on ionomer composition and environment have generally been based on scattering data where the presence and structure of clusters is inferred by fitting the data to simple models.[41] Direct experimental visualization of the clusters using, for example, dye-staining transmission electron spectroscopy (TEM) is challenged by the poor image contrast in perfluorinated ionomers and the need to create extremely thin membrane samples.[59] In addition, the inherent flexibility of the polymer opens up the possibility of changes in polymer microstructure caused by the experimental methodology. Finally, the electron microscopy techniques cannot follow changes in the ionomer structure in situ such as those caused by changes in environmental conditions.

Nonetheless, many TEM studies have been performed and have generally found evidence of small 3–10 nm ionic clusters approximately spherical in shape.[60–63] An early TEM study of Nafion® membranes by Ceynowa employed ultra-thin sections of Nafion® 125 membrane, a 1200 EW membrane.[60] The process of preparing the samples for TEM consisted of conversion to the Pb^{2+} form using 1.0 M $Pb(NO_3)_2$ for 60 h and careful washing of the films, dehydration using ethanol solutions, rehydrating in 1,2-epoxypropane and embedding into epoxy resin. Ultrathin sections were cut to 60–80 nm size. The final film was shown to consist of very small and homogeneously distributed black spots 3–6 nm size which were attributed to the ion clusters.

An early study by Handlin and co-workers on TEM of ionomers described the challenges with this experimental approach.[59] These authors examined solvent cast and microtomed thin films of four different ionomers using TEM. Solvent casting produced artifacts and no useful information on ion clustering due to the difficulty in achieving true ionomer solutions and the effects of drying and phase separation on film structure. Specific issues for consideration in electron microscopy experiments include geometry effects (2D image of 3D structure) and radiation damage of organic molecules caused by the electron beam. Staining of clusters with osmium tetraoxide led to ionic domains of 2–3 nm in size in an ethylene propylene diene monomer (EPDM)-based ionomer. These experiments required very thin sections to visualize the clusters accurately.

Xue *et al.* carried out a TEM study of both solution cast and stained N117 membranes.[63] Staining was done using the common process of exposing the system to RuO_4 vapor which reacts with water to form RuO_2 microparticles. Images showed nearly spherical black spots uniformly distributed across the film with diameters of 2.5–5.0 nm, similar to those found with SAXS analyses. Grey areas around the black spots were visible and attributed to the interfacial region proposed in three-phase structural models. The remainder of the membrane was white and assigned to the semi-crystalline PTFE-like region of the polymer.

Porat and co-workers carried out a TEM study of very thin recast Nafion® solution-coated films cast from ethanol/water mixtures.[64] Zero-loss bright field images were obtained as well as specific sulfur imaging and Dage silicon intensified target (SIT) low-light images with minimum specimen damage. Single crystals with an average distance of several micrometers were seen scattered randomly across the film. An orthorhombic crystal structure similar to polyethylene was found. The results suggest that the fluorocarbon backbone is in the form of linear zigzag chains as in polyethylene and not in twisted chain as in PTFE. Sulfonate groups were seen in a nonrandom distribution primarily in clusters of 5 nm size based on the sulfur imaging. A recent dye-stained TEM study of a heavily sulfonated styrene-ethylene-butylene-styrene triblock polymer exhibited lamellar shaped ionic regions consistent with the phase-separated structure of the base polymer.[65] This result demonstrated that spherical cluster shapes do not result from all TEM studies, but rather other morphologies such as lamellar ones are possible.

A number of fascinating and important issues related to ionomer membrane surface structure still exist. One pervasive and unexplained phenomenon is the difference in water uptake for perfluorinated ionomer membranes exposed to liquid water versus saturated water vapor under otherwise identical conditions. The presence of this difference has been referred to as Schroeder's paradox and continues to receive study due to the uncertainty in its resolution.[66, 67] Recent theories to explain this experimental finding postulate different regions in the membrane or different mechanisms for water uptake from the two environments. Another possible explanation which has support based on contact angle measurements involves changes in the surface morphology of the membrane exposed to the different environments.[68] Atomic force microscopy (AFM) can have the resolution required to elucidate polymer microstructural features at the nanometer scale. In the ionomer field, AFM has been applied to both the examination of surface textural features as well as the direct examination of ionic clustering.[69]

Lehmani and co-workers carried out an early AFM study of N117 membranes with the purpose of achieving the necessary resolution for imaging ion clusters.[70] However, these authors concluded that they could not achieve the necessary resolution to see ion clusters with transmission mode AFM. James and coworkers carried out tapping mode (TM) AFM studies of Nafion® membranes such as N115-H^+.[71] Typical image sizes were 1 × 1 μm. An environmental chamber was used to control the humidity of membrane samples during the TM AFM experiments. TM phase imaging was used to identify hydrophobic and hydrophilic regions of the membrane. Clusters with a range of sizes from 5–30 nm were visible, larger than the 4–6 nm typical of XRD studies, which the authors attributed to formation and visualization of cluster aggregates. The number of clusters decreased while the size of clusters increased with increasing humidity during the experiments as one would expect.

In a further study by this same research group, TM AFM was complemented with shear force microscopy to examine the cause of phase contrast in images of both Cs^+ and H^+ form Nafion® membranes.[72] The measured phase contrast was much greater (60° rather than 10°)

for Cs^+-form N115 whereas there was no significant difference in the topographic images. The higher water content of the H^+-form ionomer coupled with the larger charge density of the Cs^+ ion was speculated to be the cause of the higher phase contrast difference. The authors demonstrated that the differences in probe-sample adhesion caused by an inhomogeneous distribution of surface water were important phase contrast mechanisms.

McLean *et al.* showed that it is possible to image ionic clusters in a number of different ionomer systems, and also provide additional morphological information not available from any other real-space technique.[73] They used TM AFM to characterize the fluorine-rich crystal aggregates within perfluorinated ionomers in addition to determining the relative morphological positions of the ionic species and domains. Images of non-ionic polymers including the Nafion® precursor polymer in its sulfonyl fluoride form served as controls to assign various phases. McLean *et al.* demonstrated that TM AFM in phase-contrast mode can be used to characterize the positions in space of both ionic domains and crystalline lamellae or lamellar stacks in Nafion® membranes. Three different AFM phase imaging methods were utilized to examine different depths into the ionomer and different structural features. Normal tapping under moderate forces can resolve stiffness differences from the top surface down to about 5–10 nm into the bulk polymer. Low oscillation amplitude tapping resolves ionic domains down to about 5 nm below the surface and only provides contrast for ion-containing systems. The third technique of very light tapping is sensitive to hydrophobicity differences in the near surface region from 0.2 to 1.0 nm within the polymer and does not require ionic species for its contrast mechanism.

Low oscillation amplitude tapping of Nafion® membranes generated remarkable images of ion clusters and their dependence on various conditions such as humidity. Figure 2 illustrates the low-energy phase images of N117-K^+ after exposure to room temperature humidity (a) versus deionized water exposure (b). Images of non-ionic sulfonyl fluoride form ionomer under identical conditions produced no contrast in these experiments. The white regions in the images are the ionic domains which exhibit a high degree of uniformity in spacing with an approximate size of 4–10 nm in diameter for sample (a). Images taken of ionomers of varying EW show a relationship between the quantity of white region and the EW, although higher EW ionomers tend to appear less homogeneous in their distribution of ionic rich regions. The swollen images (b) present clumps of ionic regions that have increased to 7–15 nm in size in the narrow dimension while appearing to have coalesced into channel-like shapes. The authors speculated that the technique provides direct images of ion clusters in their aggregated form which when swollen with water are constrained by crystalline regions into the channel-like morphology.

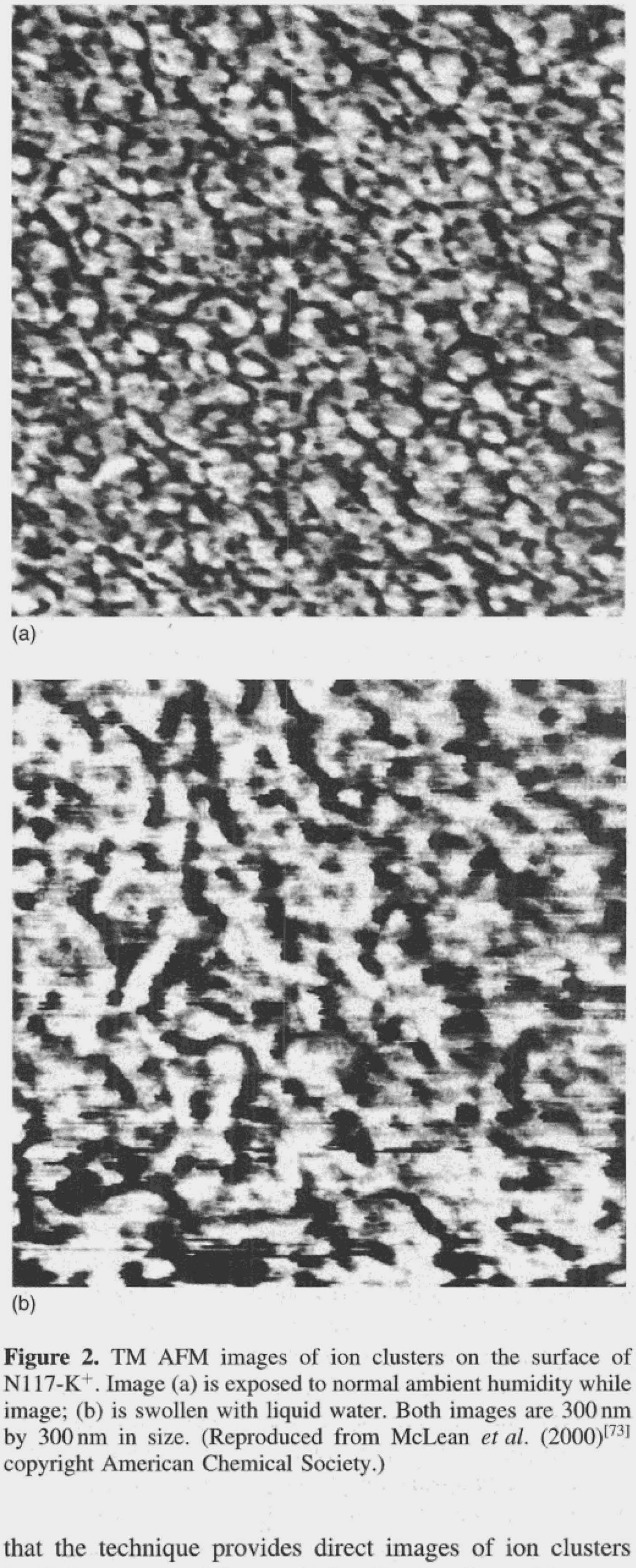

Figure 2. TM AFM images of ion clusters on the surface of N117-K^+. Image (a) is exposed to normal ambient humidity while image; (b) is swollen with liquid water. Both images are 300 nm by 300 nm in size. (Reproduced from McLean *et al.* (2000)[73] copyright American Chemical Society.)

McLean *et al.* also examined the near surface region of Nafion® membranes using very light TM.[73] The surface of Nafion® membranes exposed to a vapor-phase environment consists of a thin fluorine-rich skin region with low surface energy that is estimated to be about 1 nm thick. Based on the results using different AFM techniques, the authors concluded that this region contains essentially no ionic species when exposed to vapor-phase water but rearranges rapidly when exposed to liquid water to allow diffusion of ionic groups to the surface. The rearrangement time for this process is very fast due to the high concentration of ion groups as well as their relatively high mobility within the fluorocarbon matrix. This process is contrasted to the rearrangement process in poly(ethylene-co-methacrylic acid) ionomers neutralized with Zn metal ions where the ionic species take substantially longer to migrate to the surface. Rearrangement times of hours, compared to seconds for Nafion® membranes, are typical for these ionomers.[73]

4.4 EW measurement

The well-known challenges of creating true ionomer solutions with fully dissolved and extended polymer chains cause difficulty in molecular weight measurements on ionomers. EW, on the other hand, a measure of the ionic concentration within the ionomer, is readily determined using a number of different techniques. As many key properties of ionomers such as ionic conductivity, water uptake, and degree of swelling depend directly on EW, it is an important physical property for correlating data on ionomers of all types.

The EW of a Nafion® membrane can be expressed using equation (1) where n is the number of TFE groups on average per PSEPVE monomer.

$$\mathrm{EW}(\mathrm{g\,eq}^{-1}) = 100 \times n + 446 \tag{1}$$

Copolymers of TFE and PSEPVE having a wide variety of EW have been synthesized and studied. EW values as low as 700 are readily achievable in standard polymerization processes. The PSEPVE homopolymer is difficult to synthesize due to the sluggish self-polymerization of PSEPVE thus limiting the low end of EW (446 is the theoretical low-end value for the PSEPVE homopolymer). Very high EW copolymers can be synthesized although control over EW becomes increasingly challenging. Copolymers with EW greater than approximately $1500\,\mathrm{g\,eq}^{-1}$ have sufficiently dilute ionic groups to afford too low an ionic conductivity for practical application.

EW is conveniently measured by either FTIR techniques, measurements of atomic sulfur content, or by acid–base titration. FTIR is generally believed to be more accurate. FTIR techniques for EW measurement are described in the literature.[28] Acid capacity measurements using titration are another route to calculate ionomer EW as described within Nafion® membrane products technical literature. Atomic sulfur content measurements provide another check on EW and can be employed in precursor sulfonyl fluoride form unlike the titration methods.

4.5 Electroactive and luminescent probe studies

One means for studying the various internal structures and environments within ionomer films is through the electrochemical and photochemical studies of electroactive and luminescent probe molecules incorporated into the polymer film. Fluorescent probe studies of the environment within Nafion® membranes have become more common in recent years due to the wealth of information possible if the probe molecules are selected properly or designed for the desired properties.

A number of studies have been done on the incorporation of $\mathrm{Ru(bpy)_3}$ into Nafion® membranes due to its well understood luminescent properties. Researchers have shown that $\mathrm{Ru(bpy)_3}$luminescence is enhanced within the Nafion® membrane indicating that the probe molecules reside within the interfacial region of the ionomer. Anson *et al.* studied the incorporation of $\mathrm{Ru(bpy)_2dppz^{2+}}$ into Nafion® films as this probe molecule is strongly quenched in aqueous solutions allowing for direct measurement of the luminescence dynamics during the probe molecule uptake into the membrane.[74]

Robertson *et al.* performed another fluorescent probe study where probe molecules pyrene and $\mathrm{Ru(bpy)_3}$ were used to determine the location of various ions within the ionomer structure.[75] These fluorescent probes reside mainly within the interfacial region separating the hydrophobic and hydrophilic regions of the ionomer. The quenching of the fluorescent probes by $\mathrm{Cs^+}$ and $\mathrm{I^-}$ was studied and used to infer the locations and mobilities of these ions within the polymer. $\mathrm{Cs^+}$ was located within the aqueous hydrophilic region, whereas $\mathrm{I^-}$ was found to reside deeper into the interfacial region and farther away from the hydrophilic region. The location of these ions within carboxylate ionomers was compared to the results for sulfonate ionomers and used to explain the differences in selectivity for these types of polymers.

Incorporation of electroactive probe molecules into ionomer films represents another rich area of study for potential applications in areas such as electrochromic devices and electrocatalysis. For example, Komura *et al.*, investigated the partitioning and charge-transport behavior of viologens within Nafion® solution-cast films.[76] Increasing quantities of the 1,1′-dibenzyl-4,4′-bipyridinium (BV^{2+}) cation could be incorporated into Nafion® films with the effect of partially dehydrating the polymer and reducing the mobility of the BV^{2+} cation within the film and hence its charge-transfer rate.

4.6 Thermal studies — DSC and TGA

The thermal properties and behavior of Nafion® membranes have been studied extensively due to their practical importance in the performance of membranes in processes operating at elevated temperatures. Thermal characterization of ionomers also provides fundamental information on polymer structure and properties. Starkweather carried out an early study of the thermal properties of Nafion® ionomers having EWs ranging from 1050 to 1790.[77] This study reported melting temperature and heat of fusion data for both SO_2F and SO_3H polymers. These data are reproduced in Table 4. The heat of fusion was a linear function of EW and extrapolated to zero at an EW of 910 g eq^{-1} which corresponds to a TFE/PSEPVE ratio of about five. This suggests that some crystallinity remains in the copolymer to very high comonomer contents. An XRD study of the sulfonyl fluoride precursor suggested that the unit cell is hexagonal as in the PTFE homopolymer with crystal dimensions of 3.0–4.0 nm. XRD data are claimed to support Gierke's bilayer model for the Nafion® membrane backbone and side chain organization wherein ionic domains having 4.0 nm diameter are separated by 1.0 nm thick fluorocarbon wall regions.

Glass transition temperatures for various Nafion® membranes were reported by Yeo and Eisenberg.[78] They found that the T_g was lowest for the unhydrolyzed polymer, at about 0 °C, increased to 103 °C for the acid-form ionomer, and increased further into the 210–240 °C range for alkali-metal-cation-exchanged ionomers. Higher T_g values are a result of ionic crosslinking within the structure which is clearly more efficient at reducing chain mobility for certain cations. Further studies of T_g for Nafion® membranes as a function of polymer EW and membrane humidity could not be found in the literature at this time.

Table 4. Thermal data from DSC for Nafion® membranes having a range of EW values.

EW (g eq^{-1})	T_m (°C) peak/end	ΔH_f (cal g^{-1})
SO_2F-form polymers		
1050	236/254	1.16
1100	231/257	1.48
1350	251/278	3.34
1500	256/283	4.13
1790	266/286	6.92
SO_3H-form polymers		
1100	207/235	1.06
1350	231/253	1.68
1500	249/265	4.98

A recent study of the thermal behavior of Nafion® membranes reported an analysis of the thermogravimetric and DSC behavior of membranes having different ionic forms.[79] The thermal behavior of N117 membranes in H^+, Na^+, K^+, Rb^+, and Cs^+ forms were studied using both thermogravimetric analysis TGA and DSC measurements. Fluoropolymers exhibit very good thermal stability although incorporation of ions into the structure reduces stability. Thermal treatment of H^+-form membranes caused them to become dark above 120 °C and increasingly darken to 300 °C. Na^+-form films showed no darkening up to 300 °C. Gradual mass loss on heating to 290 °C was attributed to the loss of water.

First stage mass loss between 290 and 400 °C is due to desulfonation while the second stage from 400 to 470 °C is related to side-chain decomposition and the third stage from 470 to 560 °C to PTFE backbone decomposition.[79] The Na^+-form ionomer exhibits higher thermal stability with an onset of thermal decomposition about 150 °C higher than the acid-form ionomer. The formation of the Na^+-SO_3^- ion pair stabilizes the C–S bond since SO_2 production is not seen during degradation of the salt form of N117. This study did not measure gases found in decomposition but did quote results from earlier studies that made these measurements.[79] Mass loss products in the first stage are H_2O, SO_2, and CO_2 while the later stages contain HF, SiF_4 and COF_2. SiF_4 is presumably from exposure of HF-containing gases to glassware used in these experiments.

DSC data show one strong endothermic peak T_1 at 115 °C and a weak and broad endothermic peak near 230 °C for both the acid and salt forms. Thermal events over 250 °C are likely related to decomposition reactions. The broad peak near 230 °C is attributed to melting of the crystalline regions occurring at lower temperatures than it would for the PTFE homopolymer. The lower temperature T_1 peak is attributed to the ionic clusters, possibly related to an order–disorder transition within the clusters. The T_1 temperature depended on the cationic form of the polymer with other cations having higher T_1 values except for Cs^+. Other authors have attributed T_1 to the glass transition temperature of the polymer.[79]

Thermal property data necessary for modeling thermal conduction within Nafion® membrane-containing systems are more difficult to find in the open literature. We have found no citations for heat capacity of Nafion® membranes.

Maggio *et al.* utilizes an effective thermal conductivity for the Nafion® membrane of $0.21\,\mathrm{W\,m^{-1}\,K^{-1}}$.[80] One would hope that these data would be measured and confirmed in the future as the use of Nafion® membranes in large fuel cell stacks necessitates better understanding and control of temperature distributions and local heating within the stacks.

4.7 Mechanical studies and properties — melt flow, dynamic mechanical analyzer (DMA), and QCM

Research on mechanical properties of perfluorinated ionomers are often coupled with other techniques, including thermal and scattering studies to learn more about ionomer structure than can be derived from the individual techniques. Mechanical properties become important for robust operation of membrane-containing systems and devices as the membrane will often be the most fragile component in a large cell stack containing metallic or graphite-based bipolar plates and carbon cloth or paper gas-diffusion electrodes. The Nafion® membrane technical literature quotes the values given in Table 5 for mechanical properties of 1100 EW membranes (e.g., NE112, NE1135, N115, and N117) based on American Society for Testing and Materials (ASTM) standard tests. Each property depends on the degree of humidification which must be properly controlled to obtain reproducible results. Tear resistances listed in the table depend on membrane thickness and values quoted are for NE112 membranes.

Table 5. Mechanical properties reported for Nafion® membranes within product technical literature. MD indicates machine direction and TD transverse direction.[87]

Physical property	Typical value	Test method
	Tensile modulus, (MPa)	
50% RH, 23 °C	249	ASTM D 882
Water soaked, 23 °C	114	ASTM D 882
Water soaked, 100 °C	64	ASTM D 882
	Tensile strength, maximum, (MPa)	
50% RH, 23 °C	43 in MD, 32 in TD	ASTM D 882
Water soaked, 23 °C	34 in MD, 26 in TD	ASTM D 882
Water soaked, 100 °C	25 in MD, 24 in TD	ASTM D 882
	Elongation at break, %	
50% RH, 23 °C	225 in MD, 310 in TD	ASTM D 882
Water soaked, 23 °C	200 in MD, 275 in TD	ASTM D 882
Water soaked, 100 °C	180 in MD, 240 in TD	ASTM D 882
	Tear resistance – initial, ($\mathrm{g\,mm^{-1}}$)	
50% RH, 23 °C	6000 in MD, TD	ASTM D 1004
Water soaked, 23 °C	3500 in MD, TD	ASTM D 1004
Water soaked, 100 °C	3000 in MD, TD	ASTM D 1004
	Tear Resistance – propagating, ($\mathrm{g\,mm^{-1}}$)	
50% RH, 23 °C	>100 in MD, >150 in TD	ASTM D 1922
Water soaked, 23 °C	92 in MD, 104 in TD	ASTM D 1922
Water soaked, 100 °C	74 in MD, 85 in TD	ASTM D 1922

Miura *et al.* performed dynamic viscoelastic spectral and DSC measurements on N117 membranes in various cationic forms for the purpose of understanding the effect of water and alcohols on the molecular motion of the ionomer.[81] The Nafion® membrane showed five tan delta peaks in the dry state (α, β, β', γ' and γ). Absorption of water did not affect the transitions greatly, however, alcohol had a pronounced effect on the spectra. A further study by Miura *et al.* employed dynamic mechanical analysis, SAXS, and electron probe microanalysis to probe the structure of N117 membranes exchanged into different cation forms and swollen with ethanol.[82] The ethanol uptake was measured for N117 in the following cationic forms: Li^+, Na^+, K^+, $NH_4{}^+$, and several organic ammonium cations. The cluster diameter in ethanol-swollen membranes was calculated to be smaller than water-swollen clusters.

Moore and co-workers carried out an important study of the melt processability of the Nafion® membrane exchanged into the TBA cationic form.[83] Physical properties of perfluorinated ionomer membranes are dominated by the semi-crystalline fluorocarbon backbone and the ionic side chain aggregates. Semi-crystalline perfluorinated ionomers are insoluble in any solvent at temperatures below 200 °C. Once hydrolyzed into ionic form, perfluorinated ionomers are not melt processable and solution processing techniques are necessary to create novel structures such as thin coatings. Prior to hydrolysis, perfluorinated ionomers exhibit typical melt index values of 5–15 grams after 10 min at 270 °C based on Nafion® membrane technical product literature.

A procedure for carrying out melt processing of perfluorinated ionomers was developed by Moore *et al.*, based on ion exchange of an N117-H^+ membrane using a 1 M solution of TBAOH in methanol.[83] This ion-exchanged membrane is reduced to a solution using the standard processing in a water/methanol-1-propanol mixture at 250 °C under pressure. Melt processable polymer powder could be recovered from the solutions by stripping out the alcohol solvents using boiling deionized water and drying the resulting powder. The authors surmise that the large organic TBA^+ cations reduce aggregation forces by creating internal plasticization and reducing electrostatic crosslinking between ion pairs due to their diffuse charge density. Thus, TBA^+-exchanged ionomer has a much lower T_g relative to Na^+-form ionomer. These TBA^+-form ionomers can be readily converted back to acid form by treatment with nitric acid. The procedures developed by Moore *et al.* in this work have been employed by numerous researchers to create novel composite structures with Nafion® membranes.

The quartz crystal microbalance (QCM) was developed during the last decade for purposes of allowing highly sensitive measurements of weight loss and gain of films and surfaces. Shi *et al.* created coatings of Nafion® solution onto a gold-coated crystal of a quartz crystal microbalance and used these to study the cation exchange process in Nafion® solution-based recast films.[84] Exchange of protons with a variety of cations led to a loss of mass of the coating due to the accompanying loss of water. Only Li^+-cation exchange gave an increase in mass as would be expected from the relative water uptake of various cation-form Nafion® membranes. These microbalance measurements were used to determine the relative states of hydration of various cations within Nafion® membranes. As many as 50 water molecules per cation can be expulsed for large multivalent cations such as $Ru(NH_3)_6{}^{3+}$.

4.8 Other structural studies

Among the large selection of other studies that have been reported on the structure of Nafion® membranes and related systems in recent years, we choose to focus on only a handful here for their relevance to important issues in the operation and understanding of the PEMFC. For example, Zawodzinski *et al.* performed contact angle measurements on N115 and N117 membranes equilibrated with different water vapor activities.[68] The membrane surface was shown to be very hydrophobic, presenting a significant barrier to water. The advancing contact angles were much higher than the receding angles due to the changes in the surface structure that occur in the presence of liquid water. Advancing contact angles decrease somewhat with increasing membrane water content, moving from 116° for dry N117 down to 98° for N117 in a saturated water vapor. The changes in surface structure were explained by rearrangements in response to the dielectric constant of the medium.

The study by Zawodzinski *et al.* is important as it relates to the processes of surface rearrangement that occur when Nafion® membranes are exposed to different media, i.e., liquid water or water-vapor environments. Surface rearrangements in Nafion® membranes were studied using AFM by McLean *et al.* and shown to occur very rapidly compared to similar processes for other ionomers.[73] The rearrangement process is believed to involve motion of the ionic side chains towards and away from the membrane surface which is typically composed of a thin fluorocarbon-like skin in the presence of humid air. This process has implications for water mass transport and proton conductivity at ionomer surfaces under different operating conditions.

Another recent study taking a novel approach to the characterization of the structure of Nafion® membranes was reported by Divisek *et al.*[85] The pore size distributions of Nafion® 112, 115, and 117 membranes were measured using mercury porosimetry. A wide spectrum of pore sizes were found with the average value at 2 nm and a range from 100 to 1 nm. Elevating the temperature to 80 °C did not lead to any qualitative changes in the pore structure.

The state of water within the Nafion® membrane has been studied recently using FTIR techniques on a very thin (approximately 1 μm) solution-cast film.[86] The authors designed an FTIR system allowing equilibration of the film sample with a known water activity and temperature to monitor the FTIR spectra as a function of water content within the ionomer. The study concluded that proton transfer from the sulfonic acid to water to form the H_3O^+ cation had occurred already even under very dry conditions with a single water molecule per sulfonate site.

5 THERMODYNAMIC PROPERTIES

5.1 Water uptake and swelling data

The swelling behavior of perfluorinated ionomeric membranes has been a frequent topic of study over the years due to its relationship to membrane properties such as ionic conductivity and selectivity. Membrane swelling results from a complex interplay between the affinity of the polymer and ionic sites for polar solvents and the resistance of the membrane's structure and crystallinity to volumetric expansion. The previous history and pretreatment of these polymers has a marked impact on their swelling and solubility properties largely due to the disruption or development of membrane crystallinity.

The uptake of water into Nafion® membranes having various EWs is given in Table 6 based on data reported

Table 6. Data on water uptake and ionic conductivity for various EW commercial and experimental Nafion® membranes. These data have been taken for membranes immersed into liquid water under ambient conditions.[87]

EW (g eq^{-1})	Water uptake (wt%)	Effective ionic concentration (M)	Ionic conductivity at 23 °C (S cm^{-1})
1500	13.3	1.245	0.0123
1350	19.4	1.338	0.0253
1200	21.0	1.492	0.0636
1100	25.0	1.591	0.0902
980	27.1	1.764	0.1193
834	53.1	1.761	0.1152
785	79.1	1.539	0.0791

recently.[87] Standard pretreatments consisting of hydrolysis, acid exchange, and rinsing and boiling in deionized water were followed with all membranes. Membrane samples are blotted dry prior to the measurements to remove surface moisture. The water uptake is expressed in terms of weight percent calculated based on the weight of the wet sample

$$\text{Weight }\% = \frac{(\mathrm{w_{final}} - \mathrm{w_{init}})}{\mathrm{w_{final}}} \tag{2}$$

As ionomer samples with EWs much higher or lower than the commercial 1100 EW membrane are experimental samples, the variability of the swelling data are greater and are not expected to be as accurate. The effective ionic concentration in Table 6 is calculated by dividing the membrane's wet density by the EW. This parameter correlates most closely with ionic conductivity, demonstrating that the decrease in ionic conductivity at low EW values results from excessive swelling of the membrane leading to a dilution in the ionic concentration.

Buchi and Scherer performed a recent study of the behavior of various Nafion® membranes in situ within an operating fuel cell.[88] While their focus was the in situ ionic conductivity and water content, they also reported measurements of the swollen thickness and water uptake of commercial Nafion® membranes. The final states of the various membranes are described in Table 7. The relationship between water content in terms of number of water molecules per sulfonic acid site and weight percent used to calculate water weight percent data in Table 7 is illustrated by equation (3).

$$\lambda = \frac{(\omega \times \mathrm{EW})}{M_o} \tag{3}$$

Table 7. Swollen water content and thickness of various commercial Nafion® membranes from Buchi and Scherer.[88]

Nafion® membrane	Water content λ (# H_2O/SO_3H)	Water content (wt%)	Wet thickness (μm)
N112	21–22	24–26	58–62
N115	21–22	24–26	145–150
N117	21–22	24–26	200–205
N105	27–28	32–33	160–165

where M_o is the molecular weight of water (18 g mol^{-1}) and ω is the solvent uptake in weight percent based on the weight of dry polymer. We use the common convention of referring to the water content of the membrane expressed in terms of number of water molecules per sulfonic acid site by the parameter λ.

5.2 Water activity in vapor environments and membrane drying

While solvent uptake data are useful for predicting membrane swelling and internal solvent concentrations, these data are often taken under conditions of unit solvent activity, a condition that does not generally exist in an operating PEMFC. For understanding the properties of ionomers under operating conditions and for fundamental studies of the nature of absorbed water, a preferred experimental approach is to expose membrane samples to external environments having controlled solvent activity. This condition can be achieved by exposure to salt solutions of known vapor activity followed by measurements of the solvent uptake by the ionomer.

Zawodzinski *et al.* originally measured a complete set of water activity data on acid-form N117 membranes at a temperature of 30 °C and attempted to interpret the data in terms of interactions between the water molecules and ionic side chains.[89] Membrane samples were exposed to LiCl solutions of known water activity to absorb controlled quantities of water. This technique can attain water activities ranging from 0.15 to 1.0 at room temperature. Equilibrium was reached within 4 days in these experiments. Complete drying of the membrane samples was accomplished by exposure to P_2O_5 for several days at room temperature. Based on the water absorption data as a function of the known water activity in the LiCl solutions, an isopiestic sorption curve could be calculated for N117-H$^+$ at $T = 30\,°\mathrm{C}$. These data are reproduced here in Figure 3 and also in the equations given below.

$$\lambda = 0.043 + 17.81a_0 - 39.85a_0^2 + 36.0a_0^3 \text{ for } 0 < a_0 < 1 \tag{4}$$

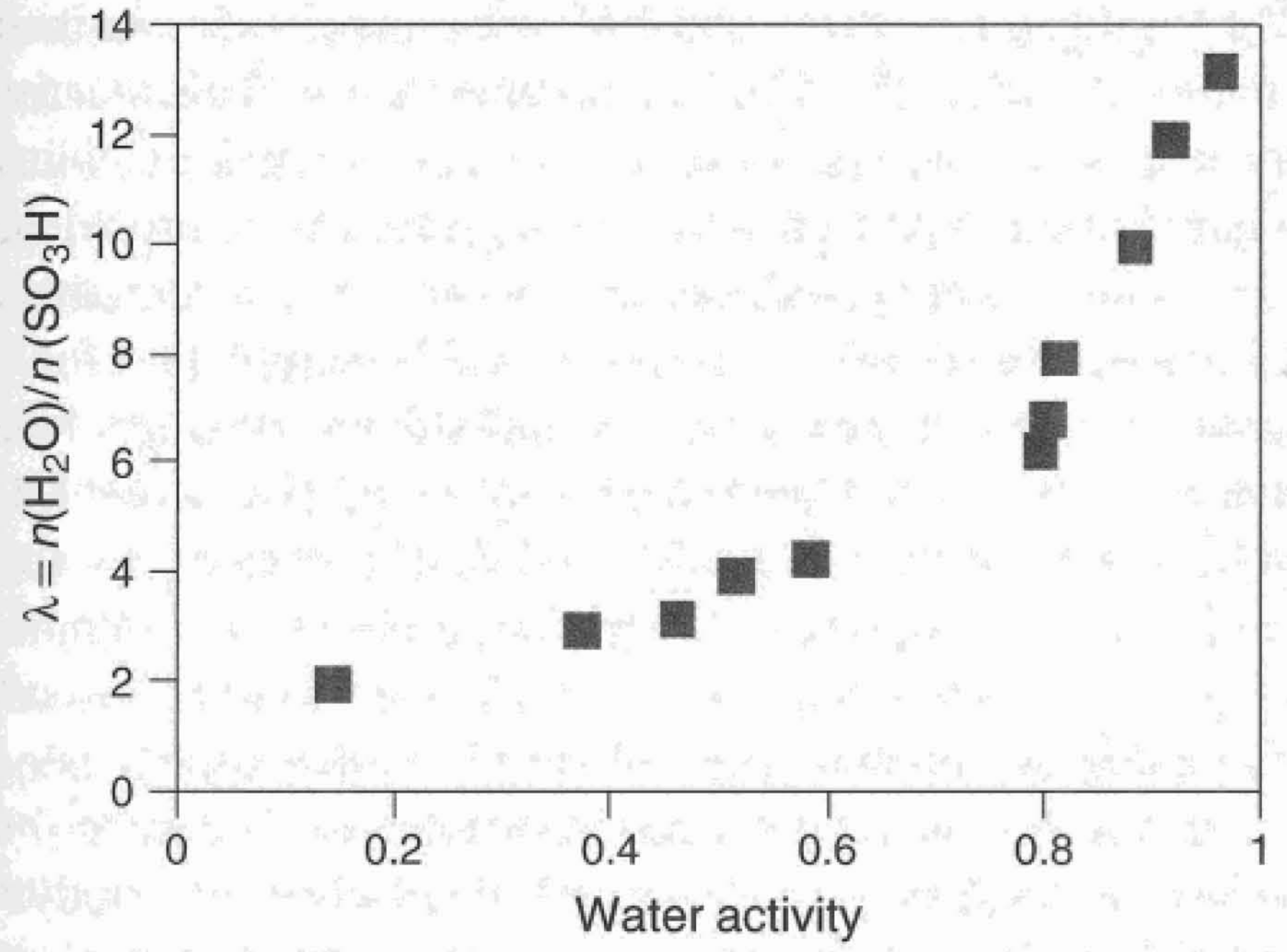

Figure 3. Isopiestic sorption curve giving water uptake as a function of water activity measured for N117-H$^+$ at $T = 30\,°C$. (Reprinted with permission from Zawodzinski *et al.* (1991)[89] copyright American Chemical Society.)

or

$$a_0 = -0.0505 + 0.1853\lambda - 0.01049\lambda^2 + 1.712 \times 10^{-4}\lambda^3 \quad (5)$$

where $a_0 = p_0/p^*$ and p^* is the water vapor pressure (in units of bars).

These water uptake data indicate that this system exhibits a small change in water content over the water activity range of 0.15–0.75. Over activities of 0.75, water content changes rapidly from 6 to 14 water molecules per sulfonate site. These results are interpreted as being due to an initial strong interaction of the first water molecules with the sulfonic acid sites of the ionomer, followed by weaker interactions at greater than six water molecules per acid site. The initial water absorbed into the polymer is considered tightly bound whereas the later water is bulk-like in its properties.

These same authors further explored the isopiestic sorption curve for N117-H$^+$ in a later paper.[67] Comparisons between the water uptake from liquid water and 100% saturated water vapor indicate that the values achieved in the two cases are notably different, with 14 waters per sulfonate absorbed from the vapor phase and 22 from the liquid phase. This difference runs counter to expectations from thermodynamic considerations as the water activity in either case is equal. This phenomenon relates to Schroeder's paradox where a lower uptake of penetrants into polymers from saturated vapor phase compared with the liquid phase is observed for a number of polymer–solvent combinations.[66] These authors speculate that this result may be caused by the difficulty absorbing water from the vapor onto walls of hydrophobic pores within the membrane.

An extensive study of the uptake of water by perfluorinated ionomer membranes was reported by Hinatsu *et al.*[7] They examined a number of different commercial membranes including N117 and N125, Flemion® FL-12 and FL-4, and Aciplex® AC-12 and AC-4. Water sorption curves were measured for membranes with and without standard swelling and pretreatments. Water uptake from both liquid water and vapor were measured as functions of temperature. The results were similar to those of Zawodzinski *et al.*, in the general shape of the isopiestic sorption curve for all the membranes studied showing the generality of the phenomena. Water uptake increased with decreasing EW of the ionomer and increased with temperature for absorption from liquid water. Water uptake from the vapor phase decreased with temperature down to 10 waters per sulfonate site at 100% RH at 80 °C. Fitting expressions for the uptake data were given which may be useful in modeling studies.

The studies described earlier generated extensive vapor–liquid equilibrium data for perfluorinated ionomer membrane–water systems and focused on the interpretation of these data. For purposes of engineering working fuel cell systems, it is valuable to have thermodynamic models of the equilibrium behavior of the water-swollen Nafion® membrane as these can be used to predict phase equilibria under any conditions. Futerko and Hsing derived an equation to represent the water activity within N117-H$^+$ membranes as a function of water uptake and temperature based on a two-parameter Flory–Huggins model.[90] Chemical equilibrium of protons between the fixed acid sites and the absorbed water molecules was accounted for explicitly in the model. Another thermodynamic study of vapor–liquid equilibrium within the Nafion® membrane was performed by Huh and Bae.[91] These authors extended the Vapor–Liquid- and Solid–Liquid-Equilibria of Electrolyte Systems (LIQUAC) model to describe the Gibbs free energy of water/perfluorosulfonic acid ionomer systems.

The challenges of drying perfluorinated ionomer membranes completely are well documented. One water molecule generally resides with each ionic site in the polymer even upon sustained drying at moderate temperatures and under vacuum conditions. Recently the issue of the performance of tubular dryers based on Nafion® membranes with selective permeability was studied.[92] These systems operate by passing a carrier gas such as a wet organic through the center of one or more tubes surrounded by a continuous countercurrent-flowing dry purge gas. In order to understand and optimize the operation of these systems, the authors studied the fundamental water vapor equilibrium properties of Nafion® membranes in comparison to other drying agents. Measurements were performed to determine the water vapor pressure, written as PWN in equation (6) below, for Nafion® membranes as a function of temperature. For temperatures ranging from −20 to 50 °C, the data were well described by the expression given as equation (6)

$$\mathrm{PWN} = -\frac{3580}{T} + 10.01 \qquad (6)$$

where PWN is in Torr and T is in Kelvin. The water vapor pressure over essentially dry Nafion® membranes is three to four orders of magnitude lower than that of liquid water at any given temperature and the difference increases with decreasing temperature. From these data, the molar enthalpy of vaporization for water was $69\,\mathrm{kJ\,mol^{-1}}$ compared to about $41\,\mathrm{kJ\,mol^{-1}}$ for bulk water. Using previously reported values of the free energy of vaporization, the authors derived an entropy of vaporization of $120\,\mathrm{J\,K^{-1}\,mol^{-1}}$. These data may be used to predict the dryness of a given atmosphere required to remove water from very dry Nafion® membranes under conditions of atmospheric pressure at any temperature. Under practical operating conditions, Nafion® dryers achieve dew points of −61 °C in removal of water from a saturated carrier stream at 25 °C. Nafion® dryers operated under ambient conditions are slightly less effective than $CaSO_4$ and operate about as well as $Mg(ClO_4)_2$ and dry ice/acetone traps at 0 °C.

5.3 Swelling with organic and methanol-containing solvents

Yeo performed one of the earliest comprehensive swelling studies of 10 mil 1100 and 1200 EW Nafion® membranes in K^+-form in various solvents including water, amines, alcohols, glycol, glycerol, and formamide.[93] The resulting swelling data were modeled and explained using a solubility parameter analysis. Two regions of behavior were found, with the separation at solubility parameter values in the range of 12–15. The highest swelling was achieved with the higher alcohols and amide solvents. These early swelling studies are the benchmark for a number of more recent studies of the behavior of Nafion® membranes when exposed to organic solvents as this topic has become of greater commercial importance with the development of processes for creating Nafion® solutions through dissolution in organic solvent mixtures. In a later study utilizing Na^+-form Nafion® 110 and Nafion® 901 membranes, Yeo showed that solvent uptake depended on membrane pretreatment and on the solubility parameter of the solvent with the maximum swelling occurring for solubility parameters of around 10.[94]

Aldebert *et al.* studied the swelling and ionic conductivity behavior of the N117 membrane in organic solvents. They utilized Li^+, Na^+, and Rb^+ form membranes in their studies, avoiding H^+ form membranes due to their reactivity with some organic solvents. Solvents studied including ethanol, triethyl phosphate, n-methyl formamide, propylene carbonate, dimethoxyethane, and water.[95] A recent study of solvent swelling in Li^+-form N117 membranes for a large range of organic solvents and solvent mixtures was reported.[27] Room temperature solvent uptake as well as ionic conductivity were measured and correlated to solvent physical properties. A correlation based on a number of properties including solvent molecular weight, viscosity, and donor number was able to give a reasonably good prediction of the solvent-swollen membrane properties.

Several studies have confined themselves to analyzing the uptake of methanol or methanol/water mixtures by Nafion® membranes due to the relevance to direct methanol PEMFCs. Nandan and co-workers studied solvent uptake by N117-M^+ for water and methanol for a variety of cations.[96] The partitioning of water–methanol into the membranes was studied by exposure to 50 mol% methanol–water solution (64 wt% methanol) followed by analysis of the methanol content absorbed into the membrane. These authors found that from 6 to 20 wt% water is absorbed by N117 with the uptakes decreasing in the order of $H^+ > Li^+ > Mg^{2+} > Sr^{2+} > Ba^{2+} > Na^+ > K^+ > Rb^+$. In comparison, they found that from 6–40 wt% methanol is absorbed by N117 with the order in this case decreasing as $Li^+ > H^+ > Na^+ > Mg^{2+} > Ca^{2+} > Sr^{2+} > Ba^{2+} > K^+ > Rb^+$. Dry densities of N117 membranes in each cationic form varied from 1.896 (H^+ form) to $2.168\,\mathrm{g\,cm^{-3}}$ (Rb^+ form). Membrane thicknesses in the dry form for the cation-exchanged N117 films varied from 168–180 μm, showing less variation than the membrane dry densities. Fractionation experiments showed that water is selectively taken up by the membrane with K_w values of 1.5–2.1. Selective uptake for water was found by all cationic forms but was strongest for the Rb^+ and Mg^{2+} form membranes.[96]

Ren *et al.* studied the behavior of Nafion® membranes in methanol/water mixtures to better understand and model performance of direct methanol PEMFCs.[97] Nafion® membranes having two different EWs (1100 EW N117 and 1200 EW N120) were pretreated using standard conditions and dried over a large excess of P_2O_5 in sealed jars. The dry membrane density was reported to equal $2.075\,\mathrm{g\,cm^{-3}}$ for acid-form N117. Previous studies using nuclear magnetic resonance (NMR) had demonstrated that the composition within the membrane was essentially identical to the external solution concentration. This finding was used to calculate methanol and water contents when membranes were exposed to solutions varying from 0 to 10 M methanol in deionized water. Increasing methanol solution concentration appeared to increase the total uptake but did not impact the water content ($\lambda = 20-21$) within the membrane. Methanol contents reached the level of 5.6 molecules per sulfonic acid at 10 M methanol. Water and methanol uptake for the Nafion® 120 membrane were approximately 70–74% of the values for N117. Water contents may start to drop off at the higher methanol concentrations (>8.0 M) for the N120 membrane. In a later study, Ren and co-workers measured transport properties for N117-H^+ exposed to 1.0 M methanol solutions in operating direct methanol PEMFCs.[98]

A comprehensive study of the equilibrium uptake of methanol/water mixtures in N117-H^+ membranes over the temperature range of 298–333 K was reported recently by Geiger *et al.*[99] The work follows from and improves upon the experimental approach of Gates and Newman.[100] Careful procedures were employed to assure minimum loss of solvents during the measurements and accurate chemical analysis of the composition of the absorbed solution phase. A model of the Gibbs free energy was used to derive a modified Wohl expansion to fit the experimental data ensuring thermodynamic consistency. In general, the presence of methanol in the external solution increased the mass uptake by the Nafion® membrane with a maximum at a methanol mole fraction of about 0.65 in the external solution. Experiments at the higher methanol concentrations were affected by the formation and volatilization of dimethyl ether. No significant temperature dependence to the uptake data was found.

5.4 Ionic selectivity and chemical modification of ionomers

Anion crossover has been a topic of strong historical interest originating with the use of Nafion® membranes for the membrane chlor-alkali process and the need to reduce hydroxyl ion crossover to improve the economics of this process. While significant work was expended to study the selectivity of Nafion® membranes over various ionic species in the 1970s and 1980s, more recent studies have been less frequent as new issues and challenges have arisen. There continues to be the occasional study on the topic of anion exclusion from the standpoint of modeling the process or attempting to gather more complete data on the phenomenon.

A novel feature of ionomer membranes that has been used with advantage in selected cases is the ability to carry out chemistry either locally at the ionic (acid) sites or within the nano-sized pores of the membrane. This attribute of perfluorinated ionomer membranes was first utilized in the research towards better, more permselective chlor-alkali membranes. In recent years, imaginative concepts for utilizing this capability for improving PEMFC performance have been reported. An early example is seen in the work of Watanabe *et al.* who modified a Nafion® solution by combining it with TiO_2 or SiO_2 colloids having 5–7 nm particles by mixing 3 wt% of the additive together with the Nafion® solution, casting a film, and drying.[101] They also explored the incorporation of Pt particles at a loading density of 0.07 mg cm^{-2} into 2 mil thick Nafion® membranes by ion exchange and reduction with hydrazine. These Pt particles were shown to catalyze the oxidation of crossover H_2 with O_2 to create H_2O whereas the ceramic particles absorb and hold onto water more effectively. In either case, useful functions for the operating fuel cell are incorporated into membranes in a facile manner.

Surface modification is another route to achieving property changes in the ionomer membrane such as improvements in selectivity that take advantage of its capability to perform local chemical changes. For example, several groups have examined the use of plasma polymerization for modification of the Nafion® membrane. Early studies of plasma polymerization involved deposition of the 4-vinylpyridine monomer by Ogumi *et al.*[102, 103] This approach yielded a membrane with very high proton permselectivity but the membrane resistance increased to 12 Ω cm² which is unacceptable for application in fuel cells. Later, Yasuda *et al.* attempted further modifications of the membrane surface with plasma induced surface modification but did not find any appreciable improvement in membrane selectivity.[104, 105]

A more recent attempt at surface modification using a plasma polymerization process was reported by Zeng *et al.*[106] They deposited a 0.5 μm thick layer with anion exchange properties onto the surface of a N117 membrane. The process employed glow discharge plasma polymerization of ethylene and ammonia to deposit a polyethylene-like film with $-NH_2$ and $-CONH_2$ groups. Selectivity for protons over divalent and trivalent cations was improved by manipulating the ratio of ethylene to ammonia in the plasma. Importantly, the resistance of the membrane was only slightly higher with the polymerized surface layer and this layer was stable over several months.

Precipitation of inorganic compounds on the surface and within the Nafion® membrane has been known and studied for many years because of its relevance to stable long-term operation of chlor-alkali cells. The strong caustic environment at the cathode of these cells can lead to precipitation of compounds within the membrane near this surface, causing damage to membranes including microcracks and tears. Silica-containing species such as aluminum silicates have been studied in detail. Membrane impurity studies on a variety of di- and trivalent cationic species have been performed over the years by the chlor-alkali industry. These studies have led to firm limits down to part per million (PPM) and part per billion (PPB) levels for a number of species (Ni, Mg, Fe, Ca, Al, SiO_2, etc.) within the anolyte and catholyte solutions for the chlor-alkali industry. Some of these findings have general implications for the fuel cell industry also, such as the strong binding of multivalent cationic species within Nafion® membranes that must be avoided at all costs for stable long-term operation. Unfortunately, not all of these studies translate directly to useful information in the fuel cell environment and hence new studies will continue to be needed on these issues in realistic fuel cell operating conditions before lifetime issues for membranes are as well understand in this industry.

Many studies were performed in the early years of use of Nafion® membranes on their selectivity for various cationic species. For example, Yeager found an order of selectivity that goes as $Cs^+ > Rb^+ > Ba^{2+} > K^+ > Mg^{2+} > Na^+ > H^+ > Li^+$.[107] Similar sequences have been found by other studies. Pintauro and co-workers derived a partition coefficient model that can describe the equilibrium uptake of ionic species from a multicomponent external solution.[108] Theoretical results show that univalent cations with the highest surface charge density or smallest hard sphere radius are excluded from the membrane pore wall region in a manner similar to that observed for anions which explains the selectivity relationship between the univalent cations. Pintauro *et al.* continued to develop and expand upon this model with detailed comparisons with experimental partitioning data.[109]

6 THEORETICAL AND MODELING STUDIES

6.1 Macroscopic transport modeling in ionomer membranes

Macroscopic modeling of transport processes in ion-exchange membranes has been a topic of study for several decades. Helfferich's textbook "Ion Exchange", first published in Germany in 1959, remains a classic work on this topic although it predates the Nafion® membrane and fuel cell applications of ionomer membranes.[110] The challenges of modeling transport in multicomponent electrolyte solutions are well understood.[111] As the number of species increases, the number of transport properties required to describe the system also rises and quickly reaches the point where exhaustive measurements of all of the necessary transport properties and their dependence on thermodynamic variables (T, p, c_i) becomes untenable. For the simplest case of the acid-form Nafion® membrane in an aqueous environment, the situation is tractable as three species (protons, water, and membrane) give way to three transport properties (water diffusion coefficient, ionic conductivity, and water transport number) and each of these has known techniques for their independent measurement. However, as soon as a fourth species is added, such as methanol for the direct methanol fuel cell, the situation becomes much more complex as six transport properties are required.

Verbrugge and Pintauro wrote an excellent review of transport processes in ion-exchange membranes in 1989 that can still serve as a starting point for any current modeling effort.[112] This review article gives a comprehensive overview of the modeling of transport processes in ion-exchange membranes, including microscopic or capillary pore models such as phenomenological models based on the Nernst–Planck equation, electrokinetic models starting from an assumed pore structure, and true macroscopic models that make no assumptions about microscopic structure and only arbitrary designations of speciation. In addition, common methods of measuring equilibrium properties (concentrations, density, porosity, activity coefficients) are elaborated and transport property measurements, including transference numbers and diffusion coefficients, are reviewed.

Macroscopic modeling has been put to its best use in the many detailed mathematical modeling studies of the performance of PEMFCs.[113–117] Several different models were published during the first half of the 1990s that provided a wealth of information on performance aspects, including membrane water transport and thermal behavior, transport of gases within and across the cell, and predictions of cell current–voltage curves under different operating conditions. These models incorporated the latest compilations of thermodynamic and transport property data available at the time on the Nafion® membrane and the comparisons with experimental data represent a valuable tool for checking the validity of physical property data. As physical properties of Nafion® membranes are strongly dependent on water content and temperature, the relevant transport equations are nonlinear and require computer simulations for an exact solution.

More recently, the performance of direct methanol fuel cells has begun to see detailed modeling, presenting the challenge of multi-component transport and partitioning of methanol/water mixtures within the ionomer regions of the cell.[118–121] In addition to the direct current (d.c.) performance of the PEMFC, a comprehensive modeling study of the steady-state impedance response of the cathode side of the PEMFC has been published.[122] Early 1D PEMFC models have also been extended recently into two dimensions.[123–126] Finally, some efforts have been made to examine the dynamic behavior of fuel cells and ionomer membranes.[127, 128] Many of these recent models are extensions of the earlier classic models of Bernardi and Verbrugge,[114] Springer *et al.*,[113] Nguyen and White,[116] and Fuller and Newman.[115]

6.2 Molecular modeling of perfluorinated ionomers

While macroscopic models are generally preferred for several purposes, including the construction of complex device models to predict and understand large-scale fuel cell performance, microscopic models based on first principles, are needed for a deeper understanding of structure and transport in perfluorinated ionomer membranes. Without these models, it is not possible to draw detailed conclusions on the relationship of local structures, such as side chain length and degree of branching, to transport properties of membranes and solutions.

Din and Michaelides developed a molecular dynamics simulation of water and protons in pores of various radii with fixed wall charge densities, a system meant to describe a Nafion® membrane.[129] Water, proton, and potential profiles within the pores are calculated. Transport properties such as the proton diffusivity are calculated from the simplified molecular dynamics model and compared to experimental data. Elliott *et al.* performed molecular dynamics simulations using 26 anions composed of fluorosulfonate fragments as well as hydronium cations (H_3O^+) and water molecules as the solvent medium.[130] These simulations provided evidence for clusters in the form of small aggregates. Phase separation into ionic-rich aggregates was due to the electrostatic terms in the force fields. Two types of water were found, *bound* water strongly associated with sulfonic acid groups and a *free* water phase loosely attached.

In addition to molecular dynamics simulations, several groups have embarked on fundamental molecular modeling efforts to describe the potential energy surfaces of model systems meant to describe perfluorinated ionomer membranes. Recent years have seen multiple groups initiate ab initio quantum mechanical calculations with the purpose of constructing potential energy surfaces for key portions of the Nafion® membrane such as the sulfonic acid side chain. The purpose of these studies is to build a more sophisticated modeling framework and also to study structural questions related to ionic conduction through these systems.

Johansson *et al.* reported ab initio quantum mechanical calculations on model side chains having the structure $(CF_3)_2CFOCF_2CF_2SO_3H$ to study the energetics of bond rotation.[131] The energetic barrier to rotation about the C–C bond was found to be about $10\,\mathrm{kJ\,mol^{-1}}$ compared to $\sim 30\,\mathrm{kJ\,mol^{-1}}$ for rotation about the C–O bond. The effect of increasing membrane hydration or changes in solvent type was studied by changing the dielectric constant employed in the supercritical fluid (SCF) simulations, illustrating that the rotational barriers increase sharply with decreasing dielectric constant. This phenomenon is relevant to ionomers with low water levels, caused, for example, by drying of the anode side of an operating PEMFC. These authors also studied the possibility that inter-chain hydrogen bonding is responsible for the slow rehydration kinetics of perfluorinated ionomers.

Paddison and co-workers have engaged in an extensive molecular-level simulation research program focused on perfluorinated ionomer membranes. Their work has included ab initio molecular structure and energy calculations as well as molecular dynamic and statistical mechanical simulations of transport processes and built a fundamental understanding of the critical structures and mechanisms involved in the transport process.[132–134] More details can be found in **First principles modeling of sulfonic acid based ionomer membranes**, Volume 3. A primary motivation of their work has been to give guidance to synthetic chemists on directions for new ionomers with improved physical and transport properties.

7 TRANSPORT PROPERTIES — TECHNIQUES EMPLOYED AND PROPERTY DATA

7.1 Ionic conductivity

Proton conductivity in solids is a topic of substantial theoretical as well as practical importance to engineers and scientists. In addition to the importance for industrial processes such as fuel cells, the remarkably high proton conductivity of Nafion® membranes makes them an important class of proton conductors for fundamental studies and modeling of the conduction process. An excellent recent review of the general topic of proton conductors with a focus on solid systems and fundamental understanding of the mechanism of the conduction process exists.[135]

Proton conductivity is most frequently measured from the alternating current impedance of a standard cell design. For single-ion conductors that exhibit little to no concentration polarization, it is also possible to utilize d.c. techniques to measure ionic conductivity although alternating current (a.c.) techniques are still preferred. An a.c. signal can be established between two electrodes in any cell design including the a.c. response of an operating fuel cell. However, for purposes of accurate measurements, several general rules should be followed for measuring conductivity data on ionomer membranes.

While a uniform current distribution is not necessary for accurate measurements, a known current distribution is essential as it allows a measured cell resistance to be related to the bulk material property referred to as the ionic conductivity. A uniform current distribution is the most simple to handle as the relationships that describe the ohmic drop (IR) loss in the cell become simple equations that are easily manipulated to extract physical properties. Unfortunately, very few cell designs provide a uniform current distribution and not all are easy to use in practice. Three cell designs used in many studies and worth discussing in more detail are described below.

An imposed potential gradient has an influence on all of the mobile charged species within an ionomer membrane. Ionic fluxes through solvent-swollen ionomers exert an influence on the solvent molecules and can dry out one side of the membrane if not exposed to a sufficient rehydration rate. The potential gradient measured across an ionomer membrane at zero current will be non-zero after a period of polarization due to the solvent gradients that build up under conditions of current flow. The decay of this potential is one means for measuring transport properties other than ionic conductivity. Under a.c. conditions, these solvent concentration gradients can be neglected and a more straightforward measurement of the ionic conductivity is afforded.

While measuring voltage differences between electrodes is straightforward under either a.c. or d.c. conditions, there are numerous electrode effects that must be considered in order to make accurate measurements of bulk material properties such as the ionic conductivity. Under d.c. conditions, passage of current between working and counter electrodes will affect chemical changes at the interfaces that may by nature change the bulk system being probed. a.c. techniques are preferred for their ability to pass current via double-layer charging processes that are not necessarily accompanied by chemical changes. However, even with a.c. techniques, the electrode surface cannot necessarily be ignored as the resistance of a cell will include contributions from electrode kinetic (charge-transfer) resistances. This last consideration is the primary motivation for the use of high-surface-area electrodes such as roughened Pt in order to reduce or minimize the surface resistance. Even more preferred is the use of four-electrode cell geometries where two reference electrodes that pass only negligible current densities are used to probe the cell resistance.

A final challenge with ionic conductivity measurements in solvent-swollen ionomers is control of the environment. The ionic conductivity of perfluorinated ionomers depends strongly on the solvent content and temperature. Equilibrium water uptake depends on temperature and the water activity of the surrounding medium in which the ionomer is immersed. Controlling these variables, while making electrochemical measurements, is an important consideration in cell design that has led researchers to employ a small number of common experimental arrangements. When temperature-dependent measurements are desired, the equilibrium solvent activity can be controlled in a number of ways. The simplest approach is to utilize a liquid solvent medium such as immersion into water and confine the measurements to temperatures over the liquid range of the solvent. More appropriate for fuel cell measurements, the water activity is controlled to a specific value using a vapor phase equilibrated with a salt solution of known activity. This latter approach requires a prolonged period of equilibration at each temperature to assure that the equilibrium solvent content throughout the ionomer membrane has been reached.

Next we discuss the strengths and weaknesses of three common cell designs.

7.1.1 Cylindrical body two-electrode design

This is the most common cell design for measurements of ionic conductivity in other solid systems including polymer electrolytes for lithium battery applications. The cylindrical cell is simple to construct and assemble and allows relatively easy temperature control. The disadvantages of this cell design are the challenge of installing reference electrodes, the difficulty in maintaining thickness control and calibration of the pressure applied to the membrane, and the small aspect ratio (length : area) for the cell. Additionally, it is challenging to expose a membrane sample to a known humid environment in a cell having this design as little contact area is exposed for the equilibration process.

7.1.2 Parallel line electrode two or four-point-probe design

The parallel linear electrode cell design is probably the most commonly used design at present for Nafion® membranes and related ionomers available as free-standing films. The advantages of this design are its excellent control of thickness and contact area, its ability to be fitted with reference electrodes for three and four-electrode measurements, and the control of environment allowed by the large membrane area exposed on the surface of the cell. The primary disadvantage is that current flow occurs parallel to the surface of the membrane rather than across the membrane as is the case in operating devices. In addition, the large exposed membrane area makes humidification control more challenging as the membrane equilibrates rapidly with the environment. Four-electrode cell designs are independent of the experimental parameters critical to two-electrode designs such as electrode area and electrode compression or pressure. Four-electrode cells can give frequency-independent resistances in a.c. measurements over several decades of frequency making the conductivity measurement more accurate.[27]

7.1.3 Microdisk two or three-electrode designs

A classic cell design for studying properties of Nafion® membranes and recast films, especially in electrode kinetics research, is the film-coated microelectrode described for example by Uribe *et al.*[136] These authors employed a 100 μm diameter Pt disk electrode coated with a recast Nafion® membrane with an outer series of counter and reference electrodes. The microelectrode design has advantages such as its capability to maintain high current densities without reaching mass-transport limiting currents due to the large field that the electrode draws upon. Microelectrodes can have controlled and known current distributions and are frequently used in electrochemical studies.

Conductivity Data

Early studies of ionic conductivity of Nafion® membranes generally employed membrane systems in the presence of other electrolyte solutions, such as NaCl or acidic or basic electrolytes.[137] While this was appropriate for these studies, the current operation of fuel cells without added electrolytes makes these earlier studies irrelevant and in some cases misleading. The presence of electrolytes in the external solution causes two significant changes in the Nafion® membrane, one being the sorption of electrolyte species into the membrane and the other being the equilibration of water between the two regions. The ionic conductivity of the Nafion® membrane under these conditions may be raised or lowered compared to its value in the presence of pure water, accounting for some of the variability in literature data. To measure the conductivity under operating PEMFC conditions, the membrane must be exposed to environments free from added electrolytes and with controlled water activity or, in the case of the direct methanol fuel cell (DMFC), water/methanol solutions of known concentration.

Other causes of the well-known variability in ionic conductivity data are differences in membrane pretreatments and other experimental procedures such as cell design, data analysis, and humidification. Differences in cell design were discussed earlier. A significant influence on ionic conductivity comes from the water content of the membrane sample. Simple actions such as blotting dry the membrane can cause a large variability in measurements. Whenever possible, researchers should seek to follow similar procedures to earlier studies in order to facilitate comparisons between different studies. Table 8 provides a summary of a number of conductivity measurements from the literature. In all cases, similar membrane pretreatments giving the expanded form of the membrane were employed. This section will review many of the focused studies of ionic conductivity performed in recent years on Nafion® membranes.

Table 8. Ionic conductivity of Nafion® membranes in proton form and in the presence of various environments at ambient temperatures (23–25 °C).

Nafion® membrane	Cation type	External electrolyte (wt%)	Ionic conductivity ($S\,cm^{-1}$)	Reference
1100 EW	H^+	H_2O liq.	0.092 (20 °C)	[147]
1100 EW	H^+	100% RH vapor	0.060 (30 °C)	[142]
1100 EW	H^+	100% RH vapor	0.078 (20 °C)	[146]
1100 EW	H^+	0.05 M HNO_3	0.060	[149]

The dependence of ionic conductivity on the volume fraction of conductive phase has been studied by several authors in an attempt to model the conduction process using percolation theory. Percolation theory holds for conduction in heterogeneous media and expresses the conductivity of a system in terms of the volume fraction of the conducting phase raised to a critical exponent. Given the well-known dependence of ionic conductivity on solvent swelling or uptake in ionomer membranes, it is natural to attempt to predict this dependence under the assumption that the swelling process expands the volume of the ion-containing channels and clusters within the ionomer, allowing more facile transport of ions through this interconnected phase. However, one must consider that extensive swelling as seen in some organic solvents or in low EW membranes in water causes a decrease in conductivity even though the volume fraction of the conducting phase is increasing, which contradicts the simple percolation theory.

Hsu and Gierke presented an early analysis of conductivity data on Nafion® 125 membranes in Na^+ form based on percolation theory, finding that the critical exponent had a value of 1.5 for this system.[34] Wodzki *et al.* studied conductivity data on Nafion® 120 and Nafion® 427 membranes exposed to various electrolyte solutions for purposes of fitting the conductivity data to a percolation equation.[138] The conductivity data obtained in the study were fit to a critical volume fraction of the conductive phase and to critical exponents. Pourcelly and Gavach summarized previous percolation studies on Nafion® membranes and pointed out that percolation theory does not hold at higher water contents due to the presence of a fully connected conducting network under these conditions.[2]

Rieke and Vanderborgh reported one of the earlier studies on ionic conductivity of the acid-form N117 membrane having applications in PEMFCs as the motivation.[139] The conductivity cell was designed for a flow stream of humidified nitrogen gas and could also control the cell temperature during measurement. Ionic conductivity was about 0.06–0.08 S cm^{-1} at room temperature and 100% relative humidity (RH) and increased with temperature up to about 50–60 °C then decreased to 0.08 S cm^{-1} at 95 °C. The maximum conductivity occurred in the temperature range of the minimum in water content, an unexpected result given the importance of water in the conduction process. These results illustrate one of the challenges in conductivity measurements in a vapor-phase environment. As the temperature is increased, the water content in the membrane varies as the water vaporizes into the nitrogen stream. Other studies have shown that ionic conductivity continues to increase up to temperatures of nearly 100 °C when the water content in the membrane is held constant.[87] These authors measured an activation energy for conductivity at constant water content of 21 kJ mol^{-1} at low temperatures (30–40 °C) which decreased to 12 kJ mol^{-1} in the higher temperature range (up to 70 °C).

Slade *et al.* studied the effect of pretreatment on the ionic conductivity of acid-form N117 membranes.[140] This study also presented pulsed field gradients (PFG) NMR data that were used to measure the 1H proton self-diffusion coefficient. The measured diffusion coefficients were much higher than that calculated for H^+-form membrane conductivity data, from which the authors inferred that the NMR-based self-diffusion coefficient is a combination of transport of water as well as free protons or hydronium ions. Another study of the temperature dependence of various physical properties of the N117 membrane was carried out by Parthasarathy *et al.*[141] Using impedance data over a wide frequency range, they were able to extract the membrane's ionic conductivity over the range of 30–80 °C.

The temperature and humidity dependences of the conductivity of N117 in acid form were examined by Zawodzinski and co-workers.[142] Ionic conductivities over the temperature range of 25–90 °C were measured at various water contents for fully hydrated membranes immersed into liquid deionized water ($\alpha = 22$). Activation energies were not extracted from the temperature-dependent conductivity data as the data were not strictly Arrhenius; at the lower temperatures the conductivity appeared to become less dependent on temperature.[67] At constant temperature of 30 °C, conductivity decreased nearly linearly with water content down to a value of <0.01 S cm^{-1} at the lowest water content. Based on these measurements, Springer *et al.*, correlated the ionic conductivity using the expression[113]

$$\kappa(\mathrm{S\,cm^{-1}}) = (0.5139\lambda - 0.326)\exp\left[1268\left(\frac{1}{303} - \frac{1}{T}\right)\right] \qquad (7)$$

An activation energy of 10.5 kJ mol^{-1} is used in the expression and the linear dependence on α is clear. This expression also goes to zero as the water content approaches a value of 0.6 with the physical implication that at least 0.6 water molecules per acid group are required for conduction.

An important study related to proper cell design for accurate conductivity measurements was published by Cahan and Wainright.[143] The two cell designs consisted of a two-electrode cell with two Pt electrodes in the standard sandwich configuration and a four-electrode cell with two platinized Pt foil electrodes at the ends and two Pt probe wire electrodes 1 cm apart near the center of the film sample. Temperature and humidity were both controlled using an environmental chamber. Their study showed that the two-electrode cell could not separate the bulk resistance of the sample from the interfacial (electrode) impedances until very high frequencies were reached, at which point other cell-design related artifacts appeared in the spectra. The impedance of the four-electrode cell, on the other hand, exhibited a constant impedance over several decades of frequency allowing a straightforward isolation of the membrane conductivity.

One drawback of the parallel electrode four-probe design is that the ionic conductivity is measured parallel to the film direction rather than in the perpendicular direction that current must flow for fuel cell applications. This difference could be significant if the Nafion® membrane shows an anisotropic behavior in its ionic conductivity. Measurements of the normal (perpendicular) component of the conductivity of membranes take much ingenuity due to the challenge of attaining a uniform current distribution in the membrane in this direction. To study the anisotropy of the conductivity, Gardner *et al.* published a series of papers using a coaxial probe conductivity cell with a ring-disk design focusing on the issue of the anisotropy of the conductivity of N117 in H^+-form.[144] This study was the first to report a directional dependence to the ionic conductivity of Nafion® membranes. These measurements should be confirmed by other researchers, preferably with different probe designs meant to eliminate potential measurement errors associated with the two-electrode coaxial probe such as the pressure dependences and the potential for non-uniform current distributions.

Several authors have studied the temperature dependence of the ionic conductivity in Nafion® membranes in more detail. Control of the solvent content for volatile solvents such as water is the critical experimental variable in these studies. Cappadonia *et al.* carried out an interesting study of the temperature dependence of conductivity for acid-form N117 membranes over the temperature range of 140 K and room temperature.[145] These low temperatures reduce the problems with control of membrane water content. Temperature was held constant with a liquid-N_2 cryostat and the temperature at the surface of the membrane sample was monitored. A two-electrode cell design with Au electrodes deposited on each side of the membrane in the standard sandwich configuration was employed. Ionic conductivity exhibited Arrhenius behavior with two different slopes indicating that a phase transition occurs over the temperature range studied. The transition temperature between the two different regions was 225 K for pretreated samples with an activation energy of 0.11 eV at higher temperature and 0.53 eV below 225 K. Non-pretreated samples showed a transition at 260 K with an activation energy of 0.14–0.21 eV above this temperature and 0.55 eV below 260 K. The authors speculated that frozen water was responsible for the much higher activation energy below the transition temperature and noted that the transition temperature depended on the water content of the membrane but the activation energy below the transition was relatively constant for all samples. The activation energy above the transition temperature depended on the water content of the membrane (Table 9).

A comprehensive study of the temperature and humidity dependences of the conductivity of N117-H^+ was reported by Sone *et al.*[146] These authors used a four-electrode cell and controlled temperature and humidity by circulating humidified nitrogen across the cell. The authors employed a 30 min equilibration period each time the temperature or humidity was changed to assure that a stable impedance was reached. These authors reported a conductivity of $7.8 \times 10^{-2}\,\mathrm{S\,cm^{-1}}$ under conditions of 100% RH and 20 °C for N117-H^+; this same value was obtained with a two-electrode conductivity cell in order to confirm the validity of their four-electrode cell design. The temperature dependence of the conductivity at fixed percentage RH values showed a complicated behavior with the conductivity at first decreasing from 20 to 45 °C due to a decrease in water content in the membrane followed by increases from 45 to 80 °C as the water content stabilized. Above 45 °C, the activation energies were in the range of 1–2 $\mathrm{kJ\,mol^{-1}}$ which is lower than reported by other studies. By combining water content data with conductivity data versus percentage RH, a plot was constructed of the conductivity as a function of water content (expressed as λ) at fixed temperature. The plot was roughly linear with the conductivity increasing by over three orders of magnitude as the water content increased from under two to over 12 waters per acid site.

Table 9. Activation energies for ionic conduction in Nafion® membranes measured under various conditions. All membrane samples were in their expanded form during the measurements indicating similar pretreatments.

Membrane	Humidification	Temperature range (°C)	Activation energy ($\mathrm{kJ\,mol^{-1}}$)	Reference
N117-H^+	H_2O liq.	30–80	21.8	[141]
N117-H^+	H_2O liq.	20–170	7.82	[147]
N117-H^+	100% RH vapor	45–80	1–2	[146]
N117-H^+	100% RH	30–40	21	[139]
N117-H^+	100% RH	50–70	12	[139]
N117-H^+	100% RH	−33–27	31.5	[140]
N117-H^+	H_2O liq.	25–70	17.2	[87]

Another recent study of the temperature dependence of the ionic conductivity of N117 membranes was carried out by Kopitzke *et al.* in their study of aromatic hydrocarbon ionomers.[147] The conductivity of acid-form N117 was equal to $9.2 \times 10^{-2}\,\mathrm{S\,cm^{-1}}$ at 20 °C with a water content of 11.5 H_2O per sulfonic acid site. An activation energy of 7.82 $\mathrm{kJ\,mol^{-1}}$ was calculated from the conductivity-temperature plot over the full temperature range. Alberti *et al.*, recently studied the temperature and humidity dependence of the ionic conductivity of N117-H^+ in comparison to sulfonated polyether ether ketone membranes to temperatures up to 160 °C.[148]

A number of other conductivity studies have been reported for Nafion® membranes that examine the effect of properties such as the external solution environment, the cation exchange process, and the effect of various additives on the ionic conductivity. Lehmani and co-workers studied the conductivity of N117 membranes in the presence of external solutions of nitric acid and sodium chloride of various concentrations.[149] In addition to ionic conductivity, the membrane density, porosity, and water content were also measured as a function of electrolyte concentration. Okada and co-workers performed an extensive study of transport property data, including ionic conductivity on N115 and N117 in various cation forms (immersed in dilute solutions of the metal chloride salts) such as a number of ammonium salts, alkali and alkali earth salts.[150] Data measured and analyzed in the study included ionic conductivity, cation transference number, water transport number and permeability, and water diffusion coefficient. By plotting the membrane resistance (inverse conductivity) versus the measured water transport number for various cations, it was shown that resistance will generally decrease with decreasing water transport number, especially for the alkyl ammonium salts. The authors concluded that for purposes of designing improved ionomers, one should attempt to achieve a high concentration of sulfonic acid groups, high water content, and an alignment of channel structures for ease of transport.

Means for increasing the ionic conductivity of Nafion® membranes have become an important focus of research in recent years. With ionic conductivity under various operating conditions well explored, fuel cell researchers are more concerned with improving ionic conductivity to reduce cell resistance under standard operating conditions. Additionally, any solution to the problem of the decrease in ionic conductivity at elevated temperatures in the presence of water vapor would allow systems to operate at higher temperatures, which is advantageous for a number of reasons. Arimura *et al.* published a recent study on the effect of various additives on the ionic conductivity of Nafion® solution-cast films.[151] For films without additives in a dry state (dried for 12 h in vacuum at elevated temperature), low conductivities of $1.9 \times 10^{-2}\,\mathrm{S\,cm^{-1}}$ were measured. Addition of 5 wt% of moisture absorbants such as P_2O_5, molecular sieves, or silica gels increased conductivity into the $2{-}4 \times 10^{-2}\,\mathrm{S\,cm^{-1}}$ range. Addition of 10 wt% naphthalene-sulfonate additives reduced conductivity somewhat (to 75–95%) from the value in the *wet* state of $0.13\,\mathrm{S\,cm^{-1}}$. Addition of vinyl sulfonate ionic copolymers with certain oriented structures increased conductivity to the highest levels of $0.21{-}0.23\,\mathrm{S\,cm^{-1}}$. This effect was believed to be caused by a rearrangement of the ionic cluster/channel system due to the influence of the long alkyl side chain attached to the hydrophilic end group. These final conductivities are impressive and deserve further study.

Beyond the use of additives to influence conductivity, some authors have examined the use of novel solvents as the primary component within the Nafion® membrane. The purpose is to eliminate or reduce the necessity of using a hydrated membrane due to the substantial volatility of water that precludes operation of PEMFCs at temperatures much in excess of 100 °C. Kreuer *et al.* recently imbibed pyrazole and imidazole liquids into sulfonated polyether ketone ionomer membranes under anhydrous conditions as potential high-temperature solvents to replace water.[152] They showed that protonic conductivities approaching $0.01\,\mathrm{S\,cm^{-1}}$ could be reached at 200 °C in these novel systems. In a similar approach, Doyle *et al.* imbibed ionic liquids such as 1-butyl, 3-methyl imidazolium trifluoromethane sulfonate (BMITf) into Nafion® membranes to obtain anhydrous proton conducting systems that can operate at elevated temperatures.[153] Ionic conductivities were reported for BMITf imbibed into a number of different ionomers. Lower EW membranes such as the 890 EW Nafion® membrane absorbed larger quantities of the ionic liquid and achieved lower activation energies and higher conductivities. Conductivities as high as $0.1\,\mathrm{S\,cm^{-1}}$ could be achieved at temperatures of 180 °C. Activation energies were in the range of $19{-}22\,\mathrm{kJ\,mol^{-1}}$ for the lower EW membranes and 30.5 for N117-H^+ with BMITf. Measurements of the conductivity of the ionic liquid without the ionomer present gave lower conductivities in the higher temperature range demonstrating that the protons contributed by the ionomer are mobile in these systems.

While numerous experimental studies of ionic conductivity in Nafion® membranes have been described, few studies have focused on the theoretical and mechanistic aspects of proton transport in these systems. Kreuer and coworkers used comparisons between the proton conductivity and hydrogen self-diffusion coefficient to make inferences about the mechanism of proton conduction in ionomers.[154] Additional details on these studies can be found in **Hydrocarbon membranes**, Volume 3. PFG NMR measurements of the H self-diffusion coefficient were performed on N117-H^+ membranes having a range of water contents. This measurement probes the self-diffusion process for hydrogen atoms located both as protons and within water molecules. The activation energy for the hydrogen diffusion process ranged from 0.215 to 0.16 eV over the range of water contents and temperatures from 300 to 360 K. The actual diffusion coefficients were in the range of 10^{-7} to $10^{-5}\,\mathrm{cm^2\,s^{-1}}$. A comparison between these self-diffusion coefficients and ionic diffusion coefficients extracted from ionic conductivity data showed that similar values were achieved at low water contents indicating a vehicular mechanism for proton conduction under these conditions. A similar approach was used previously by Zawodzinski *et al.* for the same purpose.[89] These authors refer to the ratio of diffusivities as the *amplification factor*. At higher water contents, the amplification factor increases from unity to reach a value of 2.5 illustrating the decoupling of proton transport from water diffusion. The amplification factor in dilute aqueous solutions is 4.5.[155] The authors concluded that there was little restriction to proton transport within the ionomer from the polymer chains at high water contents.

Fontanella's research group has carried out several studies of the pressure dependence of the ionic conductivity of perfluorinated ionomer membranes with the purpose of understanding the mechanism of the conduction process and its rate-limiting behavior in more detail.[156] One recent study compared data on N117 membranes with Dow short-side chain ionomers having EWs of 800 and $1000\,\mathrm{g\,eq^{-1}}$.[157] The pressure dependence of the ionic conductivity was measured over the range of 0–0.2 GPa (2 kbar). From these data, the activation volume could be calculated and used to infer information about the rate-limiting process in conduction. Activation volume for a low water content N117 membrane was $54\,\mathrm{cm^3\,mol^{-1}}$, a large value that indicated polymer chain segmental motion was influencing conductivity. The activation volume decreased continuously for increasing water content and became negative at the highest water contents. This indicated that conductivity became similar to the process in liquid water, unaffected by the ionomer itself.

A number of studies of the dielectric relaxation spectra of Nafion® membranes have been published over the years. Most of these studies operated in a relatively low frequency range (<100 MHz) compared to the frequencies of molecular motions. Dielectric spectroscopy is fraught with experimental challenges of the same nature found in ionic conductivity measurements as the intent is to measure bulk material properties but electrode artifacts can be difficult to eliminate. A study performed recently by Paddison *et al.* reported data in the 45 MHz–30 GHz range with the purpose of finding molecular motions such as water rotational processes that are coupled to the ionic conduction process.[158] These measurements are extremely challenging due to the prevalence of experimental artifacts at these high frequencies and the difficulties associated with proper membrane pretreatment and equilibration during the measurements. Measurements on Teflon® film samples were done to show that the technique could give the expected results for dielectric constant and loss on this well-characterized polymer. The ionic conductivity was extracted from the low-frequency dielectric data and compared well to previous measurements; the ionic conductivity was shown to be independent of frequency up to at least 50 MHz.

While all the previous studies cited utilized specially designed probes to measure conductivity, it is also possible to make measurements in situ in an operating fuel cell. These measurements are generally made using voltage step or impedance-based perturbation techniques. These measurements do not lend themselves to the accurate determination of physical property data due to the complexity of the high-frequency or short-time response of electrochemical cells. A particular challenge for fuel cells is the separation of ionic conduction through the catalyst layers from conduction through the membrane and cell components. However, in situ measurements provide a wealth of information on the transient response of the cell resistance to changes in operating conditions and can elucidate the conditions that lead to membrane drying and its impact on cell resistance. One such study performed recently by Buchi and Scherer measured in situ conductivity in an operating fuel cell using an auxiliary current-pulse technique with 5 A pulses with a 1 μ, ms time window.[88] Membrane resistances (in $\Omega\,\mathrm{cm}^2$) were measured for commercial Nafion® membranes (N112, N115, N105, and N117) at current densities from 0 to 1 A cm^{-2}. Cells with multiple membranes sandwiched together were used to plot apparent membrane conductivity versus thickness over the range of 50–400 μm. These results showed that a slight increase in resistance existed for thinner membranes below 100 μm. This was interpreted to mean that a slightly higher resistance existed at the membrane surface which has a larger relative contribution for thinner membranes. Another explanation could be the resistance of the electrodes causing an additive factor in the measurements.

7.2 Water and methanol diffusion coefficients

The water diffusion coefficient within the Nafion® membrane is important for modeling and understanding the water content and dynamics within the PEMFC. Water diffusion is the primary process by which non-uniformities in water content within the membrane are equilibrated. These non-uniformities are brought about by either electroosmotic drag processes or exposure to different water environments on either side of the membrane. Water diffusion also determines one of the critical time constants for the dynamic response of Nafion® membrane-based fuel cells to processes such as changes in current density, humidification, or temperature. Finally, transport limitations due to water diffusion can be one of the limiting current density mechanisms in membrane-based processes, thus presenting a ceiling on the maximum achievable current density.

Unlike the case with ionic conductivity measurements where one technique, that of high-frequency impedance measurements, is used by most researchers, nearly every measurement of water diffusion coefficients in Nafion® membranes employs a new approach. Classical techniques based on the measurement of transient uptake curves or radiotracer labeling techniques have been used since the earliest measurements of diffusivity in Nafion® membranes. More recent approaches have included PFG NMR measurements of water self-diffusion coefficients and the streaming potential approach. Self-diffusion coefficients measured using NMR must be converted into Fickian diffusion coefficients for purposes of comparison with other macroscopic measurements or utilization of these data in macroscopic transport models.

Early measurements of the water diffusion coefficient followed the process of water sorption into a dry membrane from which diffusion rates and activation energies could be calculated. Yeo and Eisenberg found an activation energy of 18.8 kJ mol^{-1} and diffusion coefficients ranging from 1 to $10 \times 10^{-6}\,\mathrm{cm}^2\ \mathrm{s}^{-1}$ over the temperature range of 0–99 °C.[78] The diffusivities were extracted from the short-time slope of the uptake curve. This technique relies upon a constant diffusion coefficient over the course of the sorption experiment, which is generally not the case for water-swollen ionomers. Radiotracer and other labeling techniques have also been used to extract diffusion coefficients for water in Nafion® membranes. Yeager *et al.* measured the diffusion coefficient of water in fully hydrated N120 containing various alkali metal cations using radiotracer techniques.[44] They reported a diffusivity of $2.5 \times 10^{-6}\,\mathrm{cm^2\ s^{-1}}$ at 25 °C for the Na^+-form membrane and slightly smaller values for the K^+ and Cs^+-form membranes.

Using another probe technique, Zawodzinski *et al.* employed PFG spin echo NMR measurements to determine the 1H self-diffusion coefficient in N117-H^+ at various water contents.[89] Diffusion coefficients obtained by this technique were compared with proton diffusivities from conductivity measurements in a similar procedure to the one later used by Kreuer.[152] Similar diffusion coefficients were found using either approach at low water contents implying a vehicular transport mechanism. At higher water contents, on the other hand, the two values diverged consistent with a Grotthus mechanism for conduction. As self-diffusion coefficients are not relevant to macroscopic transport processes of interest for modeling the behavior of PEMFCs, these values were converted to Fickian or macroscopic water diffusion coefficients, D_{chem}, using the known activity data and the expression

$$D_{chem} = \left(\frac{d\ln a}{d\ln C}\right) \times D_s \tag{8}$$

where a is the thermodynamic activity of water, C is the water concentration, and D_s is the self-diffusion coefficient of water calculated using the NMR data and reproduced in Figure 4. The water diffusion coefficient expressed in equation (8) is the proper transport property to use in macroscopic studies of water diffusion.[111] The Fickian water diffusion coefficient has a weaker dependence on membrane water content with values of $1.3 \times 10^{-6}\,\mathrm{cm^2\ s^{-1}}$ at $\lambda = 2$ and $1.5 \times 10^{-6}\,\mathrm{cm^2\ s^{-1}}$ at $\lambda = 14$ under conditions of vapor-phase water at ambient temperature. A fitting expression for these data will be given in equation (9).

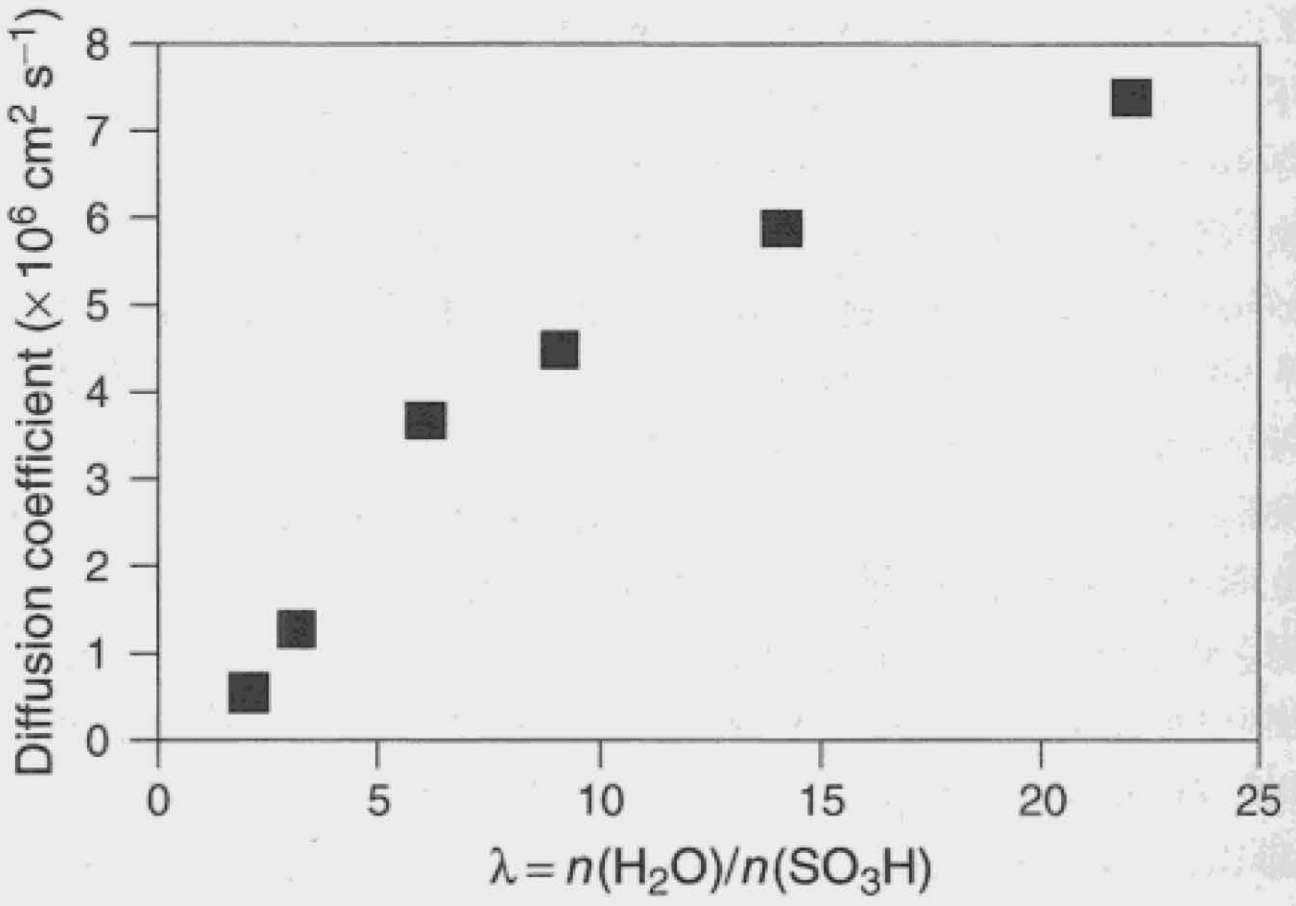

Figure 4. Water self-diffusion coefficient in N117-H^+ as a function of water content in the membrane measured using the PFG NMR technique. (Reprinted from Zawodzinski *et al.* (1991)[89] copyright American Chemical Society.)

Okada *et al.* made measurements of all three of the independent transport properties for the N117 membrane in both H^+ and Na^+ form over the temperature range of 25–80 °C.[159] The membranes were immersed into 0.03 N HCl or NaCl during the measurements. The supporting electrolyte was necessary for the two-compartment two-electrode cell design employed in the work. Both the transport number of water and the water diffusion coefficient were extracted from streaming potential measurements. The streaming potential could be used to measure the water permeability, from which the water diffusion coefficient was calculated. This water diffusion coefficient should be the same Fickian diffusion coefficient as calculated in equation (8). A diffusion coefficient of $1.25 \times 10^{-5}\,\mathrm{cm^2\ s^{-1}}$ at 80 °C and an activation energy of $11.6\,\mathrm{kJ\,mol^{-1}}$ were reported. The reasons this value is larger than the previous cited values may be due to the use of liquid water equilibrated membrane here as well as the elevated temperature.

Many of the literature values for the water diffusion coefficient (D_{chem}) in Nafion® membranes are collected in Table 10. Even under similar conditions such as a fully

Table 10. Compilation of water and methanol diffusion coefficients in Nafion® membranes from the literature.

Membrane	Penetrant	Conditions	Diffusion coefficient ($\mathrm{cm^2\ s^{-1}}$)	Reference
N117-H^+	H_2O	0.03 N HCl, 80 °C	1.25×10^{-5}	[159]
N117-H^+	H_2O	1.0 M methanol, 30 °C	1.0×10^{-5}	[103]
N117-H^+	H_2O	100% RH H_2O, $\lambda = 14$, 30 °C	1.5×10^{-6}	[89]
N117-Na^+	H_2O	H_2O liq., 25 °C	2.5×10^{-6}	[44]
N117-H^+	methanol	1.0 M H_2SO_4, 25 °C	1.15×10^{-5}	[161]
N117-H^+	methanol	0.5–8.0 M methanol, 30 °C	6.0×10^{-6}	[103]
N117-H^+	methanol	2.0 M H_2SO_4, 60 °C	4.9×10^{-6}	[162]

hydrated N117-H^+ membrane, the values in the literature vary over nearly one order of magnitude. Based on the data in Table 10, it appears that the water diffusion coefficient for H^+-form membranes is higher than that for the salt form, and that water-vapor equilibrated membranes have a lower value than liquid water equilibrated membranes. However, a comprehensive study on water diffusion under various conditions has not been done so these interpretations are best considered speculative.

The variation in literature values of water diffusion coefficients was addressed in a study of water transport in Nafion® membranes reported by Motupally *et al.*[160] Water flux measurements were made across an N115-H^+ membrane at 80 °C by varying the water activity in a flowing nitrogen gas stream exposed to one side of the membrane. These measurements were modeled using a macroscopic transport model making use of various expressions from the literature for the water-content dependence of the diffusion coefficient. Based on comparisons with their experiment, the most accurate expression for the dependence of the diffusion coefficient on water content was exhibited by using the Fickian diffusion coefficient data of Zawodzinski *et al.* The fitting expression used by Motupally was

$$\mathrm{D}_{\mathrm{chem}} = 3.1 \times 10^{-3}\lambda(\mathrm{e}^{0.28\lambda} - 1) \times \exp\left(\frac{-2436}{T}\right) \text{ for } 0 < \lambda < 3 \qquad \text{(9a)}$$

and

$$\mathrm{D}_{\mathrm{chem}} = 4.17 \times 10^{-4}(1 + 161\mathrm{e}^{-\lambda}) \times \exp\left(\frac{-2436}{T}\right) \text{ for } 3 < \lambda < 17 \qquad \text{(9b)}$$

where $\mathrm{D}_{\mathrm{chem}}$ has units of $\mathrm{cm}^2\ \mathrm{s}^{-1}$. The activation energy used in this expression was based on the data of Yeo and Eisenberg who measured an enthalpy of diffusion of $20.25\ \mathrm{kJ\ mol}^{-1}$.[78] This study demonstrated that the accurate prediction of water concentration profiles across Nafion® membranes requires a valid expression for the water-content dependence of the diffusion coefficient. Hence, researchers should be careful with their choice and application of physical properties from the literature in situations where a wide variation exists.

Another important penetrant of interest for Nafion® membranes is methanol, due to its use as a liquid fuel in direct methanol PEMFCs. Methanol is somewhat easier to characterize than water because of the ability to expose the membrane to solutions of methanol in water at various concentrations and measure the methanol released from the other side of the membrane. Verbrugge utilized a two-reservoir cell to measure the methanol diffusivity through N117-H^+ in an aqueous solution of $1.0\ \mathrm{M}\ H_2SO_4$.[161] A diffusion coefficient of $1.15 \times 10^{-5}\ \mathrm{cm}^2\ \mathrm{s}^{-1}$ was obtained. Comparison with the dilute solution value of $1.6 \times 10^{-5}\ \mathrm{cm}^2\ \mathrm{s}^{-1}$ at 25 °C in water showed that methanol transport through the membrane was extremely facile.

Several different techniques have been used to measure the diffusion of methanol through Nafion® membranes. Kauranen and Skou used an electrochemical technique to measure the methanol permeability in N117 membranes in the presence of $2.0\ \mathrm{M}\ H_2SO_4$ solutions.[162] The anodic peak current measured at electrodes in adjacent liquid solutions was used to calculate a diffusion coefficient of $4.9 \times 10^{-6}\ \mathrm{cm}^2\ \mathrm{s}^{-1}$ at 60 °C with an activation energy of $12\ \mathrm{kJ\ mol}^{-1}$. Techniques such as this one that involve electrochemical measurements in adjacent solutions are straightforward experimentally but the transport properties in the membrane phase are affected by the electrolyte solution present. Ren and co-workers measured both water and methanol diffusion coefficients in N117-H^+ membranes exposed to 1.0 M methanol solutions using the PFG NMR technique.[97] The methanol self-diffusion coefficient was $6 \times 10^{-6}\ \mathrm{cm}^2\ \mathrm{s}^{-1}$ and roughly independent of concentration over the range of 0.5–8.0 M at 30 °C. A diffusion coefficient for water of $1 \times 10^{-5}\ \mathrm{cm}^2\ \mathrm{s}^{-1}$ was measured similar to the value in other studies. Measurements of methanol diffusion over the temperature range of 30–130 °C yielded an activation energy of $20.1\ \mathrm{kJ\ mol}^{-1}$ for the diffusion process.

Useful information on the transport behavior of Nafion® membranes is often found from non-fuel cell studies due to the many non-electrochemical uses of Nafion® membranes such as dryers and permselective membranes. Cabasso and co-workers examined the use of Nafion® membranes and hollow fibers in the separation of water/alcohol mixtures.[163, 164] They found that the permeation and selectivity behavior of the membranes depended strongly on the ionomer's cationic form. The permeate flux decreased and the water selectivity increased as the atomic number of the alkali cation form increased. Additionally, alkyl ammonium-exchanged membranes exhibited a higher permeate flux and selectivity than alkali metal cation-exchanged systems.

7.3 Electroosmotic drag coefficient

Transport processes in a system composed of three components, in this case water, protons, and a negatively charged polymer, should be characterized fully by three independent transport properties. These properties can be chosen to be the ionic conductivity, the water diffusion coefficient, and a third property representative of the influence of the electric field on water transport. This third property is generally referred to as either the water electroosmotic drag coefficient or the transport number of water. As with the other transport properties, this coefficient has significant practical influence on the operation of fuel cells. As the operating current density is increased in the cell, water transport due to drag increases proportionally and can exceed the ability of diffusion to redistribute the water across the membrane. This process leads to drying out at the anode side of the cell, and increases in membrane resistivity.

Several methods have been utilized in the literature to measure drag coefficients for water in Nafion® membranes including streaming potential, concentration cells, and water flux measurements. As with measurement of any transport or transference number, this property is challenging to extract accurately because its presence creates concentration gradients that lead to diffusion which can obscure the electroosmotic drag process. The key challenge of these measurements is thus the separation of electroosmotic drag from diffusional transport. The electroosmotic drag coefficient has been defined as the ratio of the flux of water through the membrane to the flux of protons in the absence of water concentration gradients. Equation (10) illustrates the equality of the water drag coefficient with the water transport number (t_0^{m}/z_0) for an acid-form Nafion® membrane as can be shown using concentrated solution theory.[111]

$$\xi = \frac{N_0}{N_+} = \frac{t_0 z_+}{z_0 t_+} = \frac{t_0}{z_0} \tag{10}$$

In the expression above, the subscript 0 refers to water and the + to protons; z is the valences of the species, t is the transference numbers, and N the molar fluxes.

Early methods to measure ξ were based on measurements of the water flux across the membrane at constant current with the membrane exposed to liquid water or aqueous solutions on both sides. The assumption here is that the water content is equal across the membrane due to the equilibrium conditions at each boundary. While this may be true for low values of the current density, it is an assumption that is inherently difficult to verify and certainly breaks down at low water contents within the membrane making measurements of ξ over the full range of water contents impossible. The resulting water drag coefficients tend to underestimate the true value, often values in the range 0.3–1.0 are found using this approach.[165] Although this technique is not appropriate for accurate physical property measurements, due to its simplicity it is still pursued in some cases as a means to compare between different membranes.

Fuller and Newman presented an early technique for extracting drag coefficients based on an equilibrium measurement of the potential of a concentration cell created by exposing a N117-H^+ membrane to a different water activity on either side.[166] The difference in water activities leads to the imposition of a potential gradient across the membrane that can be related to the drag coefficient. The measurement requires the slope of a plot of potential versus activity difference to extract ξ and requires a significant amount of time for equilibrium to be reached at each data point. The resulting drag coefficient was 1.4 at $\lambda = 11$ and 25 °C and decreased sharply below $\lambda = 5$ towards a value of zero. These authors utilized the second law of thermodynamics to demonstrate that the drag coefficient must be bounded by zero and the value of α, at a given water content. This implies that ξ must go to zero as the membrane dries out. The physical explanation for this condition is based on the understanding that ξ is related to the ratio of fluxes of water and protons and values of ξ larger than λ would imply that the membrane is accelerating rather than retarding the flow of water.

The traditional measurement of water flux across the Nafion® membrane under conditions of zero concentration gradient was utilized by Zawodzinski *et al.* to measure drag coefficients at two different water contents.[67] The technique utilized two identical Pd hydride electrodes pressed against the membrane to pass current. The water carried through the membrane was monitored by measuring the height on capillary columns during the experiments. Constant water activities were set on either side of the membrane to assure that no diffusional process occurred. These measurements resulted in electroosmotic drag coefficients of 2.5–2.9 at 30 °C with a fully hydrated N117-H^+ membrane having a water content of $\lambda = 22$. Similarly, a value of 0.9 was obtained from a membrane having a water content of $\lambda = 11$.

The technique of Fuller and Newman was applied by Zawodzinski *et al.* in a later publication to measure electroosmotic drag coefficients for N117-H^+ over a wide range of water contents.[167] These authors found straight-line behavior for the potential difference as a function of the ratio of water activities giving a value of 1.0 for the drag coefficient over the full range of vapor-phase water contents ($\lambda = 1-14$). The results were interpreted as indicating that each proton travels through the membrane with a single bound water molecule when the membrane is equilibrated with vapor-phase water. Earlier measurements of the drag coefficient when exposed to liquid water gave a value of 2.5 for $\lambda = 22$. This previous result is an indication of a transition to a different state with a much more swollen pore structure leading to proton transport more analogous to membrane-free aqueous solutions. Figure 5 illustrates

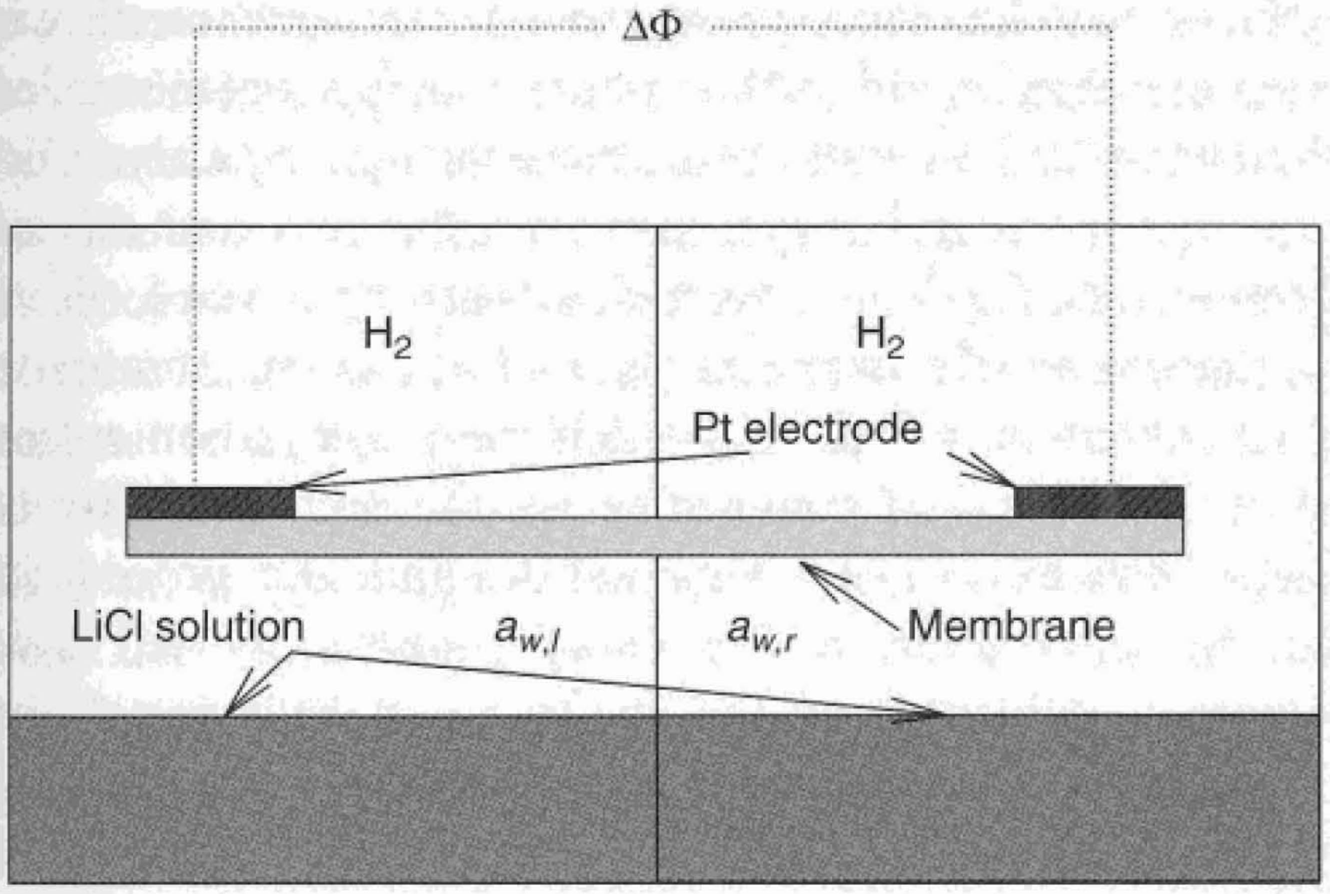

Figure 5. Schematic of experimental arrangement for concentration cell measurements of drag coefficient by Zawodzinski *et al.*[167] If we keep $a_{w,l}$ constant and measure $\Delta\Phi$, this equation will determine the relation between ξ and $a_{w,r}$. The local slope of a plot of normalized potential (in the form $F\Delta/RT$) vs. the logarithm of the ratio of water activity is the electroosmotic coefficient $\xi = \xi(a_{w,r}) = \xi(\lambda)$.

$$\xi(a_{w,r}) = F/RT[d(\Delta\Phi)/d\ln(a_{w,r}/a_{w,l})]$$

the schematic process utilized for measurement of drag coefficients.

Okada and co-workers have pioneered the application of the streaming potential technique to measure the transport properties of water in Nafion® membranes.[168] This technique is based on the imposition of a pressure difference between aqueous electrolyte solutions on either side of the Nafion® membrane and measurement of the resulting potential difference. The transport number can be extracted from the slope of a plot of potential difference as a function of pressure drop. Membranes with a variety of cationic forms were studied to illustrate the changes in water drag brought about by the charge carrier. In these measurements, a 0.03 N metal chloride solution is exposed to either side of the membrane. The transport number for N117-H^+ was shown to equal 2.6 for a fully-hydrated membrane ($\lambda = 21$) based on this method. The temperature dependence of the transport number reported in another publication increased modestly with temperature to a value of 3.2 at 80 °C.[159] Values for other monovalent and divalent cations were much higher, for example 15.6 for N117-Li^+ and 12.3 for N117-Ca^{2+}. For these alkali and alkali earth cations, the transport number of water was lower than the measured water content as is required by thermodynamic considerations.[166] The measured water transport numbers correlated with the surface charge density of the various cations, with higher charge densities leading to higher transport numbers.

Later studies by Okada and co-workers utilized hydrophobic cations based on alkyl ammonium cation exchanged membranes.[169] Unlike the previous studies, these hydrophobic cations exhibited drag coefficients higher than the respective water contents of the membranes in disagreement with the thermodynamic considerations mentioned previously. These water transport numbers increased with size of the alkyl ammonium cations unlike the results for alkali cations unless the hydrated radius was used to correlate results for the alkali cations. This implied that ions moving through hydrophilic channels pump water by physical motion through the channel, so larger-sized cations move more water.

Another new technique for measuring water drag coefficients was introduced by Ise *et al.*, based on an electrophoretic NMR approach.[170] The approach involves passing current through a thick membrane sample and measuring the phase shift of the NMR signal. Drag coefficient data for N117-H^+ at various water contents and temperatures were presented. The values for higher water contents were in good agreement with previous studies, in the 2.5–2.6 range. The value decreased with decreasing water content down to about 1.7 at $\lambda = 11$. The drag coefficient increased roughly linearly with temperature.

Table 11 compares a number of water drag coefficient values from measurements in the literature. The second of the two values based on the streaming potential measurement with an identical equilibrating solution (0.03 N

Table 11. Compilation of water electroosmotic drag coefficients in Nafion® membranes from the literature.

Membrane	Conditions	Technique	Drag coefficient	Reference
N117-H^+	H_2O liq., 30 °C, $\lambda = 22$	Water flux	2.5–2.9	[67]
N117-H^+	Water vapor, 30 °C, $\lambda = 11$	Water flux	0.9	[67]
N117-H^+	Water vapor, 25 °C, $\lambda = 14$	Conc. cell	1.4	[166]
N117-H^+	Water vapor, 30 °C, $\lambda = 1$–14	Conc. cell	1.0	[167]
N117-H^+	0.03 N HCl, 25 °C, $\lambda = 21$	Streaming potential	2.6	[168]
N117-H^+	0.03 N HCl, 80 °C, $\lambda = 21$	Streaming potential	3.2	[159]
N117-H^+	0.03 N HCl, 25 °C, $\lambda = 10$	Streaming potential	1.5	[168]
N117-H^+	H_2O liq., 25 °C, $\lambda = 19$	ENMR	2.6	[170]
N117-H^+	Water vapor, 25 °C, $\lambda = 11$	ENMR	1.7	[170]

HCl at 25 °C) but a lower water content ($\lambda = 10$) was prepared by dehydrating the membrane through extensive drying followed by reexposure to the electrolyte solution. One might summarize the data in Table 11 as demonstrating that despite modest variations between researchers, there is general agreement that 100% RH vapor-phase equilibrated drag coefficients are in the 0.9–1.7 range and liquid water equilibrated values are in the 2.5–3.2 range.

Water drag coefficients in DMFCs are more readily measurable using a technique described by Ren and Gottesfeld.[171] They took advantage of the fact that both sides of the cell can be equilibrated with liquid water under conditions of high current densities and hence the drag coefficient can be extracted from measurements of water flux across the cell. They operated cells with 1.0 M methanol at the anode side and dry oxygen at the cathode and characterized a variety of ionomer membranes including N117, 940 EW, 1000 EW, and 1200 EW Nafion® membranes and an 800 EW Dow membrane. By plotting water flux versus current density, a linear portion is found at high current densities where the water activity at the cathode is unity and diffusion no longer contributes to the water flux. These measurements allow the drag coefficient to be calculated over a range of operating temperatures. Based on their results, the water drag coefficient increased with increasing temperature from 20 to 120 °C for all membranes tested. The drag coefficient also increased with decreasing EW from about 2 to about 2.5 from a 1200 EW to a 940 EW Nafion® membrane. The exception to this was the short side chain 800 EW Dow ionomer which had a lower drag coefficient than the Nafion® membranes suggesting higher crystallinity or less formation of large ionic clusters/pores where water flow is not impeded. The drag coefficient for N117 increased from about 1.9 to about 5.0 when temperature increased from 20 to 120 °C. A fully hydrated Nafion® membrane had a larger drag coefficient than a vacuum-dried Nafion® membrane. These results were interpreted to indicate that membrane crystallinity interferes with the formation of regions of bulk water where a larger drag effect is realized; drying the membrane to reduce the regions of bulk water consequently reduces drag in a similar manner.

7.4 Solubility and diffusion of gases

The solubility and transport behavior of oxygen and hydrogen gases in the Nafion® membrane are important for application in fuel cells as these gases must reach the active catalyst surface for the system to operate. A number of studies of the transport behavior of these gases have been done over the years, generally employing electrochemical measurements based on chronoamperometry or voltammetry. The fuel cell membrane–electrode interface is often modeled as a thin-film system, where a water-swollen Nafion® solution-coated film covers the active catalyst surface and the reactant gas must dissolve into and diffuse through this region to reach the electrode surface. From the earliest experiments comparing Nafion® membranes to other ionomers, it was found that the fluorocarbon region of the polymer was responsible for the high solubility of gases such as oxygen. This implies that the procedures used to cast membranes or solution-cast films will have important influences on the gas transport behavior as the crystallinity of the films can be influenced by the preparation procedures.

In two separate studies, Yeo and McBreen and Ogumi *et al.* characterized the solubility and diffusivity of hydrogen and oxygen gas in the N120 membrane. While this membrane has a higher EW (1200 g eq^{-1}) than the more commonly employed membranes used in PEMFCs, the physical property data for these gases should represent a good starting point for current research. Ogumi reported that the oxygen diffusion coefficient in N120 depended on temperature in the following manner[172]

$$\mathrm{D(O_2)} = 3.1 \times 10^{-3} \exp\left(\frac{-2768}{T}\right) \tag{11}$$

with T in units of Kelvin and D in cm^2 s^{-1}. This expression equates to a value of 1.22×10^{-6} cm^2 s^{-1} at 80 °C. Similarly, Yeo and McBreen reported the following diffusivity for hydrogen in N120[173]

$$\mathrm{D(H_2)} = 4.1 \times 10^{-3} \exp\left(\frac{-2602}{T}\right) \tag{12}$$

with T and D in the same units used in equation (11) which equates to 2.59×10^{-6} cm^2 s^{-1} at 80 °C. The oxygen solubility was reported by Ogumi and translated into a Henry's law expression by Bernardi *et al.*, as follows:[114]

$$\ln K(\mathrm{O_2}) = \frac{666}{T} + 14.1 \tag{13}$$

with K in units of atm cm^3 mol^{-1} and T in Kelvin. Yeo and McBreen reported H_2 solubility at 25 °C in N120;[173] these data were used to determine a Henry's law constant of 4.5×10^4.[114]

Another common system for studying gas solubility is the Pt microelectrode. Often this is combined with Nafion® solution-cast films or Nafion® membranes and used for characterization of electrode kinetics and gas transport. Slow-sweep voltammetry or chronoamperometry can be used to estimate the concentration of dissolved gas and the diffusion coefficient to the electrode surface. These experiments can be done without supporting electrolytes and under exposure to either liquid or vapor-phase water. Parthasarathy *et al.* performed one of the earliest and broadest studies of the oxygen transport behavior in Nafion® membranes using a microelectrode-based cell over a temperature range of 30–80 °C.[141] They employed chronoamperometric plots of i (i = current density) versus $t^{-1/2}$ (t = time) to extract the diffusion coefficient and solubility of oxygen in Nafion® membranes and solution-cast films. The temperature dependence of the oxygen diffusion coefficient in Nafion® membranes exhibited two regions both showing Arrhenius behavior but with a change in slope around 40 °C. The oxygen diffusion coefficient had a value of $9.95 \times 10^{-7}\,\mathrm{cm^2\,s^{-1}}$ at 30 °C increasing to $8.70 \times 10^{-6}\,\mathrm{cm^2\,s^{-1}}$ at 80 °C. The solubility was $9.34 \times 10^{-6}\,\mathrm{mol\,cm^{-3}}$ at 30 °C decreasing to $4.43 \times 10^{-6}\,\mathrm{mol\,cm^{-3}}$ at 80 °C. The product of diffusion coefficient and solubility, a parameter of practical importance for mass-transport processes, increased with temperature. The activation energy for diffusion was $23.8\,\mathrm{kJ\,mol^{-1}}$ over the temperature range of 40–80 °C. Using the same technique, these authors found an oxygen diffusion coefficient of $2 \times 10^{-6}\,\mathrm{cm^2\,s^{-1}}$ and a solubility of $3.8 \times 10^{-6}\,\mathrm{mol\,cm^{-3}}$ under ambient conditions for a Nafion® solution-cast film immersed into phosphoric acid.[174] The higher diffusion coefficient and lower solubility were attributed to the substantially higher water content in this system.

A more recent microelectrode study of the oxygen reduction reaction kinetics and oxygen diffusion and solubility behavior was carried out by Beattie *et al.*, for purposes of comparing N117 to a new experimental ionomer membrane.[175] These authors also utilized chronoamperometry to measure the oxygen diffusion coefficient and solubility as functions of temperature. The oxygen diffusion coefficient increased with temperature while the solubility decreased with temperature. The diffusion coefficient was $5.96 \times 10^{-6}\,\mathrm{cm^2\,s^{-1}}$ at 30 °C and increased to $1.31 \times 10^{-5}\,\mathrm{cm^2\,s^{-1}}$ at 70 °C, somewhat higher than the values reported previously. Their oxygen solubility data, on the other hand, were of the same order as the earlier study by Parthasarathy. These authors found an Arrhenius behavior for the diffusion process but with two slopes and a break in the region of 50 °C.

Another electrochemical technique that can be used to measure the transport behavior of gases is the measurement of limiting currents at electrodes. Haug and White used this approach to measure the oxygen diffusion coefficient and solubility in N117-H^+ at 25 °C.[176] They solved the diffusion equation analytically to give an expression for the time-dependent current density that was used to fit the values of the two unknown parameters. Their technique resulted in a diffusion coefficient of $0.62 \times 10^{-6}\,\mathrm{cm^2\,s^{-1}}$ and an oxygen solubility of $18.7 \times 10^{-6}\,\mathrm{mol\,cm^{-3}}$. These values compared reasonably well to the data of Parthasarthy *et al.* In some cases it may be preferred to study the gas solubility and diffusion in recast ionomer films rather than in Nafion® membranes. A cell design employing a recast film coated on a microelectrode was described by Uribe *et al.*, without the use of any supporting electrolyte.[136] Although these authors focused on the kinetics of the oxygen reduction reaction, their cell design could also be used for transport studies.

8 NEW DIRECTIONS IN PERFLUORINATED IONOMER MEMBRANE SYNTHESIS

Much of the fundamental research carried out on Nafion® membranes has the purpose of relating ionomer structure to physical and transport properties of the membrane. This research is based on the belief that a deeper understanding of this relationship will allow synthetic chemists to create novel ionomer membranes with improved physical properties. A challenge exists in that a limited number of chemical structures are available for the ionic side chains of perfluorinated ionomers and this limits the flexibility that one has in devising new polymers. It is highly likely that for some future fuel cell applications it will not be necessary to utilize perfluorinated ionomers, and this degree of freedom will open up new avenues for polymer synthesis expanding far beyond what is possible with perfluorinated systems.

The most common approaches for synthesis of new ionomers are the modification of either the backbone or side chain structure. If one believes that non-perfluorinated ionomers have sufficient stability to withstand fuel cell operating conditions, then a nearly infinite number of structures can be created and tested. On the other hand, perfluorinated ionomers do not present as large a selection of novel structures:

- The backbone is generally composed of monomers such as TFE, hexafluoropropylene (HFP), none of which offer much opportunity for crosslinking or controlled branching.
- The side chain can be varying in length, degree of branching, presence of functional groups such as ether linkages, and the type of anion group.

Several modifications to the anion group within the side chain are not generally pursued due to the belief that they would disrupt ionomer cluster formation. These include placement of the anion group within the polymer main chain, side chains with multiple anion groups, or placement of the anion group on the side chain somewhere other than on the unteathered end, all of which would restrict anion mobility. Accessibility of the anion end groups to one another is also determined partially by side chain mobility, so side chains need to have a certain minimum length for a given number density or concentration within the polymer. Clearly the number of possible structures is still vastly greater than the number that have been synthesized and characterized in practice, so these recommendations on structure should be viewed with some skepticism. These considerations do not preclude the use of any number of novel anion groups such as those listed earlier in Table 3, nor do they indicate the optimum side chain length or structure from the standpoint of the number of perfluoroether or other linkages.

In addition to novel polymer structures approached from a molecular standpoint, a tremendous number of novel structures can be created using new film formation procedures and polymer pretreatments for any given ionomer. Also, composite systems that contain a given ionomer combined with other additives, blends with other polymers, or fillers present a rich variety of systems for discovery research. As many of the exciting developments in novel ionomers are already covered fully in other sections, we provide only a brief overview with a focus on new directions in polymer synthesis for improved ionomer structures.

The patent literature contains the most extensive description of novel ionomer systems that have been synthesized within industrial research laboratories as well as data on physical properties such as ionic conductivity of many of these ionomers. Clearly the basic variations in the Nafion® membrane copolymer of TFE and PSEPVE have been well studied over the years. Copolymers with a large range of EWs, terpolymers with other monomers, and certain simple modifications to the side chain have been reported. One of the more powerful means for improving conductivity under certain conditions such as in the presence of poor dielectric media (e.g., organic solvents) is the use of stronger acid groups such as the perfluorosulfonimide and perfluorosulfonyl methide (carbon anion) groups.

The first published study of the use of acid-form perfluorosulfonimide-based ionomers for fuel cell applications appeared in 1993 from Appleby *et al.*, using ionomers synthesized within the DesMarteau group.[177] Sulfonimide-containing ionenes of the form CF_3–$[CF_2SO_2NHSO_2CF_2]_n$–CF_3 with n up to 40 were synthesized from CF_3SO_2F and NH_3 in a five-step process. Carbon anion ionenes were also attempted using the same synthetic route but could not be synthesized. The $n = 40$ sulfonimide ionene was a stable, whitish-colored solid with a high solubility in water expected to have the excellent chemical stability and inertness of Nafion® membranes but with higher conductivity and potentially superior oxygen reduction kinetics due to the stronger and more densely packed acid groups. Ionic conductivity was high, greater than $0.1\ \mathrm{S\ cm^{-1}}$ up to 90 °C, but then dropped steadily over 100 °C and reached an approximate value of $0.004\ \mathrm{S\ cm^{-1}}$ at 130 °C. These results demonstrated that the perfluorinated sulfonimide ionenes required water for proton transport in a similar manner to other perfluorinated ionomers and will lose conductivity at temperatures over the boiling point of water.

Over the last several years, the DesMarteau research group has synthesized a variety of perfluorinated ionomers and ionenes having sulfonimide and related strong acid sites. DesMarteau has described a number of the challenges faced by researchers working in this field.[26] One is the problem of obtaining the necessary purified functional monomers for the polymerization processes. For example, synthesis of the most commonly used monomer within the DesMarteau group research, the PSEPVE-sulfonimide analogue $CF_2{=}CFOCF_2CF(CF_3)OCF_2CF_2SO_2N(Na)SO_2CF_3$, begins with rather expensive and exotic reactants ($SO_2N(Na)SiMe_3$ and $FSO_2(CF_2)_4SO_2F$). The copolymerization process generally employed is an aqueous redox initiation system in an emulsion polymerization. Functional monomers are used in their Na^+-salt form in this process to afford good water solubility and to control pH. Often purification requires formation of the acid-form of the monomer followed by distillation and reneutralization. In the case of the sulfonimide copolymer, the ionic monomer has been copolymerized with TFE giving a white powdery polymer capable of being pressed into films in its acid form. DesMarteau has described a number of novel ionenes of interest but cautioned that obtaining high purity products can be very challenging.

A number of studies have suggested that perfluorosulfonimide-based acid groups would present a superior electrolyte system to the sulfonic acid groups used in the commercial Nafion® membrane. Perfluorosulfonimides have the highest known gas-phase acidities of any compound while retaining excellent thermal stability and promoting good oxygen reduction kinetics. Sumner *et al.* reported conductivity data for the H^+-form sulfonimide analogue of the Nafion® membrane having an EW of about $1100\ \mathrm{g\ eq^{-1}}$.[178] The perfluorosulfonimide ionomer had an equilibrium water uptake of 116% by weight of the dry ionomer under 100% RH conditions corresponding to 70 water molecules per acid site. Ionic conductivity versus % RH was consistently higher than N117 by a margin of about ×2 until very low %RH at which point the sulfonimide polymer achieved over an order of magnitude improvement. The temperature dependence of the ionic conductivity for both ionomers were similar and both systems showed a decreasing conductivity with increasing temperature over 60–70 °C under a fixed water partial pressure of 150 torr. The study concluded that both systems required a certain quantity of water to achieve proton transport and that the proton transport mechanism was basically the same in the two systems.

A number of modifications to the basic perfluorosulfonic acid side chain have been reported over the years, generally motivated by the desire to simplify the synthesis and polymerization process for the ionic monomer. Feiring and Rozen reported partially fluorinated ionomers consisting of TFE and $CF_2{=}CFOCH_2CF_2(CF_2)_nSO_2F$.[179] These copolymers have a shorter side chain than PSPEVE due to the absence of the second ether group. Presumably the presence of the single CH_2 linkage in the side chain will provide a relatively weak site for oxidation; however, testing would need to be done to determine whether this would have any practical negative effect within a fuel cell. It was shown that these ionomers can be produced from monomers of the form $CF_2{=}CFOCH_2CF_2(CF_2)_nSR$ by converting the end groups to sulfonyl chloride functional groups after polymerization. Another modified side chain reported by Farnham and Yang was the $CF_2{=}CF(CF_2CF_2)_nSO_2F$ group where $n = 1{-}5$.[180] The synthesis of these monomers was reported in the patent literature and polymerization with monomers such as VF2, VF2/HFP, and TFE/ethylene was described. However, these allyl monomers are difficult to copolymerize directly with TFE, making good comparisons with Nafion® membrane analogues impossible. In another patent, Yang reported ionomers based on partially fluorinated sulfonimide-type monomers of the form $CH_2{=}CH(CF_2)_nOCF_2CF_2SO_2N(M)SO_2R_f$ where M=H or alkali metal cations.[181] Copolymers with VF2, TFE/ethylene, and TFE/VF were described. Yang showed that these monomers can be prepared from $CF_3SO_2NH_2$ and $CH_2{=}CHCF_2CF_2OCF_2CF_2SO_2F$ without protection of the double bond, thus saving steps in the synthesis process.

The simplicity of styrene sulfonic acid ionomers has motivated research on variations to this system over the years. Often new approaches to locate more fluorine atoms within the structure have been attempted for purposes of alleviating the poor stability of these systems under typical fuel cell operating conditions. Feiring *et al.* reported ionic monomers based on aromatic groups such as styrenic and isophthalate monomers with pendant fluorosulfonate and fluorosulfonimide groups.[24] These monomers have the functional groups attached to the aromatic ring via an ether linkage, providing greater thermal stability and synthetic versatility than approaches without this linkage. Styrenic monomers can be polymerized using a variety of means such as anionic, cationic, coordination, free radical and living polymerization offering a wide range of polymers with novel architectures. Additionally, these monomers can be prepared by straightforward means with relatively few steps giving high yields and including the minimum desired quantity of fluorine atoms to give strong acid sites. However, it is unclear whether these ionomers would be stable enough for fuel cell applications. More highly delocalized electron withdrawing functional groups, such as sulfonimide and sulfonyl methide groups have also been attached to the aromatic group via ether linkages. Copolymerization of the novel monomer $CH_2{=}CH{-}C_6H_4{-}OCF_2CF_2SO_2N(Li)SO_2CF_3$ with acrylates, acrylonitrile, styrene, and other monomers was performed and data on some of these ionomers were reported.[182]

Another variation on the poly(styrene sulfonate) system are copolymers of α, β, β-trifluorostyrene which can be sulfonated using a number of approaches. This system was first synthesized in the 1950s and pursued for fuel cell applications in the 1960s.[183, 184] The partially fluorinated system is highly resistant to oxidative degradation, making it a substantial improvement over non-fluorinated styrenic ionomers.[185] The copolymer will commonly be crosslinked to improve mechanical performance at high levels of sulfonation where ionic conductivity and water swelling are optimized. Most recently, Ballard have introduced a family of ionomers based on copolymerization of α, β, β-trifluorostyrene and a series of substituted α, β, β-trifluorostyrene comonomers. These new ionomers are referred to as the BAM3G membrane.[186] These copolymers reportedly have good oxidative stability and can possess high water uptake and conductivity with the proper control of the degree of sulfonation and crosslinking. Among other properties, the oxygen diffusion coefficient and solubility for these polymers have been measured and reported.[175]

A number of patents have described ionomers with partially fluorinated backbones of TFE/ethylene, VF2, and vinyl fluoride (VF). Metallocene organometallic polymerization catalysts have been used to generate copolymers of ethylene and other olefinic monomers with comonomers of the form $CH_2{=}CH(CH_2)_n(CF_2)_mSO_2F$ ($n = 2$ or greater) as well as their sulfonimide and sulfonyl methide analogues.[187] While it is clear that the hydrocarbon backbone will compromise oxidative stability for these ionomers, this highly active and controllable polymerization process affords a number of means for manipulation of final polymer properties, such as solubility, mechanical strength and solvent uptake due to the control of the degree of branching and structure.

Another partially fluorinated ionomer system that has benefited from substantial development efforts are copolymers of the VF2 monomer ($CH_2{=}CF_2$). VF2 is a highly polar monomer with good stability and is relatively active in polymerization with a variety of comonomers. Its polarity imparts in its polymers a higher affinity for certain organic solvents than most other standard fluorinated monomers. Copolymers of VF2 and PSEPVE with termonomers such as TFE, CTFE, ethylene, HFP, and VF were reported.[188] The challenge in producing these ionomers is the base instability of the VF2 monomer, which is readily attacked by strong alkali solutions. The hydrolysis reaction to convert the sulfonyl fluoride precursor of the PSEPVE monomer to the fluorosulfonate group can be achieved via the use of weak carbonate bases such as aqueous carbonate solutions which attack the sulfonyl fluoride group preferentially to the VF2 backbone. The acid-form ionomer can be obtained through simple ion exchange. The patent literature contains solvent uptake and ionic conductivity data on these ionomers revealing that their ionic conductivity can reach similar levels to the Nafion® membrane. Beyond the simple fluorosulfonate ionomers, VF2 copolymers with sulfonimide and sulfonyl methide groups have also been synthesized.[189]

Ideally one would like to reduce the cost of Nafion® membranes while improving on their key performance properties such as ionic conductivity and mechanical strength in the swollen state and maintaining the desirable features such as chemical and electrochemical stability and film forming ability. A likely place to search for such an ionomer is in the short side chain Dow ionomer, as this system has shown excellent performance in fuel cell testing and its lower molecular weight holds the promise for a less expensive polymer with higher ionic conductivity. While no one has yet managed to demonstrate a synthesis of this monomer that is simple enough to realize this low-cost potential, an interesting variation was reported.[190] Blau has shown that the PSEPVE monomer's precursor cyclic sulfone can be reacted with $CF_3SO_2NNa_2$ (formed from $CF_3SO_2NH_2$ and NaH) to give the monomer $CF_2{=}CFOCF_2CF_2OSO_2N(Na)SO_2CF_3$ which is the short side chain sulfonimide variant of the Dow monomer. As this reaction makes use of a small number of steps from the cyclic sulfone, it is appealing in its simplicity compared to other approaches reported to sulfonimide monomers. Unfortunately, no fuel cell data has appeared on the TFE-based copolymers of this new monomer so one cannot yet say whether these will realize the performance potential promised by the combination of the short side chain monomer and the strong acid sulfonimide group.

9 METHANOL CROSSOVER

9.1 Methanol crossover in DMFCs

Due to several practical problems associated with hydrogen fuel, such as safe handling, storage and distribution, there has been tremendous effort in identifying alternate fuels for use in fuel cells. Methanol is considered to be one of the strong contenders since, unlike hydrogen, it offers high volumetric energy density and ease of handling the liquid fuel. Methanol as a fuel can be utilized in two ways in typical PEMFCs. Methanol is either reformed to produce hydrogen-rich gas, which is then fed into the anode structure of the PEMFC, or fed directly into the anode structure of the fuel cell where it is consumed to produce energy through electrochemical reactions. The latter approach is an attractive option since it eliminates the bulky reformers, thus increasing the overall energy efficiency as a result of system simplicity.[191] Despite these advantages, DMFC technology is not well advanced due to two major technical hurdles: the sluggish methanol oxidation reaction kinetics and methanol crossover through the membrane both significantly lower fuel cell performance.[192, 193] Since the focus is perfluorinated membranes, issues related to the Nafion® membrane are reviewed.

9.1.1 Methanol crossover in Nafion® membranes

Nafion® membranes work very well as a separator when neat hydrogen or hydrogen-rich reformed gas is used as a fuel, since diffusion of the reactant gases is negligible for practical membrane thicknesses above 25 µm. When methanol is used as a fuel in DMFC technology, the Nafion® membrane suffers from methanol crossover issues. Methanol is transported through the membrane by two modes, namely diffusion and electroosmotic drag.[194, 195] When methanol comes in contact with the membrane, it diffuses through the membrane from anode to cathode and is also dragged along with the hydrated protons under the influence of current flowing across the cell. The phenomenon of transporting methanol from anode to cathode through the membrane is known as methanol crossover. The diffusive mode of methanol transport dominates when the cell is idle, whereas the electroosmotic drag dominates when the cell is operating, meaning current flowing across the cell. Methanol that is transported to the cathode adversely affects the cathode performance.[196, 197]

9.1.2 Implications of methanol crossover in DMFC

- Methanol transported through the membrane by diffusion and electroosmotic drag recombines chemically with oxygen at the cathode and therefore, the fuel conversion efficiency is lowered;
- Methanol at the cathode depolarizes the oxygen electrode and establishes a mixed potential thus lowering the cathode potential;
- Methanol competes with the oxygen reduction reaction at the cathode and predominantly reacts with oxygen;

- This undesired reaction increases the demand for oxygen and therefore requires higher stoichiometric flow rates;
- Because of the negative impact of methanol crossover, currently DMFC developers are forced to use thicker membranes thus increasing cell resistance.

N112 membranes are preferred for hydrogen-based fuel cells since they offer lower specific resistance and help in easing water management within the cell. Unfortunately, due to very high methanol crossover rates with 2 mil membranes, N117 is currently the most desirable candidate for DMFC technology. N117 reduces the methanol crossover rate >60% compared to N112. Use of N117 not only increases the material cost, but also reduces the fuel cell performance, particularly in the high current density region (>500 mA cm^{-2}) due to the higher specific resistance. Therefore, it is important to address the membrane-related issues to advance DMFC technology to become a commercially viable alternative.

9.2 Factors affecting methanol crossover

There are several factors influencing the methanol crossover rate, namely membrane thickness, membrane EW, electrode structure and the cell operating parameters such as cell temperature, methanol feed concentration, air flow rates and cell current density. All of these factors play a significant role in methanol crossover.

9.2.1 Membrane thickness and EW

Membrane thickness and EW have a major impact on the methanol crossover rate. Several research groups have reported methanol crossover data for the various commercial Nafion® membranes.[193, 198] Although the magnitude of the crossover rate varies from one group to another, the trend is the same. The reasons for variation in the crossover data, despite using similar membranes, are differences in electrode preparation method, thickness and composition of electrode structure such as Nafion® solution to catalyst ratio, and percentage composition of Teflon® or other added components. In addition, the nature of diffusion backings, such as their relative hydrophobicity and hydrophilicity, has an influence on the crossover rate.

Figure 6 compares the methanol crossover rates for various thicknesses of Nafion® membranes (N112, N115 and N117) as well as for a given thickness (5 mil thick) of commercial (N115 and NE105) and non-commercial EW Nafion® membranes (1200 and 1500 EW) relative to a 2 mil commercial (N112) membrane.[199] As shown in the figure, the methanol crossover rate decreases with increasing membrane thickness. The methanol crossover rate is reduced more than 60% going from 2 to 7 mil thick membranes. Also, for a given thickness of membrane (5 mil), the crossover rate decreases with increasing EW of the Nafion® membrane. The crossover rate can be reduced as much as 85% by employing 1500 EW membranes compared to N112.

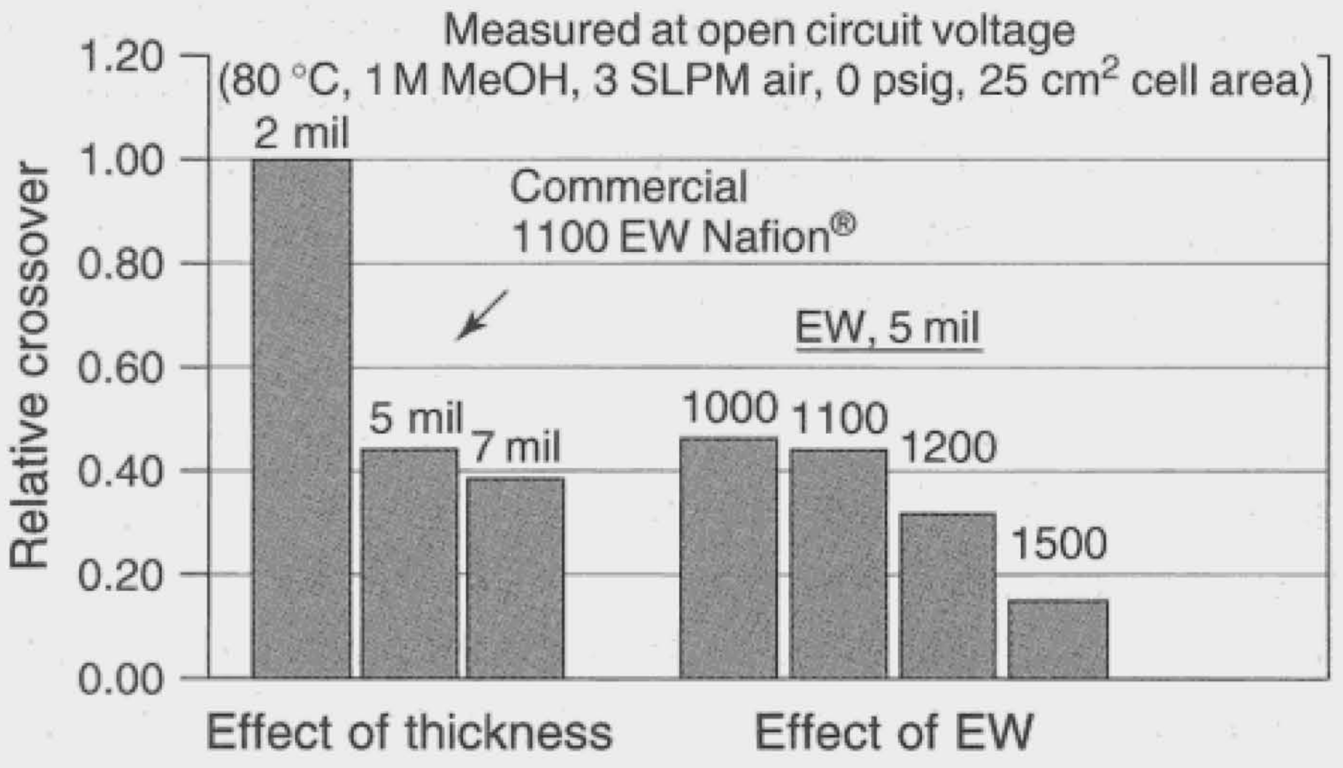

Figure 6. Effect of membrane thickness and EW on methanol crossover rate, operating the cell with 1 M methanol at 80 °C and 3 standard L/min air with 25 cm^2 active area.

Therefore, it may be advantageous to use either a thicker membrane or a higher EW membrane to reduce the methanol crossover rate. However, the disadvantage is the penalty of paying higher voltage losses due to higher specific resistance as a result of thicker and higher EW membranes. The voltage loss is particularly severe at higher current density operation. An optimum membrane should be determined for a given application after carefully reviewing the combined effects of specific conductivity and methanol crossover rate. For example, it is beneficial to use thicker or higher EW membranes for applications relating to consumer electronics, which require very low current and power densities where the voltage loss is negligible and also the fuel efficiency increases as a result of lower methanol crossover rates. On the other hand, thinner membranes would be beneficial for applications relating to higher current density/power density requirements since the voltage loss due to specific conductance is critical. Higher fuel efficiency could also be achieved by operating the cell at higher current densities since the methanol crossover rate is greatly reduced.[193, 200, 201]

As previously mentioned, the electrode structures, particularly the methanol electrode structure and diffusion backing, play a role in influencing the methanol crossover rate, but their impact is minimal compared to other factors such as membrane thickness and membrane EW. If methanol is consumed effectively in the anode structure, the concentration of methanol at the membrane–electrode interface is significantly reduced and therefore the overall methanol crossover rate is also reduced. Increasing the thickness of the electrode structure and using more active catalysts compared to the currently used Pt/Ru black catalysts would help to reduce the methanol crossover rate.

9.2.2 Cell operating parameters

Methanol feed concentration

In theory, the DMFC cell can be operated with ∼17 M methanol/water mixtures based on theoretical stoichiometric reactions. However, the most commonly used feed concentration is 1 M methanol, since higher operating methanol concentrations (>1 M) significantly increase the methanol crossover rate as a result of higher methanol diffusion and electroosmotic drag.[193] Also there is really no advantage in operating the cell with higher methanol concentrations with the currently utilized Pt/Ru black catalysts, as the methanol oxidation reaction follows zeroth-order kinetics above the concentration of 1 M methanol which is current practice and therefore, is essentially concentration independent. However, there are some reports indicating the anode kinetics are half order for concentrations lower than 1 M methanol down to 0.01 M.[202, 203]

Even though the use of 1 M methanol is common practice today, the feed methanol concentration can be further fine-tuned depending on the current density requirements needed to achieve higher fuel efficiency since methanol crossover rate decreases with decreasing methanol feed concentration. Figure 7 shows the methanol crossover rate when operating the cell at various methanol feed concentrations ranging from 0.25 M to 1 M. The crossover rate was measured and compared both at open circuit voltage and at 200 mA cm^{-2}. The crossover rate clearly decreases with methanol feed concentration and further, for a given feed methanol concentration, the crossover rate decreases with increasing cell operating current density.[200, 204] It has been reported in the literature that methanol crossover could be totally eliminated by consuming the methanol at the anode catalyst and not letting any diffuse through the membrane. This may be achieved by feeding the cell with very low methanol concentrations (<1 M) and flow rates typically in a steady-state operation. The difficulty is finding an application that suits these operating conditions since many practical applications demand variable load changes.

While it is advantageous to operate the cell with lower methanol concentrations, the downside is the higher anode overpotential due to concentration polarization as a result of inadequate fuel supply to the reaction site and also the poor reaction kinetics as detailed previously.[205] Therefore, it is necessary to identify the optimum methanol concentration to achieve higher fuel efficiency and the required power output for a given application and stack design.

Cell temperature

Methanol crossover data generated at various temperatures ranging from room temperature to 90 °C are shown in Figure 8. The feed concentration is 1 M methanol in water. The methanol crossover rate decreases with decreasing cell temperature over the temperature range studied (90–22 °C) both at open-circuit voltage (OCV) and at the current density of 200 mA cm^{-2}. These results suggest that it is advantageous to operate the cell at lower temperature to attain higher fuel efficiency but the difficulty is attaining higher power outputs since the methanol electrode exhibits poor methanol oxidation kinetics at low temperatures.

9.3 Measurements to quantify methanol crossover

Several methods are employed to determine the methanol crossover rate in the DMFC, such as voltammetry, IR,

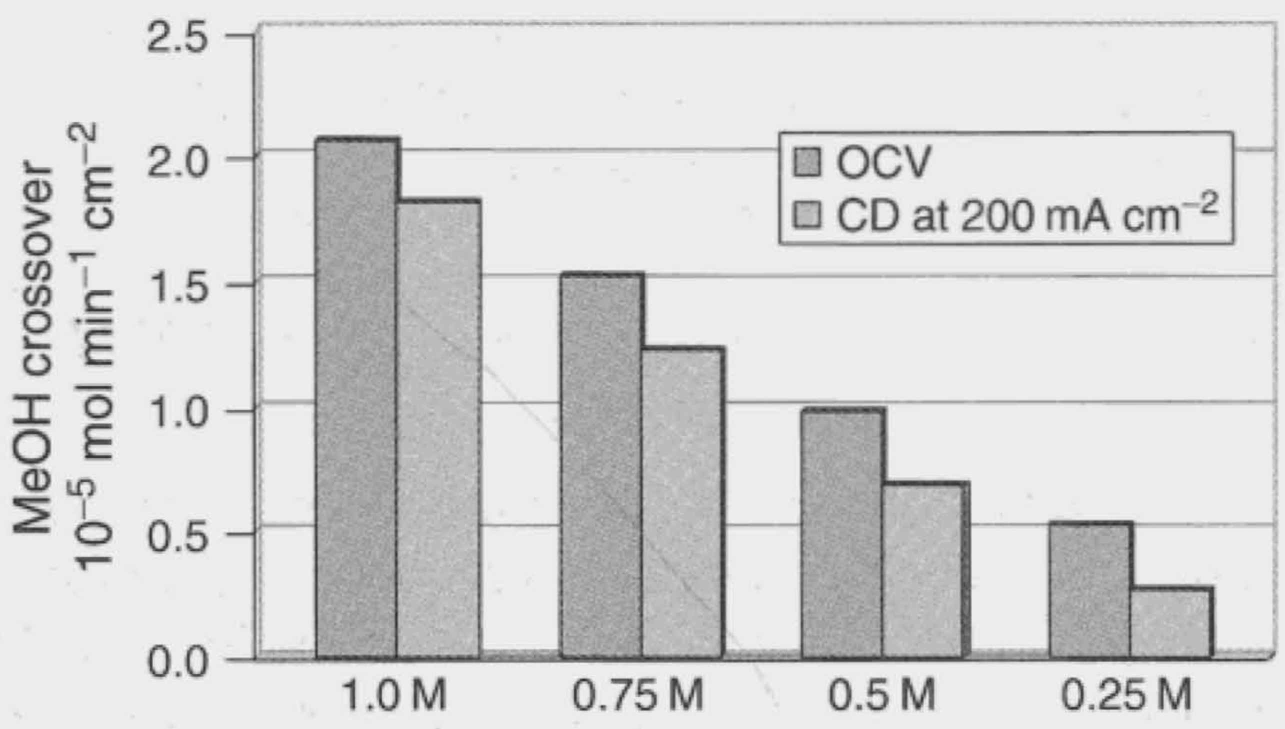

Figure 7. Effect of feed methanol concentration on methanol crossover rate at a cell operating temperature of 80 °C and a N117 membrane.

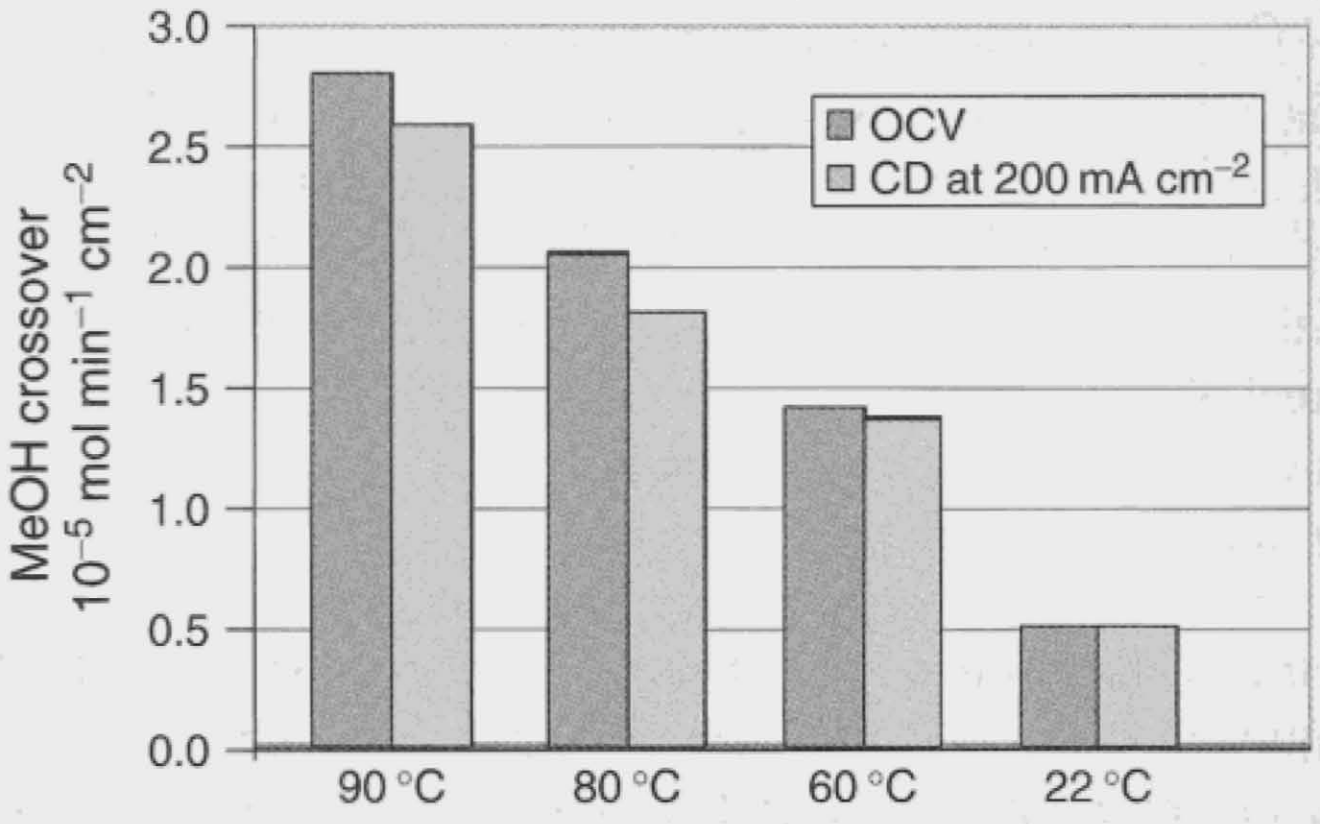

Figure 8. Effect of temperature on methanol crossover rate, operating the cell with 1 M methanol and 3 standard L/min air, at 80 °C N117 membrane, 0 psig, 25 cm^2 cell area.

NMR and gas chromatography (GC) methods. Currently both voltammetry and an optical IR method measuring the CO_2 in the cathode exit stream are the most widely used techniques. While the voltammetric method is limited to crossover measurements at open-circuit potential, the optical IR method of measuring the CO_2 in the cathode exit stream allows measurements both at open circuit and under any cell operating current density.

9.3.1 Voltammetric method

Ren and co-workers first developed the voltammetric method.[192] Standard cell hardware and membrane electrode assemblies are used for this procedure as in normal DMFC testing. But instead of air, an inert gas such as nitrogen is pumped through the positive electrode and methanol is fed through the negative electrode. Methanol that diffuses through the membrane is oxidized at the positive electrode and the protons are reduced to hydrogen at the negative electrode. The mass-transport-limited current measured from the plateau of the current–voltage voltammogram plot is the current equivalent of methanol flux across the membrane. The voltammetric method provides a very accurate measurement of methanol crossover, but the drawback is that this method cannot be used to determine the crossover rate directly in an operating fuel cell.

9.3.2 IR method

In a typical DMFC cell, the methanol transported through the membrane is oxidized at the cathode according to the reaction $CH_3OH + 3/2O_2 \rightarrow CO_2 + 2H_2O$. The methanol crossover rate can be accurately estimated by measuring the CO_2 content in the cathode exit stream. Narayanan *et al.*, developed this technique and successfully demonstrated it using a Horiba gas analyzer.[198, 201] First, the total volume of CO_2 generated was determined using the volume $\%CO_2$ read-out from the gas analyzer, then the number of $\mathrm{mol\,s^{-1}}$ of CO_2 were calculated using the ideal gas law ($PV = nRT$). The methanol crossover current density equivalent (I_x, $\mathrm{A\,cm^{-2}}$) is obtained using Faraday's law according to equation (14)

$$\mathrm{I_x} = \frac{n\mathrm{F}n_\mathrm{e}}{A} \tag{14}$$

where F is Faraday's constant, n is the number of $\mathrm{mol\,s^{-1}}$ equivalent of CO_2, n_e is the number of electrons involved in the reaction and A is the active area of the cell. As mentioned earlier, the advantage of this method is that it allows the methanol crossover rate to be determined both at open circuit and under applied loads.

There were some concerns raised about the results obtained by this procedure since part of the anode product CO_2 is believed to diffuse through the Nafion® membrane and interfere with the measurement. During cell operation a large amount of CO_2 is produced at the anode as a result of oxidation of methanol. It is possible that a portion of the CO_2 diffuses through the membrane and interferes with the CO_2 produced by the methanol crossover reaction at the cathode. The diffusion rate of anode product CO_2 through the membrane varies depending on the methanol oxidation rate or operating current density. Dohle *et al.*[206] suggested a simple method to separate the CO_2 that diffused through the membrane from the CO_2 produced as a result of methanol oxidation at the cathode. A similar cell set-up used in DMFC operation is employed, but the cathode is fed an inert gas such as nitrogen rather than air. Methanol oxidation occurs at the positive electrode and protons are transported through the membrane. Protons are reduced to hydrogen at the negative electrode under the inert atmospheric condition.

Methanol that is transported through diffusion and electroosmotic drag is unreacted at the cathode since there is no oxygen present to oxidize the methanol, and the potential of the negative electrode is too low to oxidize the methanol. Therefore, the CO_2 measured at the cathode exit stream under this condition is purely from diffusion of anode product CO_2. The true methanol crossover rate can thus be deduced from the results obtained by this method and the total CO_2 measured during the standard DMFC mode of operation.

9.4 Approaches to minimize methanol crossover

As discussed in detail, methanol crossover in perfluorinated membranes is a major concern and unavoidable as long as the membrane requires water for its best performance. The general strategies found in the literature to minimize the methanol crossover rate to achieve higher fuel and power efficiency using Nafion® perfluorinated ionomer membranes are discussed in this section.

9.4.1 Methanol concentration and cell operating temperature

The best strategy known to date to minimize the methanol crossover rate using Nafion® membrane-based cells is to operate the cell with lower methanol concentrations (<2 M) and temperatures.[193, 198, 207] Operating the cell with lower temperatures is advantageous, and the crossover rate could be, for example, reduced by as much as 50% by operating the cell at 60 °C rather than 90 °C.

9.4.2 Lean feed method

Zelenay *et al.* demonstrated that higher fuel efficiency could be achieved with a lean anode feed operation.[208] Both methanol feed concentration, to a larger extent, and methanol flow rate, to a lesser extent, were adjusted to obtain >90% fuel efficiency. The simple concept is to oxidize the majority of methanol that diffuses through the anode catalyst layer, thus reducing the presence of methanol adjacent to the membrane at the anode. This results in a lowered methanol concentration gradient across the membrane and consequently decreases the methanol crossover rate.

9.4.3 Methanol tolerant cathode catalyst

There are some efforts to use methanol-insensitive oxygen reduction catalysts to improve the cathode potential.[209, 210] See **Poisons for the O_2 reduction reaction**, Volume 2, for more information on this topic. They generally consist of macrocycles based on transition metal ions. Numerous macrocyclic compounds have been reported to show no activity towards methanol during the oxygen reduction reaction. However, such compounds have problems with respect to long-term stability and temperature. In addition their activity towards the oxygen reduction reaction is significantly lower compared to Pt-based catalyst structures. Therefore, achieving higher power output with these catalysts is quite challenging.

9.4.4 Filler approach

Approaches to modify the existing Nafion® membranes have been explored by a large number of research groups since so much is known about this basic membrane, and its structure provides numerous means for chemical and physical modification. Some of the approaches taken include incorporating inorganic proton conductors such as zirconium phosphate and silica.[211, 212] While lower methanol crossover is reported compared to the neat membrane for these composite structures, the membrane resistance increases as a result of impregnation of those compounds. These approaches are still useful for low-power fuel cell applications.

9.4.5 Blend membranes

Blended membranes are yet another way of reducing the methanol crossover. Composite membranes utilizing Nafion® membranes and polybenzimidazole (PBI) have been studied, taking advantage of the Nafion® membrane stability and conductivity and PBI's reported absence of electroosmotic drag.[213]

9.4.6 Alternate high EW membranes

The commercial Nafion® membranes currently offered are based on nominal 1100 EW polymer. Higher EW membranes lower the methanol crossover.[198, 199, 214] However, the downside is the higher membrane resistance as detailed earlier. An optimum EW membrane is possible with an acceptable trade-off between conductivity and crossover.

10 FINAL COMMENTS

The PEMFC based on polymeric ion-exchange membrane resins is approaching its 50th anniversary. The industry has nearly 35 years of experience with the use of the Nafion® perfluorinated ionomer membrane in PEMFCs. The tremendous experience and knowledge base built up over these decades on perfluorinated ionomer membrane-based fuel cells, and their steadily increasing performance over the years, confirms that these systems are likely to be the membrane of choice in PEMFCs for many years to come. The drawbacks of perfluorinated ionomer membranes such as poor elevated temperature (>90 °C) performance, oxidative degradation under relatively dry conditions, high cost, and permeability to methanol, are likely to fade in significance over time as solutions are engineered into commercial fuel cell systems to circumvent these problems.

As large-scale commercial applications of PEMFCs move closer to reality, the fundamental issues that see the greatest level of study will shift to studies of the lifetime and failure modes of these materials. Equally important will be deeper study of the optimal triple-phase boundary, and transport in composite systems essential for optimization of catalyst performance and utilization. Ultimately, as costs of perfluorinated ionomers decrease, precious metal usage will remain a fundamental limiter of system cost. Finally, novel ionomer structures with lower EW but structural stability, higher acidity, and lower cost will continue to be studied. Eventually, engineered materials may contain ion channels ideally suited to fast proton transport in relatively anhydrous conditions and operating effectively at temperatures in excess of 100 °C. This future state will only be possible through a better understanding of polymer nanostructures and their relationship to the mechanisms of proton transport.

REFERENCES

1. T. D. Gierke and W. Y. Hsu, in 'Perfluorinated Ionomer Membranes', A. Eisenberg and H. L. Yeager (Eds), ACS Symposium Series, No. 180, Ch. 13, p. 283 (1982).

2. G. Pourcelly and C. Gavach, in 'Proton Conductors, Solids, Membranes, and Gels-Materials and Devices', P. Colomban (Ed), Cambridge University Press, Cambridge (1992).
3. C. Heitner-Wirguin, *J. Membr. Sci.*, **120**, 1 (1996).
4. W. G. Grot, *Macromol. Symp.*, **82**, 161 (1994).
5. R. E. Fernandez, 'Perfluorinated ionomers', in "Polymer Data Handbook", Oxford University Press, Oxford, pp. 233–236 (1999).
6. S. A. Perusich and S. M. Reddy, *J. Appl. Electrochem.*, **31**, 421 (2001).
7. J. T. Hinatsu, M. Mizuhata and H. Takenaka, *J. Electrochem. Soc.*, **141**, 1493 (1994).
8. W. T. Grubb and L. W. Niedrach, *J. Electrochem. Soc.*, **107**, 131 (1960).
9. E. J. Cairns, D. L. Douglas and L. W. Niedrach, *AIChE J.*, **7**, 551 (1961).
10. *Chem. Eng. News*, Aug. 27, p. 15 (1973).
11. D. A. Hounshell and J. K. Smith, Jr, 'Science and Corporate Strategy – DuPont R&D, 1902–1980', Cambridge University Press, Cambridge, UK (1988).
12. K. Johns and G. Stead, *J. Fluorine Chem.*, **104**, 5 (2000).
13. T. Tervoort, J. Visjager, B. Graf and P. Smith, *Macromolecules*, **33**, 6460 (2000).
14. J. W. Weidner and M. Doyle, *J. Electrochem. Soc.*, **147**, 3953 (2000).
15. O. Savadogo, *J. New Mater. Electrochem. Syst.*, **1**, 47 (1998).
16. S. Motupally, D. T. Mah, F. J. Freire and J. W. Weidner, *Interface*, **Fall Issue**, 32 (1998).
17. DuPont, US Patent No. 5,411,641 (1995).
18. D. Eames and J. Newman, *J. Electrochem. Soc.*, **142**, 3619 (1995).
19. *Engineering Review*, January/February, p. 64 (2000).
20. D. J. Vaughan, *DuPont Innovation*, **4**, 10 (1973).
21. D. J. Connolly and W. F. Gresham, US Patent No. 3,282,875, to DuPont (1966).
22. D. P. Carlson, US Patent No. 3,528,954, to DuPont (1970).
23. Yu. E. Kirsh, S. A. Smirnov, Yu. M. Popkov and S. F. Timashev, *Russ. Chem. Rev.*, **59**, 560 (1990).
24. A. E. Feiring, S. K. Choi, M. Doyle and E. R. Wonchoba, *Macromolecules*, **33**, 9262 (2000).
25. C. Stone, T. S. Daynard, L.-Q. Hu, C. Mah and A. E. Steck, *J. New Mater. Electrochem. Syst.*, **3**, 43 (2000).
26. D. D. DesMarteau, *J. Fluorine. Chem.*, **72**, 203 (1995).
27. M. Doyle, M. E. Lewittes, M. G. Roelofs, S. A. Perusich and R. E. Lowrey, *J. Membr. Sci.*, **184**, 257 (2001).
28. S. A. Perusich, *Macromolecules*, **33**, 3437 (2000).
29. H. A. Wittcoff and B. G. Reuben, 'Industrial Organic Chemicals', John Wiley & Sons, New York, p. 408 (1996).
30. DuPont Press Release, Feb. 24 (1998).
31. M. Waidhas, A. Datz, U. Gebhardt, R. v. Helmolt, R. Hornung and G. Luft, *Mater. Res. Soc. Symp. Proc.*, **575**, 229 (2000).
32. T. R. Ralph, G. A. Hards, J. E. Keating, S. A. Campbell, D. P. Wilkinson, M. Davis, J. St-Pierre and M. C. Johnson, *J. Electrochem. Soc.*, **144**, 3845 (1997).
33. Y. A. Dyakov and Y. K. Tovbin, *Russ. Chem. Bull.*, **44**, 1186 (1995).
34. W. Y. Hsu and T. D. Gierke, *J. Membr. Sci.*, **13**, 307 (1983).
35. R. Wodzki, A. Narebska and W. K. Nioch, *J. Appl. Polm. Sci.*, **30**, 769 (1985).
36. M. W. Verbrugge and P. N. Pintauro, in 'Modern Aspects of Electrochemistry', B. E. Conway, J. O.'M. Bockris and R. E. White (Eds), Plenum Press, New York, Vol. 19 (1989).
37. X.-D. Din and E. E. Michaelides, *AIChE J.*, **44**(1), 35 (1998).
38. S. J. Paddison, D. W. Reagor and T. A. Zawodzinski, Jr, *J. Electroanal. Chem.*, **459**, 91 (1998).
39. S. J. Paddison and T. A. Zawodzinski, Jr, *Solid State Ionics*, **113**, 333 (1998).
40. S. J. Paddison, L. R. Pratt and T. A. Zawodzinski, Jr, *J. New Mater. Electrochem. Syst.*, **2**, 183 (1999).
41. A. Eisenberg and J.-S. Kim, 'Introduction to Ionomers', John Wiley & Sons, New York (1998).
42. K. A. Mauritz, *Macromol. Chem. Phys.*, **C28**(1), 65 (1988).
43. T. D. Gierke, G. E. Munn and F. C. Wilson, *J. Polym. Sci., Polym. Phys.*, **19**, 1687 (1981).
44. H. L. Yeager and A. Steck, *J. Electrochem. Soc.*, **128**, 1880 (1981).
45. A. Eisenberg, B. Hird and R. B. Moore, *Macromolecules*, **23**, 4098 (1990).
46. M. Fujimura, T. Hashimoto and H. Kawai, *Macromolecules*, **14**, 1309 (1981).
47. H.-G. Haubold, Th. Vad, H. Jungbluth and P. Hiller, *Electrochim. Acta*, **46**, 1559 (2001).
48. W. G. Grot, European Patent No. 0 066 369, to DuPont (1982).
49. C. R. Martin, T. A. Rhoades and J. A. Ferguson, *Anal. Chem.*, **54**, 1639 (1982).
50. P. Aldebert, B. Dreyfus and M. Pineri, *Macromolecules*, **19**, 2651 (1986).
51. P. Aldebert, B. Dreyfus, G. Gebel, N. Nakamura, M. Pineri and F. Volino, *J. Phys. (Paris)*, **49**, 2101 (1988).
52. B. Loppinet, G. Gebel and C. E. Williams, *J. Phys. Chem. B*, **101**, 1884 (1997).
53. R. B. Moore III and C. R. Martin, *Macromolecules*, **22**, 3594 (1989).
54. G. Gebel and R. B. Moore, *Macromolecules*, **33**, 4850 (2000).
55. G. Gebel, P. Aldebert and M. Pineri, *Macromolecules*, **20**, 1425 (1987).
56. R. B. Moore III and C. R. Martin, *Macromolecules*, **21**, 1334 (1988).
57. W. G. Grot, US Patent No. 4,433,082, to DuPont (1984).
58. M. Ludvigsson, J. Lindgren and J. Tegenfeldt, *J. Electrochem. Soc.*, **147**, 1303 (2000).

59. D. L. Handlin, W. J. MacKnight and E. L. Thomas, *Macromolecules*, **14**, 795 (1981).
60. J. Ceynowa, *Polymer*, **19**, 73 (1978).
61. M. Fujimura, T. Hashimoto and H. Kawai, *Macromolecules*, **14**, 1309 (1981).
62. M. Fujimura, T. Hashimoto and H. Kawai, *Macromolecules*, **16**, 136 (1983).
63. T. Xue, J. S. Trent and K. Osseo-Asare, *J. Membr. Sci.*, **45**, 261 (1989).
64. Z. Porat, J. R. Fryer, M. Huxham and I. Rubinstein, *J. Phys. Chem.*, **99**, 4667 (1995).
65. G. E. Wnek, B. M. Sheikh-Ali, J. M. Serpico, S. G. Ehrenberg, T. N. Tangredi, C. Karuppaiah and Y. Ye, *Am. Chem. Soc. Prepr., Polym. Div.*, **39**(1), 54 (1998).
66. P. Schroeder, *Z. Phys. Chem.*, **45**, 75 (1903).
67. T. A. Zawodzinski, Jr, C. Derouin, S. Radzinski, R. J. Sherman, V. T. Smith, T. E. Springer and S. Gottesfeld, *J. Electrochem. Soc.*, **140**, 1041 (1993).
68. T. A. Zawodzinski, Jr, S. Gottesfeld, S. Shoichet and T. J. McCarthy, *J. Appl. Electrochem.*, **23**, 86 (1993).
69. M. Chomakoba-Haefke, R. Nyffenegger and E. Schmidt, *Appl. Phys. A.*, **59**, 151 (1994).
70. A. Lehmani, S. Durand-Vidal and P. Turq, *J. Appl. Polym. Sci.*, **68**, 503 (1998).
71. P. J. James, T. J. McMaster, J. M. Newton and M. J. Miles, *Polymer*, **41**, 4223 (2000).
72. P. J. James, M. Antognozzi, J. Tamayo, T. J. McMaster, J. M. Newton and M. J. Miles, *Langmuir*, **17**, 349 (2001).
73. R. S. McLean, M. Doyle and B. B. Sauer, *Macromolecules*, **33**, 6541 (2000).
74. E. Sabatani, H. D. Nikol, H. B. Gray and F. C. Anson, *J. Am. Chem. Soc.*, **118**, 1158 (1996).
75. M. A. F. Robertson and H. L. Yeager, *Macromolecules*, **29**, 5166 (1996).
76. T. Komura, T. Yamaguchi, H. Sato, H. Shimatani and K. Takahashi, *Electrochim. Acta*, **46**, 3579 (2001).
77. H. W. Starkweather, Jr, *Macromolecules*, **15**, 320 (1982).
78. S. C. Yeo and A. J. Eisenberg, *J. Appl. Polym. Sci.*, **21**, 875 (1977).
79. S. H. de Almeida and Y. Kawano, *J. Therm. Anal. Calor.*, **58**, 569 (1999).
80. G. Maggio, V. Recupero and C. Mantegazza, *J. Power Sources*, **62**, 167 (1996).
81. Y. Miura and H. Yoshida, *Thermochim. Acta*, **163**, 161 (1990).
82. Y. Miura and H. Yoshida, *Mem. Faculty Tech. Tokyo Metropolitan Univ.*, **40**, 4349 (1990).
83. R. B. Moore, K. M. Cable and T. L. Croley, *J. Membr. Sci.*, **75**, 7 (1992).
84. M. Shi and F. C. Anson, *J. Electroanal. Chem.*, **425**, 117 (1997).
85. J. Divisek, M. Eikerling, V. Mazin, H. Schmitz, U. Stimming and Y. M. Volfkovich, *J. Electrochem. Soc.*, **145**, 2677 (1998).
86. M. Ludvigsson, J. Lindgren and J. Tegenfeldt, *Electrochim. Acta*, **45**, 2267 (2000).
87. M. Doyle, M. E. Lewittes, M. G. Roelofs and S. A. Perusich, *J. Phys. Chem. B*, **105**, 9387 (2001).
88. F. N. Buchi and G. G. Scherer, *J. Electrochem. Soc.*, **148**, A183 (2001).
89. T. A. Zawodzinski Jr, M. Neeman, L. O. Sillerud and S. Gottesfeld, *J. Phys. Chem.*, **95**, 6040 (1991).
90. P. Futerko and I.-M. Hsing, *J. Electrochem. Soc.*, **146**, 2049 (1999).
91. J. Y. Huh and Y. C. Bae, *Electrochim. Acta*, **46**, 3535 (2001).
92. K. J. Leckrone and J. M. Hayes, *Anal. Chem.*, **69**(5), 911 (1997).
93. R. S. Yeo, *Polymer*, **21**, 432 (1980).
94. R. S. Yeo, *J. Appl. Polym. Sci.*, **32**, 5733 (1986).
95. P. Aldebert, M. Guglielmi and M. Pineri, *Polym. J.*, **23**, 399 (1991).
96. D. Nandan, H. Mohan and R. M. Iyer, *J. Membr. Sci.*, **71**, 69 (1992).
97. X. Ren, T. E. Springer and S. Gottesfeld, *J. Electrochem. Soc.*, **147**, 92 (2000).
98. X. Ren, T. E. Springer, T. A. Zawodzinski and S. Gottesfeld, *J. Electrochem. Soc.*, **147**, 466 (2000).
99. A. B. Geiger, J. Newman and J. M. Prausnitz, *AIChE J.*, **47**, 445 (2001).
100. C. Gates and J. Newman, *AIChE J.*, **46**, 2076 (2000).
101. M. Watanabe, H. Uchida, Y. Seki, M. Emori and P. Stonehart, *J. Electrochem. Soc.*, **143**, 3847 (1996).
102. Z. Ogumi, Y. Uchimoto, M. Tsujikawa and Z. Takehara, *J. Electrochem. Soc.*, **136**, 1247 (1989).
103. Z. Ogumi, Y. Uchimoto, M. Tsujikawa and Z. Takehara, *J. Electrochem. Soc.*, **137**, 1430 (1990).
104. K. Yasuda, T. Yoshida, Y. Uchimoto, Z. Ogumi and Z. Takehara, *Chem. Lett.*, **250**, 2013 (1992).
105. Z.-I. Takehara, Z. Ogumi, Y. Uchimoto and K. Yasuda, *J. Adhesion Sci. Tech.*, **9**, 615 (1995).
106. R. Zeng, Z. Pang and H. Zhu, *J. Electroanal. Chem.*, **490**, 102 (2000).
107. H. L. Yeager in 'Perfluorinated Ionomer Membranes', A. Eisenberg and H. L. Yeager (Eds), ACS Symp. Ser. 180, p. 41 (1982).
108. J. R. Bontha and P. N. Pintauro, *Chem. Eng. Sci.*, **49**(23), 3835 (1994).
109. P. N. Pintauro, R. Tandon, L. Chao, W. Xu and R. Evilia, *J. Phys. Chem.*, **99**, 12 915 (1995).
110. F. Helfferich, 'Ion Exchange', McGraw-Hill, New York (1962).
111. J. Newman, 'Electrochemical Systems', Prentice-Hall, Englewood Cliffs, NJ (1991).

112. M. W. Verbrugge and P. N. Pintauro, 'Modern Aspects of Electrochemistry', B. E. Conway, J. O.'M. Bockris and R. W. White (Eds), Plenum Press, New York, Vol. 19, pp. 1–67 (1989).
113. T. E. Springer, T. A. Zawodzinski and S. Gottesfeld, *J. Electrochem. Soc.*, **138**, 2334 (1991).
114. D. M. Bernardi and M. W. Verbrugge, *J. Electrochem. Soc.*, **139**, 2477 (1992).
115. T. F. Fuller and J. Newman, *J. Electrochem. Soc.*, **140**, 1218 (1993).
116. T. V. Nguyen and R. E. White, *J. Electrochem. Soc.*, **140**, 2178 (1993).
117. R. Mosdale and S. Srinivasan, *Electrochim. Acta*, **40**, 413 (1995).
118. J. P. Meyers, 'Simulation and Analysis of the Direct Methanol Fuel Cell', Ph.D. Dissertation, U. C. Berkeley, Berkeley, CA (1998).
119. K. Sundmacher and K. Scott, *Chem. Eng. Sci.*, **54**, 2927 (1999).
120. P. Argyropoulos, K. Scott and W. M. Taama, *J. Power Sources*, **79**, 169 (1999).
121. P. Argyropoulos, K. Scott and W. M. Taama, *Chem. Eng. J.*, **73**, 217 (1999).
122. T. E. Springer, T. A. Zawodzinski, M. S. Wilson and S. Gottesfeld, *J. Electrochem. Soc.*, **143**, 587 (1996).
123. J. S. Yi and T. V. Nguyen, *J. Electrochem. Soc.*, **145**, 1149 (1998).
124. V. Gurau, H. Liu and S. Kakac, *AIChE J.*, **44**, 2410 (1998).
125. D. Singh, D. M. Lu and N. Djilali, *Int. J. Eng. Sci.*, **37**, 431 (1999).
126. S. Um, C.-Y. Wang and K. S. Chen, *J. Electrochem. Soc.*, **147**, 4485 (2000).
127. T. Okada, G. Xie and M. Meeg, *Electrochim. Acta*, **14**, 2141 (1998).
128. K. Sundmacher, T. Schultz, S. Zhou, K. Scott, M. Ginkel and E. D. Gilles, *Chem. Eng. Sci.*, **56**, 333 (2001).
129. X.-D. Din and E. E. Michaelides, *AIChE J.*, **44**, 35 (1998).
130. J. A. Elliott, S. Hanna, A. M. S. Elliott and G. E. Cooley, *Phys. Chem. Chem. Phys.*, **1**, 4855 (1999).
131. P. Johansson, J. Tegenfeldt and J. Lindgren, *Electrochim. Acta*, **45**, 3055 (2000).
132. S. J. Paddison, L. R. Pratt, T. A. Zawodzinski, Jr and D. W. Reagor, *Fluid Phase Equilib.*, **150**, 235 (1998).
133. S. J. Paddison, L. R. Pratt and T. A. Zawodzinski, Jr, *J. New Mater. Electrochem. Syst.*, **2**, 183 (1999).
134. S. J. Paddison, R. Paul and T. A. Zawodzinski Jr, *J. Electrochem. Soc.*, **147**, 617 (2000).
135. K.-D. Kreuer, *Chem. Mater.*, **8**, 610 (1996).
136. F. A. Uribe, T. E. Springer and S. Gottesfeld, *J. Electrochem. Soc.*, **139**, 765 (1992).
137. R. S. Yeo and D. T. Chin, *J. Electrochem. Soc.*, **127**, 549 (1980).
138. R. Wodzki, A. Narebska and W. K. Nioch, *J. Appl. Polm. Sci.*, **30**, 769 (1985).
139. P. C. Rieke and N. E. Vanderborgh, *J. Membr. Sci.*, **32**, 313 (1987).
140. R. C. T. Slade, J. Barker and J. H. Strange, *Solid State Ionics*, **35**, 11 (1989).
141. A. Parthasarathy, S. Srinivasan, A. J. Appleby and C. R. Martin, *J. Electrochem. Soc.*, **139**, 2530 (1992).
142. T. A. Zawodzinski Jr, T. E. Springer, F. Uribe and S. Gottesfeld, *Solid State Ionics*, **60**, 199 (1993).
143. B. D. Cahan and J. S. Wainright, *J. Electrochem. Soc.*, **140**, L185 (1993).
144. C. L. Gardner and A. V. Anantaraman, *J. Electroanal. Chem.*, **449**, 209 (1998).
145. M. Cappadonia, J. Wilhelm Erning and U. Stimming, *J. Electroanal. Chem.*, **376**, 189 (1994).
146. Y. Sone, P. Ekdunge and D. Simonsson, *J. Electrochem. Soc.*, **143**, 1254 (1996).
147. R. W. Kopitzke, C. A. Linkous, H. R. Anderson and G. L. Nelson, *J. Electrochem. Soc.*, **147**, 1677 (2000).
148. G. Alberti, M. Casciola, L. Massinelli and B. Bauer, *J. Membr. Sci.*, **185**, 73 (2001).
149. A. Lehmani, P. Turq, M. Perie, J. Perie and J.-P. Simonin, *J. Electroanal. Chem.*, **428**, 81 (1997).
150. T. Okada, G. Xie, O. Gorseth, S. Kjelstrup, N. Nakamura and T. Arimura, *Electrochim. Acta*, **43**(24), 3741 (1998).
151. T. Arimura, D. Ostrovskii, T. Okada and G. Xie, *Solid State Ionics*, **118**, 1 (1999).
152. K. D. Kreuer, A. Fuchs, M. Ise, M. Spaeth and J. Maier, *Electrochim. Acta*, **43**, 1281 (1998).
153. M. Doyle, S. K. Choi and G. Proulx, *J. Electrochem. Soc.*, **147**, 34 (2000).
154. K.-D. Kreuer, T. Dippel, W. Meyer and J. Maier, *Mater. Res. Soc. Symp. Proc.*, **293**, 273 (1993).
155. K. D. Kreuer, *Solid State Ionics*, **136–137**, 149 (2000).
156. J. J. Fontanella, C. A. Edmondson, M. C. Wintersgill, Y. Wu and S. G. Greenbaum, *Macromolecules*, **29**, 4944 (1996).
157. C. A. Edmondson, P. E. Stallworth, M. E. Chapman, J. J. Fontanella, M. C. Wintersgill, S. H. Chung and S. G. Greenbaum, *Solid State Ionics*, **135**, 419 (2000).
158. S. J. Paddison, D. W. Reagor and T. A. Zawodzinski, Jr, *J. Electroanal. Chem.*, **459**, 91 (1998).
159. T. Okada, G. Xie and M. Meeg, *Electrochim. Acta*, **14–15**, 2141 (1998).
160. S. Motupally, A. J. Becker and J. W. Weidner, *J. Electrochem. Soc.*, **147**, 3171 (2000).
161. M. W. Verbrugge, *J. Electrochem. Soc.*, **136**, 417 (1989).
162. P. S. Kauranen and E. Skou, *J. Appl. Electrochem.*, **26**, 909 (1996).
163. I. Cabasso and Z. Z. Liu, *J. Membr. Sci.*, **24**, 101 (1985).
164. I. Cabasso, Z. Z. Liu and T. Makenzie, *J. Membr. Sci.*, **28**, 109 (1986).
165. K.-H. Choi, D.-H. Peck, C. S. Kim, D.-R. Shin and T.-H. Lee, *J. Power Sources*, **86**, 197 (2000).

166. T. Fuller and J. Newman, *J. Electrochem. Soc.*, **139**, 1332 (1992).
167. T. A. Zawodzinski, J. Davey, J. Valerio and S. Gottesfeld, *Electrochim. Acta*, **40**, 297 (1995).
168. G. Xie and T. Okada, *J. Electrochem. Soc.*, **142**, 3057 (1995).
169. G. Xie and T. Okada, *Electrochim. Acta*, **41**, 1569 (1996).
170. M. Ise, K. D. Kreuer and J. Maier, *Solid State Ionics*, **125**, 213 (1999).
171. X. Ren and S. Gottesfeld, *J. Electrochem. Soc.*, **148**, A87 (2001).
172. Z. Ogumi, Z. Takehara and S. Yoshizawa, *J. Electrochem. Soc.*, **131**, 769 (1984).
173. R. S. Yeo and J. McBreen, *J. Electrochem. Soc.*, **126**, 1682 (1979).
174. A. Parthasarathy, C. R. Martin and S. Srinivasan, *J. Electrochem. Soc.*, **138**, 916 (1991).
175. P. D. Beattie, V. I. Basura and S. Holdcroft, *J. Electroanal. Chem.*, **468**, 180 (1999).
176. A. T. Haug and R. E. White, *J. Electrochem. Soc.*, **147**, 980 (2000).
177. A. J. Appleby, O. A. Velev, J.-G. LeHelloco, A. Parthasarthy, S. Srinivasan, D. D. DesMarteau, M. S. Gillette and J. K. Ghosh, *J. Electrochem. Soc.*, **140**, 109 (1993).
178. J. J. Sumner, S. E. Creager, J. J. Ma and D. D. DesMarteau, *J. Electrochem. Soc.*, **145**, 107 (1998).
179. A. E. Feiring and S. Rozen, US Patent No. 5,830,962, to DuPont (1998).
180. W. B. Farnham and Z.-Y. Yang, PCT WO 00/24709, to DuPont (2000).
181. Z.-Y. Yang, PCT WO 00/77057, to DuPont (2000).
182. C. M. Doyle, A. E. Feiring and S. K. Choi, PCT WO 99/67304, to DuPont (1999).
183. M. Prober, *J. Am. Chem. Soc.*, **75**, 968 (1952).
184. R. B. Hodgdon, *J. Polym. Sci.*, **6**, 171 (1968).
185. G. Hubner and E. Roduner, *J. Mater. Chem.*, **9**, 409 (1999).
186. J. Wei, C. Stone and A. E. Steck, US Patent No. 5,422,411, to Ballard (1995).
187. S. K. Choi, C. M. Doyle, M. G. Roelofs, L. Wang and Z.-Y. Yang, US Patent No. 6,100,324, to DuPont (2000).
188. C. M. Doyle, W. B. Farnham, A. E. Feiring, P. A. Morken and M. G. Roelofs, US Patent No. 6,025,092, to DuPont (2000).
189. A. E. Feiring, C. M. Doyle, M. G. Roelofs, W. B. Farnham, P. G. Bekiarian and H. A. K. Blau, PCT WO 99/45048, to DuPont (1999).
190. H. A. K. Blau, PCT WO 01/47872, to DuPont (2001).
191. S. J. C. Cleghorn, X. Ren, T. E. Spriner, M. S. Wilson, C. Zawodzinski, T. Zawodzinski and S. Gottesfeld, *Int. J. Hydrogen Energy*, **22**, 1137 (1997).
192. X. Ren, T. A. Zawodzinski, F. Uribe, H. Dai and S. Gottesfeld, 'Proton Conducting Membrane Fuel Cells I', S. Gottesfeld, G. Halpert and A. Landgrebe (Eds), The Electrochemical Society, Pennington, NJ, Vol. 95–23, p. 284 (1995).
193. X. Ren, T. E. Springer, T. A. Zawodzinski and S. Gottesfeld, *J. Electrochem. Soc.*, **147**, 466 (2000).
194. M. R. Verbrugge, *J. Electrochem. Soc.*, **136**, 417 (1989).
195. D. L. Maricle, B. L. Murach and L. L. Van Dine, 'The Electrochemical Society Extended Abstracts', San Francisco, CA, Vol. 94–1, Abstract 35, p. 58, May 22–27 (1994).
196. D. Chu and S. Gilman, *J. Electrochem. Soc.*, **141**, 1770 (1994).
197. P. S. Kauranen and E. Skou, *J. Electroanal. Chem.*, **408**, 189 (1996).
198. S. R. Narayanan, H. Frank, B. Jeffries-Nakamura, M. Smart, W. Chun, G. Halpert, J. Kosek and C. Cropley, 'Proton Conducting Membrane Fuel Cells I', S. Gottesfeld, G. Halpert and A. Landgrebe (Eds), The Electrochemical Society, Pennington, NJ, Vol. 95–23, p. 278 (1995).
199. G. Rajendran, presented at 'Fourth International Symposium on New Materials for Electrochemical Systems', Montreal, Canada, July 9–13 (2001).
200. X. Ren, P. Zelenay, S. Thomas, J. Davey and S. Gottesfeld, *J. Power Sources*, **86**, 111 (2000).
201. S. R. Narayanan, A. Kindler, B. Jeffries-Nakamura, W. Chun, H. Frank, M. Smart, T. I. Valdez, S. Surampudi and G. Halpert, *Annu. Battery Conf. Appl. Adv.*, **11**, 113 (1996).
202. D. Chu and S. Gilman, *J. Electrochem. Soc.*, **143**, 1685 (1996).
203. H. A. Gasteiger, N. Markovic, P. N. Ross and E. J. Cairns, *J. Phys. Chem.*, **97**, 12 020 (1993).
204. DuPont unpublished data.
205. X. Ren, T. E. Springer and S. Gottesfeld, 'Proton Conducting Membrane Fuel Cells II', S. Gottesfeld and T. F. Fuller (Eds), The Electrochemical Society, Pennington, NJ, Vol. 98–27, p. 341 (1998).
206. H. Dohle, J. Divisek, J. Mergel, H. F. Oetjen, C. Zingler and D. Stolten, in '2000 Fuel Cell Seminar Abstracts', Portland, OR, Oct. 30–Nov. 2, p. 126 (2000).
207. S. Gottesfeld and T. A. Zawodzinski, in 'Advances in Electrochemistry and Electrochemical Engineering,' C. Tobias, H. Gerischer, D. Kolb and R. Akire (Eds), Vol. 5, p. 195 (1997).
208. P. Zelenay, S. C. Thomas and S. Gottesfeld, 'Proton Conducting Membrane Fuel Cells II', S. Gottesfeld and T. F. Fuller (Eds), The Electrochemical Society, Pennington, NJ, Vol. 98–27, p. 300 (1998).
209. S. Gojkovic, S. Gupta and R. F. Savinell, *J. Electroanal. Chem.*, **462**, 63 (1999).
210. T. J. Schmidt, U. A. Paulus, H. A. Gasteiger, N. Alonso-Vante and R. J. Behm, *J. Electrochem. Soc.*, **147**, 2620 (2000).
211. W. G. Grot and G. Rajendran, US Patent No. 5,919,583, to DuPont (1999).
212. P. L. Antonucci, A. S. Arico, P. Creti, E. Ramunni and V. Antonucci, *Solid State Lett.*, **125**, 431 (1999).

213. G. Deluga and B. S. Pivovar, 'Fourth International Symposium on New Materials for Electrochemical Systems', Montreal, Canada, p. 132, July 4–8 (1999).

214. G. Rajendran, presented at 'Electrochemical Technology for the 21st Century', Clearwater Beach, FL, Nov. 12–13 (2000).